UPPSALA
UNIVERSITET

Energy from Ocean Waves

Full Scale Experimental Verification of a Wave Energy Converter

RAFAEL WATERS

Dissertation presented at Uppsala University to be publicly examined in Polacksbackens aula, Lägerhyddsv. 2, Uppsala, Friday, December 12, 2008 at 13:00 for the degree of Doctor of Philosophy. The examination will be conducted in English.

Abstract
Waters, R. 2008. Energy from Ocean Waves. Full Scale Experimental Verification of a Wave Energy Converter. Acta Universitatis Upsaliensis. *Digital Comprehensive Summaries of Uppsala Dissertations from the Faculty of Science and Technology* 580. 130 pp. Uppsala. ISBN 978-91-554-7354-9.

A wave energy converter has been constructed and its function and operational characteristics have been thoroughly investigated and published. The wave energy converter was installed in March of 2006 approximately two kilometers off the Swedish west coast in the proximity of the town Lysekil. Since then the converter has been submerged at the research site for over two and a half years and in operation during three time periods for a total of 12 months, the latest being during five months of 2008. Throughout this time the generated electricity has been transmitted to shore and operational data has been recorded. The wave energy converter and its connected electrical system has been continually upgraded and each of the three operational periods have investigated more advanced stages in the progression toward grid connection. The wave energy system has faced the challenges of the ocean and initial results and insights have been reached, most important being that the overall wave energy concept has been verified. Experiments have shown that slowly varying power generation from ocean waves is possible.

Apart from the wave energy converter, three shorter studies have been performed. A sensor was designed for measuring the air gap width of the linear generator used in the wave energy converter. The sensor consists of an etched coil, a search coil, that functions passively through induction. Theory and experiment showed good agreement.

The Swedish west coast wave climate has been studied in detail. The study used eight years of wave data from 13 sites in the Skagerrak and Kattegatt, and data from a wave measurement buoy located at the wave energy research site. The study resulted in scatter diagrams, hundred year extreme wave estimations, and a mapping of the energy flux in the area. The average energy flux was found to be approximately 5.2 kW/m in the offshore Skagerrak, 2.8 kW/m in the near shore Skagerrak, and 2.4 kW/m in the Kattegat.

A method for evaluating renewable energy technologies in terms of economy and engineering solutions has been investigated. The match between the technologies and the fundamental physics of renewable energy sources can be given in terms of the technology's utilization. It is argued that engineers should strive for a high utilization if competitive technologies are to be developed.

Keywords: wave power, wave energy converter, sea trials, ocean energy, linear generator, point absorber, search coil, wave climate, utilization

Rafael Waters, Department of Engineering Sciences, Box 534, Uppsala University, SE-75121 Uppsala, Sweden

Till min fantastiska mor
To my great dad
To my brothers who'll always be there
… and to some good, I hope.

List of Papers

This thesis is based on the following papers, which are referred to in the text by their Roman numerals.

I Stålberg, M., **Waters, R.**, Eriksson, M., Danielsson, O., Thorburn, K., Bernhoff, H., and Leijon, M. "Full-Scale Testing of PM Linear Generator for Point Absorber WEC". *Proceedings of the 6th European Wave and Tidal Energy Conference, EWTEC*, Glasgow, UK, 2005.

II **Waters, R.**, Stålberg, M., Danielsson, O., Svensson, O., Gustafsson, S., Strömstedt, E., Eriksson, M., Sundberg, J., and Leijon, M. "Experimental results from sea trials of an offshore wave energy system". *Applied Physics Letters*, 90:034105, 2007.

III Stålberg, M., **Waters, R.**, Danielsson, O., and Leijon, M. "Influence of Generator Damping on Peak Power and Variance of Power for a Direct Drive Wave Energy Converter". *Journal of Offshore Mechanics and Arctic Engineering*, 130(3), 2008.

IV Eriksson, M., **Waters, R.**, Svensson, O., Isberg, J., and Leijon, M. "Wave power absorption: Experiments in open sea and simulation". *Journal of Applied Physics*, 102:084910, 2007.

V **Waters, R.**, Stålberg, M., Svensson, O., Gustafsson, S., Danielsson, O., Strömstedt, E., Boström, C., Sundberg, J., and Leijon, M. "Power Absorption of a Wave Energy Converter". Submitted to *IEEE Journal of Oceanic Engineering*.

VI Tyrberg, S., **Waters, R.**, and Leijon, M. "On the influence of water levels on wave power absorption: experimental results". Submitted to *IEEE Journal of Oceanic Engineering*.

VII Engström, J., **Waters, R.**, Stålberg, M., Strömstedt, E., Eriksson, M., Isberg, J., Henfridsson, U., Bergman, K., Asmussen, J., and Leijon, M. "Offshore experiments on a direct-driven Wave Energy Converter". *Proceedings of the 7th European Wave and Tidal Energy Conference, EWTEC*, Porto, Portugal, 2007.

VIII Boström, C., **Waters, R.**, Lejerskog, E., Svensson, O., Stålberg, M., Strömstedt, E., and Leijon, M. "Wave energy conversion system -– experimental results from offshore operation". Conditionally accepted to *IEEE Journal of Oceanic Engineering*, Technical Communication.

IX **Waters, R.**, Danielsson, O., and Leijon, M. "Measuring air gap width of permanent magnet linear generators using search coil sensor". *Journal of Applied Physics* 101:024518, 2007.

X   **Waters, R.**, Engström, J., Isberg, J., and Leijon, M. "Wave Climate off the Swedish West Coast". Submitted to *Renewable Energy*.

XI   Leijon, M., Boström, C., Danielsson, O., Gustafsson, S., Haikonen, K., Langhamer, O., Strömstedt, E., Stålberg, M., Sundberg, J., Svensson, O., Tyrberg, S., and **Waters, R.** "Wave Energy from the North Sea: Experiences from the Lysekil Research Site". *Surveys in Geophysics, Springer*, 2008, available online, invited.

XII   Leijon, M., **Waters, R.**, Stålberg, M., Svensson, O., Boström, C., Strömstedt, E., Engström, J., Tyrberg, S., Savin, A., Gravråkmo, H., Bernhoff, H., Sundberg, J., Isberg, J., Ågren, O., Danielsson, O., Eriksson, M., Lejerskog, E., Bolund, B., Gustafsson, S., and Thorburn, K. "Conversion of wave motions to electricity – from theory to full scale experiments". *IEEE Power & Energy Magazine*, to appear in January 2009 issue.

XIII   Boström, C., Lejerskog, E., Tyrberg, S., Svensson, O., **Waters, R.**, Savin, A., Bolund, B., Eriksson, M., and Leijon, M. "Experimental results from an offshore wave energy converter". *Proceedings of the 27th International Conference on Offshore Mechanics and Arctic Engineering, OMAE*, Estoril, Portugal, 2008.

XIV   Tyrberg, S., Stålberg, M., Boström, C., **Waters, R.**, Svensson, O., Strömstedt, E., Savin, A., Engström, J., Langhamer, O., Gravråkmo, H., Haikonen, K., Tedelid, J., Sundberg, J., and Leijon, M. "The Lysekil Wave Power Project: Status Update". *Proceedings of the 10th World Renewable Energy Conference, WREC*, Glasgow, UK, 2008.

XV   Leijon, M., Skoglund, A., **Waters, R.**, Rehn, A., and Lindahl, M. "On the Physics and Economics of Renewable Electric Energy Sources – part I utilization". Conditionally accepted for publication in *World Scientific and Engineering Academy and Society (WSEAS) Transactions*, invited.

XVI   Skoglund, A., Leijon, M., Rehn, A., and Lindahl, M, and **Waters, R.**. "On the Physics and Economics of Renewable Electric Energy Sources – part II engineering". Accepted for publication in *World Scientific and Engineering Academy and Society (WSEAS) Transactions*, invited.

The following, of the above papers, also appear in conference proceedings:

A   Stålberg, M., **Waters, R.**, Danielsson, O., Leijon, M. "Influence of Generator Damping on Peak Power and Variance of Power for a Direct Drive Wave Energy Converter". *Proceedings of the 26th International Conference on Offshore Mechanics and Arctic Engineering OMAE*, San Diego, California, USA, 2007.

B   Leijon, M., Skoglund, A., **Waters, R.**, Rehn, A., and Lindahl, M. "On the Physics and Economics of Renewable Electric Energy Sources – part I utilization". Presented at *World Scientific and Engineering Academy and Society, WSEAS, Energy Planning, Energy Saving, Environmental Education, EPESE*, Corfu Island, Greece, 2008.

C   Skoglund, A., Leijon, M., Rehn, A., and Lindahl, M, and **Waters, R.**. "On the Physics and Economics of Renewable Electric Energy Sources – part II engineering". Presented at *World Scientific and Engineering Academy and Society, WSEAS, Energy Planning, Energy Saving, Environmental Education, EPESE*, Corfu Island, Greece, 2008.

Contents

Nomenclature and abbreviations

Chapter 1 – Introduction

c	m/s	Phase speed
g	m/s^2	Acceleration of gravity
T	s	Wave period
U	%	Utilization

Chapter 2 – Electricity and magnetism

B	T	Magnetic flux density
H	A/m	Magnetizing field
M	A/m	Magnetization
μ_0	Vs/(Am)	Permeability of free space
μ_r	–	Relative permeability
Φ	Wb	Magnetic flux
A	m^2	Area
E	V/m	Electric field
D	C/m^2	Electric displacement field
$\mathbf{J}_f$	A/m^2	Free current density
ρ_f	C/m^3	Free charge density
B_r	T	Remanent magnetic flux density
B_s	T	Saturation magnetic flux density
H_c	A/m	Coercive field strength
p_{Fe}	W/m^3	Ohmic loss density in iron
$k_{hysteresis}$	J/(m^{3}T^2)	Hysteresis loss material constant
k_{eddy}	Js/(m^{3}T^2)	Eddy current loss material constant
k_{excess}	Js$^{1/2}$/(m^{3}T$^{3/2}$)	Excess loss material constant
B_{max}	T	Magnetic flux density amplitude in circuit
P_{Cu}	W/m^3	Ohmic losses in copper
R	Ω	Resistance
I	A	Current
V	V	Voltage
N	–	Number of coil turns

σ	A/Vm	Conductivity
V_{noise}	V	Noise voltage
$S(f)$	V^2s	Power density spectrum
$S_{white}(f)$	JΩ	Power density spectrum for white noise
k_B	J/K	Boltzmann's constant
T	K	Absolute temperature

Chapter 2 – Linear theory of ocean waves

ρ	kg/m^3	Density of sea water
t	s	Time
$\bar{v}$	m/s	Speed
p	N/m^2	Pressure
v	m^2/s	Kinematic viscosity
$\bar{f}$	N	External force on a fluid
F	N	Force
m	kg	Mass
a	m/s^2	Acceleration
ϕ	m^2/s	Velocity potential
η	m	Free surface elevation
b	–	Constant
H	m	Wave height
ω	rad/s	Angular frequency
g	m/s^2	Acceleration of gravity
k	1/m	Wave number
h	m	Water depth
f	Hz	Frequency
T	s	Wave period
λ	m	Wave length
c	m/s	Phase speed
c_g	m/s	Group speed
J	W/m	Energy flux
E_{tot}	J/m^2	Total energy density
E_p	J/m^2	Potential energy density
E_k	J/m^2	Kinetic energy density
A	m^2	Area
ζ	m	Vertical surface displacement
z_n	m	Fourier coefficients
n	–	An integer
S	m^2/Hz	Spectral density function

m_j	*varies*	Spectral moment
j	–	An integer
H_{m0}	m	Significant wave height
T_{m0-1}	s	Energy period

Chapter 2 – Extreme waves

p	–	Probability
$F(x)$	–	Cumulative distribution function
$f(x)$	–	Probability density function
$G(p)$	–	Inverse cumulative distribution function
a	m	Probability distribution location parameter
b	m	Probability distribution scale parameter
c	–	Probability distribution shape parameter
$H_{m0,statistic}$	m	Statistical significant wave height corresponding to the probability p
R	years	Return period
τ	years	Average time between values resulting from POT
$H_{m0,max}$	m	Statistical significant wave height occurring once per return period
H_{max}	m	Statistical single maximum wave height occurring once per return period

Chapter 4 – The construction of a wave energy converter

$k_{damping}$	Ns/m	Damping factor
F	N	Force
v	m/s	Speed
P	W	Power

Abbreviations

AC	Alternating Current
CDF	Cumulative distribution function
CFE	Swedish Centre for Renewable Electric Energy Conversion
DC	Direct Current
Nd-Fe-B	Neodymium–Iron–Boron
PCB	Printed circuit board
PDF	Probability density function
PDS	Power density spectrum
PM	Permanent Magnet

POT	Peaks over threshold
Q-Q	Quantile-quantile
RET	Renewable energy technology
WEC	Wave energy converter

1. Introduction

The quest for clean sources of energy is far from the only challenge facing the societies and environments of the world. Poverty, disease, war, hunger, the destruction of natural habitats, eutrophication of water bodies, and the dwindling supply of fresh water are problems that sometimes feel almost forgotten today when most media and societal focus is on global warming and the emission of greenhouse gases. Still, with this imbalance in mind, the utilized energy sources and the energy generating processes tie into many of these problems in addition to the melting of the ice caps, and modern renewable energy technologies avoid a lot of the unwanted effects of traditional energy sources.

The road to a future with little but non-polluting energy sources is, however, both long and difficult. Today fossil fuels make up approximately 80% of the gross primary energy used in the world's societies, and the *International Energy Agency (IEA)* anticipates that the same will be true in year 2030 in addition to a projected increase in global energy consumption by 1.6% per year [1]. The quest for clean sources of energy is therefore both important and urgent, but it is simultaneously hard pressed from competition with fossil fuels. Renewable energy technology that can start to compete with traditional energy sources at an economic level, without subsidies, is greatly needed.

That ocean waves carry a vast pool of energy has been known for a long time [2, 3]. Estimates account for power levels in the order of one terawatt descending on the coastlines of the world [4]. Moreover, the potential for a relatively high utilization, see Section 1.2, in combination with the fact that moving water, due to its high density, is a dense carrier of energy, suggests that ocean waves is a viable source of renewable energy. Still, as wind and solar power industries continue to grow exponentially, wave power technologies are all but absent from the world market. It is an area of multiphysics where conventional solutions do not exist. On the contrary, the lack of them has been a defining characteristic of wave power research over the years, and this is also the case among the larger projects still being researched today [5–13]. Wave power development has faced many difficulties, hence the multitude of solutions. Some of the major challenges are the survivability of parts exposed to the forces of the ocean, investment costs associated with large structures, excessive over-dimensioning needed to handle mechanical overloads, long life mooring difficulties, transmission of energy to shore, and the transformation of wave motion into high-speed, rotating generator motion. Wave power R&D has seen many mechanical solutions to these challenges, and most inventions have had a primary focus on hydrodynamics and mechanics. The Swedish Centre for Renewable Electric Energy Conversion at Uppsala University may

be the first to take a grid-oriented approach to wave energy. This approach, in combination with a holistic perspective and a desire to minimize complexity and mechanical components, is expected to generate a viable concept of wave energy conversion.

1.1 Waves

The waves referred to in this thesis are wind generated ocean waves. As such they are in essence concentrated solar energy. The sun shines on the world and heats the air, leading to pressure differences that are the engines that drive the winds. Energy from the sun is, in this way, transferred to and concentrated in the wind. When the wind blows over a stretch of water, waves are created. Some of the energy in the winds are transferred to the waves, and the energy that originally came from the sun is concentrated once again.

It starts with small pressure differences on the ocean surface, due to turbulence in the wind, that create small irregularities or small waves on the ocean surface. Resonance between the vertical wind pressure and these small waves, together with sheer stress due to higher wind speeds at the crests compared to the troughs, then act upon the waves and make them grow. When they are big enough other processes take over, the friction of the wind on the water and the pressure differences created by the sheltering effect of the lee side of the wave compared to the wind side of the wave causes the waves to continue to grow. Energy is continually transferred from the winds to the waves throughout all of these processes. The size that they ultimately reach depends on three things; the wind speed, the length of time during which the wind blows, and the distance of water over which the wind is blowing, the *fetch* [14].

1.1.1 Definitions and characteristics

Ocean waves that are created by the wind in the above way are called *wind waves*, and as long as they are under the generating influence of the wind the corresponding physical state of the ocean is called *wind sea* [15]. Waves are however, as most people realize, not dependent on winds to exist. After they have been created they will propagate unaided by the wind. Waves that are no longer under the generating influence of the wind are called *free waves* or *swell waves* [14]. A general term for the physical state of the ocean in terms of waves is *sea state*. While a sea state represents a shorter time period, and can be thought of as having a typical wave height and period, the *wave climate* is the long term description of a site which contains the combined information found in many years of sea states.

The typical appearance of a wind sea is very chaotic. Waves are appearing and disappearing with various heights and wave lengths and in various directions in an indiscernible pattern. Most wind seas can, however, be described as an overlap of a great number of perfect sine waves. Mathematically, a combi-

nation of sine waves of various heights, lengths, directions and positions will recreate the chaotic-looking sea state.

An interesting property of ocean waves is that the speed with which they move is proportional to its wave length as described by:

$$c = \frac{gT}{2\pi},$$ (1.1)

where g is the *acceleration of gravity* and T is the *wave period*. This will be described more thoroughly in Chapter 2. The consequence of this is that when the wind has ceased its generating influence on the wind sea, and as the waves continue to propagate across the ocean, then the original chaotic sea state will gradually come apart due to the different periods of the wave components that combine to make up the wind sea. That is, the longer waves will travel at the highest speeds while the converse is true for the shorter waves. After a long stretch of ocean the separation of waves will be almost complete and if at this time the first long waves arrive at a beach somewhere then the beach dwellers will see long, almost perfect waves rolling in and hitting the shore. Perfect surf waves. This is the typical appearance of swell waves. A possibly dangerous consequence of the speed of ocean waves is that the longest and therefore largest waves will be first to arrive at shore, and they may come as an unpleasant surprise.

1.1.2 Water motion

Upon observation, ocean waves exhibit a clear sense of motion and direction, and one may be fooled into thinking that this means that the water in the waves is being transported toward shore. In reality, however, it is only the energy that is being transported, while the water moves in circles with only a very small transportation of mass taking place. An example where this phenomenon can be seen is when a piece of wood is thrown in the water. It will move toward shore at a much lower speed then that of the waves. The water in waves moves forward at the wave crests, and backwards in the troughs. In deep water (which is approximately when the depth is greater than half of the average wave length), water moves in almost perfect circles and there is only a very small average transportation of water mass taking place [14]. The circular motion of the water decreases exponentially with depth and is almost zero at the depth of half the wave length. When the waves come into shallow areas they start to be affected by the bottom, which limits the movement of the water. The water starts moving in elliptical paths and energy is dissipated through friction against the seabed. As it gets even more shallow the wave period decreases and the waves become steeper. When the wave reaches a height corresponding to the wave length divided by seven, it breaks. The nature of waves at deep water will be derived in Chapter 2.

1.2 Wave energy

1.2.1 Intermittent energy sources

Wave energy is an *intermittent energy source*. This means that the available power from the source varies in time in a way that is uncontrollable. It may be possible to predict the power of waves and time of occurrence at a particular location a few days ahead of time, but it is not possible to control the waves themselves. This is an unwanted characteristic and a fact that utility companies have to deal with if they want to harness energy from intermittent sources, which is the case for most renewable energy sources, e.g. wind, wave and solar. The intermittency of these sources also make them practically incapable of supplying all of the energy to a society because, as long as there is no means of large electric energy storage in existence, the energy consumed in a society has to be produced at the time of use. The share of the total power supply to an electric grid that may be made up of intermittent sources, while remaining stable, depends on the amount of spare capacity that is rapidly available to the grid. Furthest to the right in Figure 1.2 is an example from reality where the wind power in the E.ON controlled grid drops by almost 4 GW over a short time period [16]. In Sweden the electric grid relies on hydro power to quickly fill the gap in electricity production should the power generated from wind power plants drop. There are, however, some applications where a controlled power input is not required, and intermittent sources may be particularly competitive in these cases. Examples are the charging of batteries or the desalination of seawater at desalination plants [17, 18].

A *non-intermittent energy source*, on the other hand, is one where the power input is controllable, which is the case for hydro power plants and nuclear power plants. At such plants the produced power is controlled via the input of fuel, or water in the case of hydro power. The advantage of non-intermittent
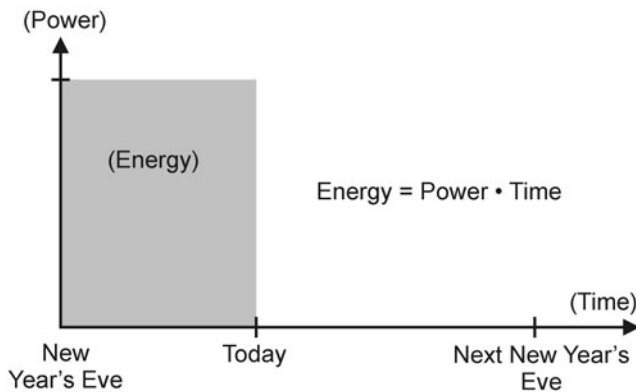

Figure 1.1: The often confused difference between power and energy. The rated power, represented here by the horizontal mark on the y-axis, corresponds to the size and investment costs of a power plant. The generated energy, represented here by the gray area, corresponds to the revenue a power plant can make by selling the energy.
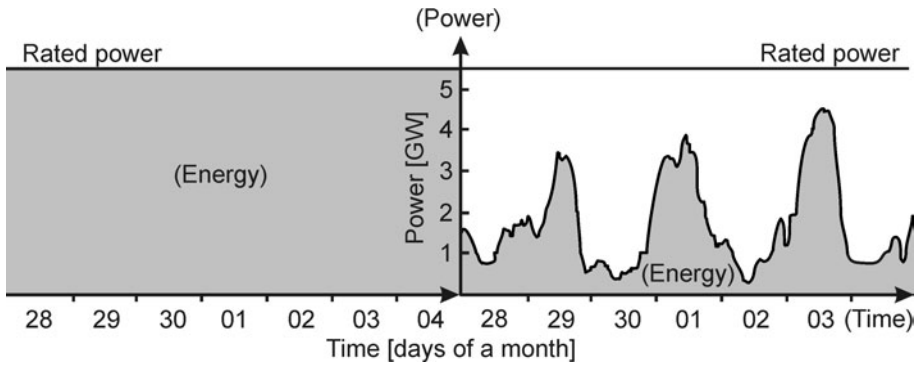
Figure 1.2: The difference between an intermittent and a non-intermittent energy source of equal rated power. The left side illustrates the ideal case of a non-intermittent energy source. The right side illustrates an intermittent energy source and is an example from a week of wind power generation in the E.ON controlled grid 28/4-4/5 2003 [16]. In reality, the non-intermittent source will have down times, at least on a longer time scale, but the general difference between the two will still be the same.
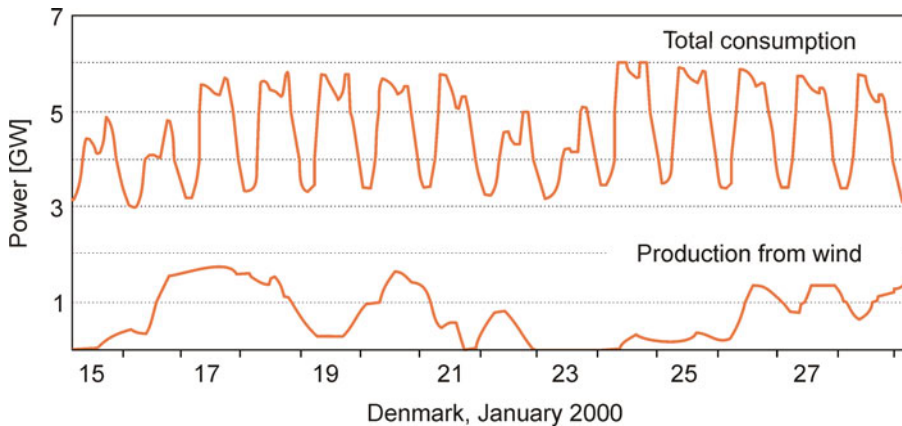

Figure 1.3: Electricity production from wind compared to gross electricity consumption. The example is taken from two weeks in the beginning of the year 2000 in Denmark [19].

sources is that they can run almost continuously at full power, also called *rated power* or *installed power*, which is good economics for a power plant simply because you get payed for generated energy, i.e. the number of produced kilowatt hours, and not for the size of the power plant, i.e. the rated power. Figure 1.1 illustrates the basic but often confused difference between energy and power. More importantly, non-intermittent sources provide stability to the electric grid since they can produce power when power is needed, unlike intermittent sources which produce power at the whim of nature. Figure 1.2 demonstrates the difference between an intermittent and a non-intermittent energy source, and Figure 1.3 presents an example of the energy production
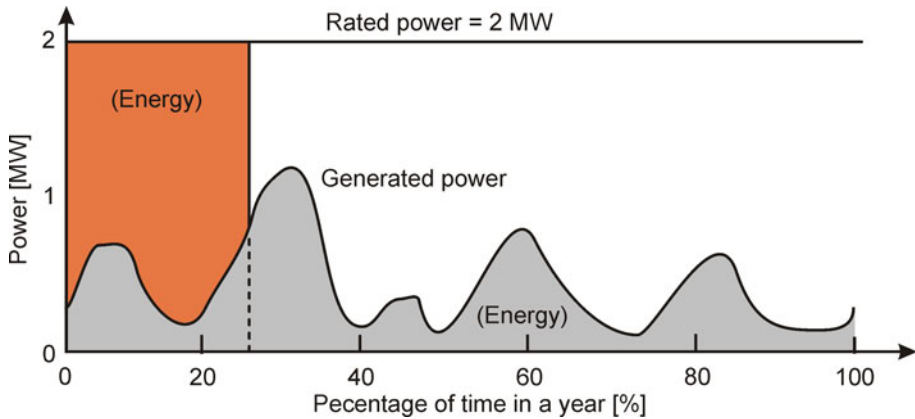
Figure 1.4: The utilization, represented by the portion of the year covered by the orange area. The energy generated at varying power during one year, the gray area, is thought of as having been generated during part of the year at rated power, the orange area.

from wind and the total consumption of electricity in Denmark during two week of the year 2000 [19].

The level of intermittency varies between energy sources and within an energy source depending on geographical location. Wind power is in general less intermittent than solar energy, and wind power at sea is generally less intermittent than wind power on land [20]. Intermittency is measured by the *utilization*, sometimes called *capacity factor* or *utility factor* (although these sometimes have other meanings as well), which is defined as the ratio of average power production over a year divided by the rated power. A low level of intermittency is desirable, and it corresponds to a high utilization:

$$\text{Utilization}, U = \frac{\text{Average annual energy production}}{\text{Rated power} \cdot 8760} \cdot 100. \qquad (1.2)$$

Utilization is presented and discussed with many examples in Papers XV and XVI. The utilization can be viewed schematically in Figure 1.4. In this figure the energy generated during the entire year, the gray area, is assumed to have been generated during part of the year but at a constant power level equaling the rated power, the orange area. The orange area is thus of equal size as the gray area and the part of the year that the orange area covers represents the utilization, here approximately 25%. Depending on location, wave energy is expected to have a potential for utilization levels between 35% and 70% [21]. It is likely that wave power will have a larger utilization than offshore wind power since the waves at any chosen site are not only generated by the wind at that site, but will also enter the site in the form of swell waves that have originated elsewhere. Since swell waves are not dependent on the wind at a site, they will contribute to the energy production of a wave energy converter whether or not there is any wind in the area.

Apart from the utilization another important aspect of an energy source is its distribution over the year, i.e. it is favorable if the energy is available simultaneously with the demand. Wave power varies to a large extent on all time scales, from the second scale of the individual waves, to the average power levels of hours, months, years and decades [14]. In Nordic countries, however, the power in waves can be predicted to be lower during the summer and higher during the winter half of the year, which is consistent with the demand for energy [22]. Wave power is often compared with wind power, which is readily done since the two energy sources have a lot in common physically and because wind already has shown itself as being a viable energy source. A positive property of the wave energy source compared to the wind energy source is that the average power delivered by waves varies more slowly compared to the sometimes very fast changes in wind speed and direction.

1.2.2   Energy density

Sea water is about 850 times heavier than air. Hence when water is in motion then so is a lot of energy. Anyone who has tried to stand up against, or has witnessed, large waves realizes that waves constitute a dense source of energy, and in comparison to other sources of renewable energy, i.e. wind and solar, they do.

When energy is transferred as swell waves across the ocean the amount of energy that is lost due to inner friction, or viscosity, is very small. For example, when waves generated in storms off New Zealand reach California in what is known as the *summer swell*, almost no energy has been lost in the journey across the pacific. Waves really start to lose energy when the depth decreases below one half wave length. At this time energy is dissipated as heat through friction against the seabed. Eventually, when the waves crash against the shore, although some is reflected, most of the energy is generally lost as heat in turbulence and friction.

The power of ocean waves, i.e. the energy flow or *energy flux*, is usually presented as the average power per meter of crest length of a wave, and the unit is thus usually [W/m]. What this given value really means is the average energy per second that is passing under one meter of wave crest, from the surface to the seabed. However, as noted in Section 1.1, the energy flux decreases exponentially with depth so that 95% of the energy is contained in depths above one fourth of the average wave length [14], see Figure 2.7 in Chapter 2. Furthermore, theoretically, a buoy on the ocean surface can capture all of the energy passing underneath it [23]. Hence, power per length of wave crest, [W/m], is a fair measure of energy flux by itself as well as in comparison to the energy flux of e.g. wind and solar energy which are given in the unit of [W/m^2].

The energy transfer from solar radiation into waves is typically in the order of 0.01 to 0.1 W/m^2, which is small compared to the average solar radiation on the earth surface. The oceans are, however, large and when the energy reaches the coasts in the concentrated form of waves, the average energy flux over a

Figure 1.5: World wave energy resource. The numbers represent average energy flux [kW/m].

year may be as high as 100 kW/m [24]. Sweden, on the other hand, has a relatively mild wave climate with an average energy flux of only approximately 5.2 kW/m on the west coast, see Paper X. This, however, corresponds to 45 MWh of energy per meter of the coast and year. By contrast, the average solar radiation in Sweden is 115 W/m^2, which corresponds to 1 MWh per square meter of land and year [25]. Moreover, at average wind speeds of 7.25 m/s near the coasts of Sweden, the average wind energy flux is 230 W/m^2 which corresponds to 2 MWh or energy per square meter of vertical surface and year [26].

1.2.3   The wave energy resource

The International Energy Agency has estimated that wave energy could eventually meet over 10% of the world's current electricity demand [27]. Calculations of the total wave energy flux in the world yeild average values between 1 – 10 TW [3, 4, 12, 27, 28]. Figure 1.5 presents the average energy flux at different locations in the world [14, 27].

   Estimates of the level of energy that descends on the coasts of the world, and how much of this that can be technically and economically harvested, varies a lot in the literature. One estimate proposes that 1000 TWh of energy descends on the coast of the UK each year, and that out of this 50 TWh could be harvested. The same source estimates that Norway receives 750 TWh/year out of which 23 TWh could be harvested, Japan receives 260 TWh/year out of

which 10 – 15 TWh could be harvested, Ireland could harvest 20 TWh/year, the US west coast 25 TWh/year, and Spain 10 TWh/year [14]. A different source proposes that Norway receives 500 – 600 TWh/year and that the harvestable amount is 50 TWh/year [22]. Estimates for Sweden say that the gross available energy is between 25 – 50 TWh/year and that, out of this, between 2 – 15 TWh is feasible for extraction [14, 22, 25, 29, 30].

1.3 Wave energy technology

Although the first patents on the extraction of wave energy from oceans are hundreds of years old [31], it was not until the oil crisis in the 70s, with sky rocketing oil prices, that the search for alternatives really picked up momentum. At that time the research was primarily undertaken in Japan, Norway and in the UK, closely followed by the US and Sweden [25]. Japanese navigation buoys, with wave energy driving air turbines to charge batteries, have been around for a long time [22]. But Japan was also first to construct a full scale device. The 2.5 MW KAIMEI, using wave energy to drive air turbines through the OWC principle described later in Section 1.3.2, was deployed in 1978 and operated for a period of time before being dismantled [14].

For a general review on early stages of wave energy research in the world, see e.g. [14, 22, 25, 27]. A comprehensive review on wave energy extraction is given in [28], and an introduction to the field of the wave energy as a whole is given in [32]. In the following, a historical recapitulation will be given that focuses on the early works on wave energy that were undertaken in Sweden during the 70s and 80s. In the wave power community, Sweden is widely know for two inventions from this era, the IPS-buoy and the Swedish hose pump.

1.3.1 Wave energy in Sweden during the 70s and 80s

The incentive for the development of alternative energy sources in Sweden was strong in the 70s. The high oil price was one important factor and the Swedish government had ruled that Sweden was going to decrease its oil dependence. The incentive was further strengthened by the fact that the government had decided that by 2010 the nuclear power program was going to be terminated [25].

In 1976 a group for wave energy research was formed at Chalmers University of Technology in Gothenburg. They were assigned to do research on wave energy at first by Nämnden för Energiproduktionsforskning (NE) and later, after 1982, by Energiforskningsnämnden (Efn). The group was unique in that it constituted four different departments within the university encompassing skills in the areas of ships and hydro mechanics, water constructions, machine parts and electrical machines, as well as an external consulting agency, Technocean. The group was very productive and by 1987 they had produced 73 group reports on wave energy as well as 43 travel reports from various visits
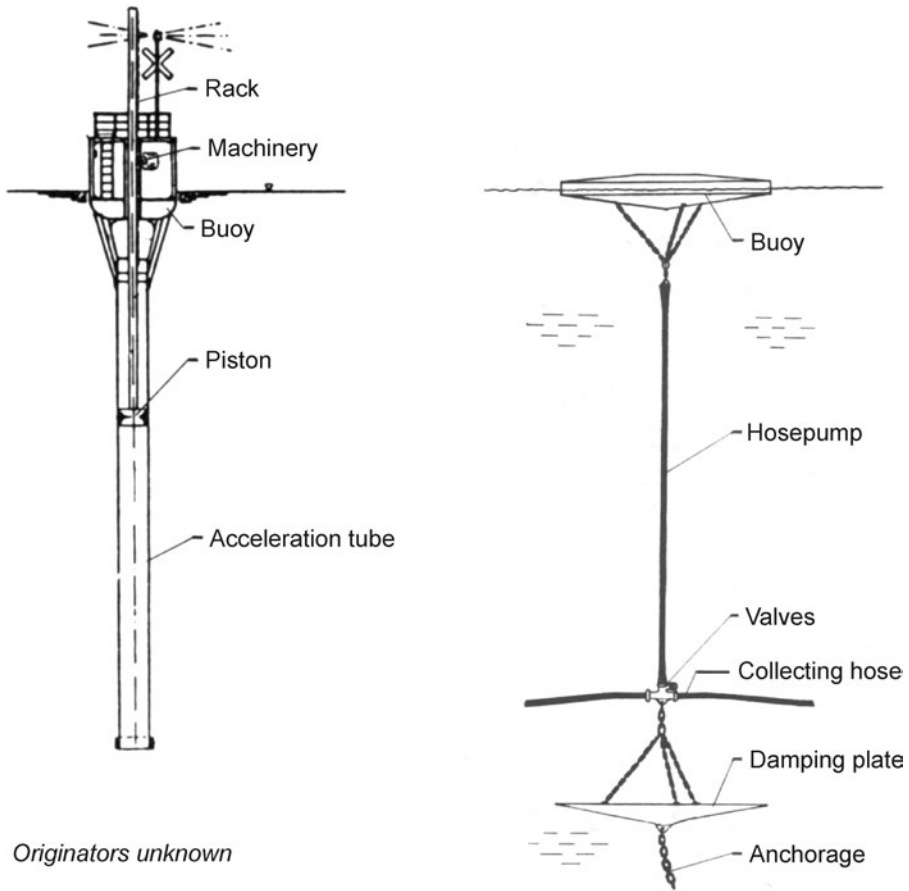
Figure 1.6: Conceptual drawings of the IPS buoy, left, and the Swedish hose pump, right [14].

to other groups connected to the subject. By this time SEK 35 million had been invested, half from the state and half from industry [14].

The Interproject Service (IPS) buoy

In 1974 a company called Interproject Service started studying wave power. They came up with a scheme for energy extraction in the shape of a buoy connected to a vertical hollow cylinder, called an acceleration tube, that moved in relative motion to a piston mechanically coupled to a generator. The idea was that as the buoy and tube move up and down in response to ocean waves, the water in the tube, which is connected to non-moving water at greater depth, would not move. This relative motion between the buoy and acceleration tube on the one hand, and the water in the tube on the other hand, was used to drive the piston. See Figure 1.6 for a conceptual drawing and Figure 1.7 for a picture of the device deployed at sea. During 1980 and 1981 sea trials were performed in the ocean outside Gothenburg, and during 1982-1983 in lake
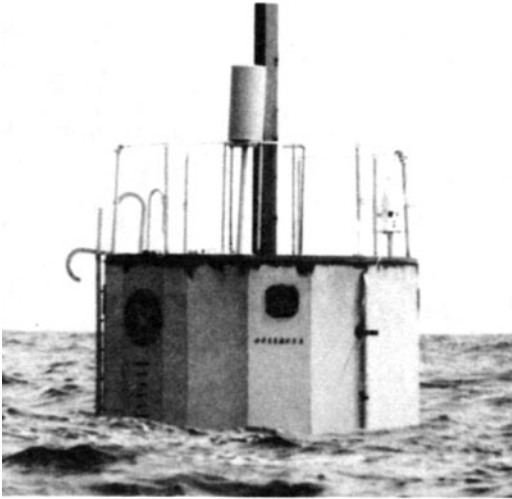
Figure 1.7: Photographs of the IPS-buoy, left, deployed at sea, and the Swedish hose pump as it is being deployed, right.

Lyngern. Mooring forces and energy production were part of what was measured on the nine tonne device, named Elskling.

The Swedish hose pump

Starting in 1980 Svenska Varv AB, later Celsius AB, pushed the development of a wave energy concept that has become known as the Swedish hose pump. The core of the technology was a steel reinforced rubber hose that had the property of decreasing in internal volume as it was stretched. When the hose was equipped with two check valves and connected in one end to a buoy and at the other end to the sea floor, a pumping action was achieved. The idea was to interconnect the combined flow of seawater from numerous buoys and lead the water to a turbine driving a generator [33]. See Figure 1.6 for a conceptual drawing and Figure 1.7 for a picture of the device as it is being deployed at sea. In the sea trials of the 80s, buoys of 4 – 5 m in diameter were used and the internal diameter of the rubber hoses was 0.2 m. At most three buys were coupled together and the water was fed in to land via a 600 m long hose.

1.3.2 General categories of wave energy converters

Many systems have been proposed that aim to divide the myriad of existing wave energy conversion concepts into a few general categories, see e.g. [24, 34, 35]. Here, a very basic division is presented where the converters are arranged into three categories: *wave activated bodies*, *overtopping devices*, and *oscillating water columns*. See Figure 1.8 for illustrations of the main principle of each category.
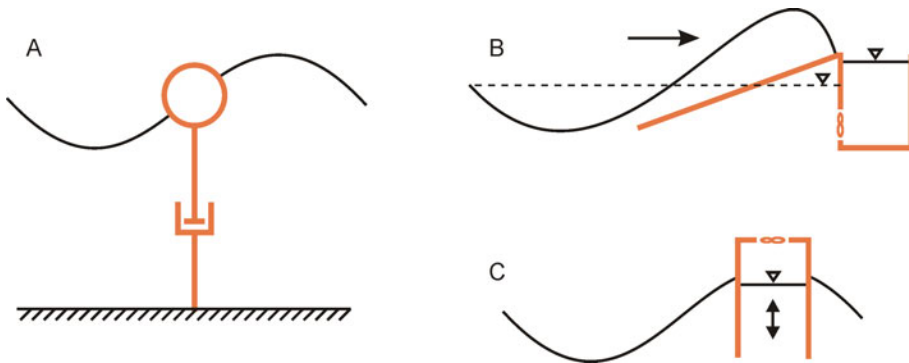
Figure 1.8: General categories of wave energy converters. A – Wave activated bodies. B – Overtopping devices. C – Oscillating water columns.

Wave activated bodies include all concepts where the motion of the ocean is transferred directly to the motion of the device, such as for example the Pelamis in Figure 1.9. A subcategory of wave activated bodies that is worth mentioning are *point absorbers*. The main characteristic of point absorbers is that they are small in the horizontal dimensions compared to the length of the waves from which they aim to capture energy. In other words, they take up a relatively small area of the ocean surface. The IPS buoy and the Swedish hose pump are both examples of point absorbers, and so is the concept presently researched at Uppsala University, the concept upon which this thesis is based.

Overtopping devices consist of a ramp or a tapered channel that forces the water of incoming waves to rise up and spill into a pool or reservoir. In this way, since the water surface of the reservoir is elevated relative to the ocean surface, the energy of the waves has been converted to potential energy. In a manner resembling hydro power plants the water is lead back into the ocean through a turbine. The Wave dragon in Figure 1.9 is an example that falls into this category.

Oscillating water columns (OWCs), have an oscillating pillar of water that pumps air through a turbine. This motion of the water pillar is achieved by e.g. taking a pipe and placing it partly submerged in the sea. The waves that roll against the pipe will make the internal water surface oscillate. This oscillation is normally used to pump air which drives a turbine. The KAIMEI mentioned in Section 1.3 functioned according to this principle, as does the Limpet OWC in Figure 1.9.

A useful expansion of the above categories is to add information on the location of the device. A typical set of definitions is to say that the device may be located onshore, near shore, or offshore. Onshore is exactly what it sounds like. Near shore are relatively shallow areas and offshore sites have depths were the waves are not affected by the bottom. Most energy can be found offshore since the waves have yet to lose energy in friction against the seabed.
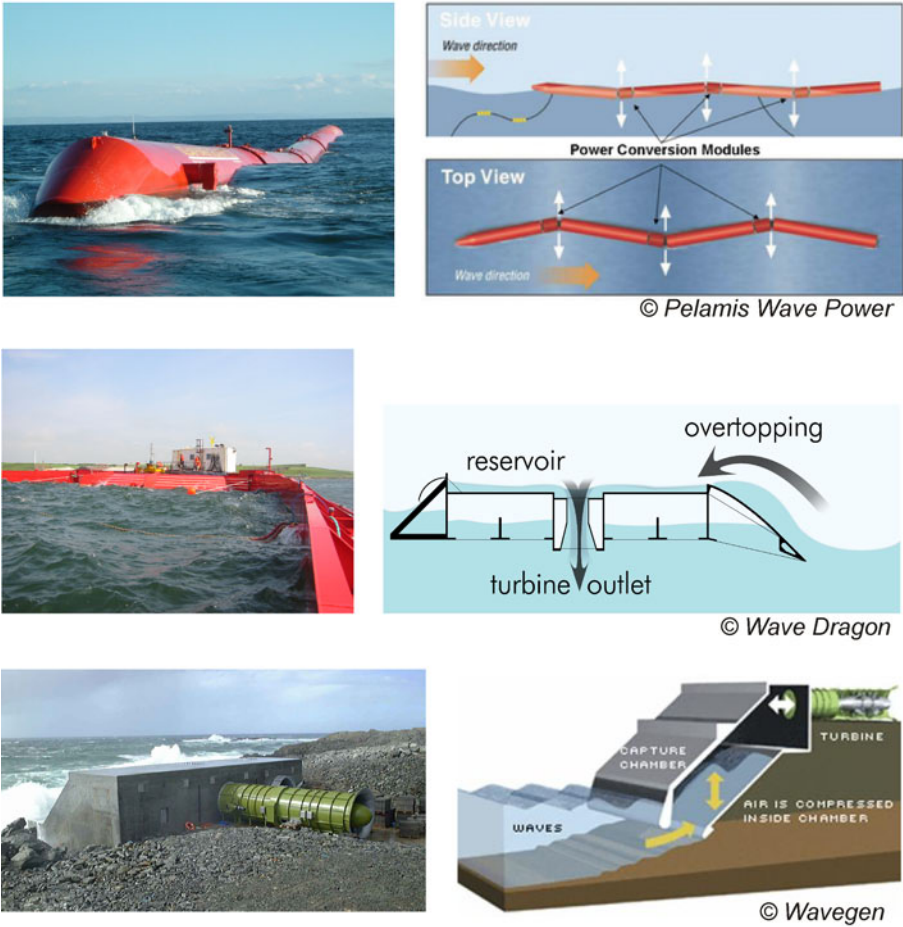
Figure 1.9: A sample of wave energy converters that have come far in development. Top: Pelamis. Middle: Wave dragon. Bottom: Limpet

1.3.3 Current wave power projects – a small sample

The general term for technologies that harness the energy of ocean waves is *wave energy converter (WEC)*. Today there are numerous wave power projects all around the world. The European Commission, in the framework of the *Co-ordinated Action on Renewable Energy* [36], presents an overview of ocean energy conversion in Europe with detailed descriptions of nine technologies in [37]. A comprehensive report on wave energy technologies around the world is given by the International Energy Agency in [38]. Some of the technologies are said to have reached commercial or close to commercial stage, some are performing small scale prototype testing of their technology, and still some technologies have not left the drawing board. Figure 1.9 presents a small sample of advanced WECs. The drawings to the right show the principles of operation, and to the left are pictures of the real devices. The basic operation of the sampled technologies can be described very shortly as follows:

The *Pelamis* is a device that falls into the wave activated bodies category. It is composed of semi-submerged cylinders linked by hinged joints. The waves induce motions in the joints which are resisted by hydraulic rams that pump a high-pressure fluid through hydraulic motors. The hydraulic motors drive electric generators. The *Wave dragon* is a large, floating, overtopping device that has arms which focus the waves up a ramp and into a water reservoir. The water is then led from the elevated reservoir back to the ocean, driving turbines in the process. *Limpet* is a traditional OWC located onshore on the island of Islay, off the west coast of Scotland. It was installed in year 2000 and produces power to the electric grid. For more information and updates on the technologies see [39–41].

1.4 Challenges

Some of the positive features of wave energy have been discussed above, and there are several more that all together seem to make wave energy an obvious choice as a source for renewable energy. Some of the features are: the relatively high utilization; the magnitude of the resource in the world; the slow variations in energy flux noted above when compared to wind power; the high energy density; that the energy is free in contrast to fuel based energy sources; installations are likely to have positive artificial reefing effects; and the degree to which wave energy would pollute the environment or add to greenhouse gas emissions is potentially insignificant compared to for example fossil fuels. If all of this is true then why is wave power, unlike the closely related wind power, hardly noticeable in the global energy system? The reason is that although research has been carried out since the 70s, similar to wind power, wave power has received less funding and fundamentally faces bigger challenges:

- Extreme forces: Although the energy density in waves is high on average as seen in Figure 1.5, it often reaches really great proportions during storms. Average power levels of storms may reach 50 times higher than the overall average. The consequences of this are large mechanical loads on the WECs, stress levels that need to be considered in the design stage. A standard practice in offshore constructions is to design the device so that it will survive the statistical 50 or 100 year wave. In general, however, it is not the extreme power levels that produce the energy, i.e. the revenue, for a WEC. Depending on the strategy used to avoid particularly high stress levels (requiring a device to hold for a 50 or 100 year wave) a heavy burden may be placed on the economy of the device. With this in mind, if possible, it is desirable to choose wave energy sites that naturally exhibit relatively small peak power levels in relation to the average power level.
- Fatigue: One year of waves may easily result in over a million load cycles on the WEC. Although storm load levels will be relatively few the total number will be significant and the WECs resistance to fatigue needs to be

carefully considered if the structure is intended to survive for years in the ocean.

- Corrosion: Metal objects are sensitive to corrosion in the saltwater environment. Its weakening affects on the durability of a structure, together with fatigue, can have dire consequences and some form of cathodic protection is often warranted.
- Working environment: The ocean is a difficult place to work. Unless it is a calm day it may be difficult to reach the WEC for the purpose of performing research, repairs, or maintenance. This plays a big role in the large development costs associated with wave energy.
- Intermittency: As noted previously in Section 1.2.1 the intermittency of modern renewable energy sources such as wind, wave and solar is an unwanted characteristic of these energy sources. It makes them practically incapable of constituting the sole electric energy sources used in a society, at least as long as there is no capability for electric energy storage large enough to store energy from the time it is supplied, at the whim of nature, to when it is needed in society, at the whim of humans.
- Marine life: Although biological life in the oceans may enjoy offshore structures to live on and around, they may hinder the operation of WECs. This problem is, however, likely to decrease with depth. In Scandinavia for example, depths greater than 65 m exhibit little but slimy bacteria [14].
- Societal conflicts: Fishermen, military, commercial ships and private boats all make use of the ocean. There is potential for conflicts of interest which can make the process of receiving permits for a wave energy installation very lengthy.
- Energy price: The cost of energy produced by the WECs has to be able to compete with other energy sources, and this is difficult for an immature technology. A few countries, Ireland, Portugal and the UK in particular, have implemented policies that promote the development and market introduction of ocean energy technologies [38]: In March 2007 the Irish government launched a target deployment of 500 MW of ocean energy by the year 2020. The Portuguese government has launched a feed-in tariff of up to 26€c per kWh supplied to the electric grid depending on the development stage of the technology. Portugal also has a pilot zone in the ocean where the process of gaining permits is simplified. The UK has a specific market-based energy policy directed toward the development of wave energy. Some specific instruments are capital grants, feed-in tariffs and regulatory and administrative rules.

Harnessing ocean energy is truly a challenge spanning over many areas of physics, e.g. hydrodynamics, mechanics, solid mechanics, fatigue, electromagnetism, electrochemistry, electronics, power electronics, marine biology etc. If all of the above challenges are to be met, then a holistic perspective is critical to the designers of wave energy converters. Wave energy is an unforgiving field of engineering, and a smart solution at one end of the path, from energy in ocean waves to electricity on the national grid, may create great challenges at the other end.

1.5 Wave energy research at Uppsala University

In awareness of the above challenges, the Swedish Centre for Renewable Electric Energy Conversion has devised a concept for wave energy conversion that hopes to result in a viable technology for harnessing the energy of ocean waves. Some of the most important principles that the concept rests upon are:

- Simple mechanics in order to minimize the need for maintenance and repairs.
- A system design that, when possible, chooses to have high electrical loads in place of high mechanical loads or complex mechanics.
- Keeping sensitive and expensive parts protected from direct contact with the high forces and the highly corrosive environment of the surface.
- Always prioritizing a holistic perspective where decisions are made keeping in mind the entire chain from capturing to supplying energy of good quality to the electric grid.

A wave energy converter, based on these principles, has been designed, constructed and installed offshore. This work, together with the studies performed on the device, is the main focus of this thesis.

2. Theory

This chapter begins with some theory on electricity and magnetism that describes the basic considerations that went into the design and operation of the generator. Furthermore, the theory used to perform the study of Paper IX, i.e. the design of a sensor for measurements of varying magnetic fields, is also presented.

The second part of this chapter gives an introduction to the linear theory of ocean waves. This leads to the fundamental equations commonly used in wave energy studies which describe ocean waves and sea states. This theory is necessary in all papers that to some degree require the study of sea states, i.e. Papers II – VIII and X – XIV.

The third and last part of the chapter presents theory for the calculation of statistical extreme waves, e.g. the highest wave occurring in 100 years. This theory was used in the writing of Paper X, which presents a detailed study of the wave climate off the Swedish west coast.

2.1 Electricity and magnetism

Regardless of the concept for wave energy conversion, somewhere along the line between capturing the energy of the waves and supplying the energy to the electric grid, a generator is needed in order to convert the mechanical energy into electrical energy. In the following sections theory on generators and circuits is presented that provides understanding of the function of the generator described in Chapter 4 and the air gap measurements described in Chapter 5. For further readings on electromagnetism, magnetism and magnetic materials see [42, 43]. For definitions of the different parts of the generator discussed here, see Figure 3.2 in Chapter 3.

2.1.1 Fundamental entities

The *magnetic flux density*, **B**, also called *magnetic induction field* or simply the *B-field*, is given by:

$$\mathbf{B} = \mu_0(\mathbf{H} + \mathbf{M}), \tag{2.1}$$

where $\mu_0 = 4\pi \cdot 10^{-7}$ is the permeability of free space, **M** is the *magnetization*, and **H** is the *magnetizing field*, also called the *magnetic field*. The magnetization, **M**, is a material specific attribute which describes how a material

responds to an externally applied magnetizing field, **H**. Some materials, e.g. iron, have the intrinsic property that if subjected to an external magnetizing field, **H**, the internal microscopic magnetic dipoles of the material will align themselves with the externally applied field, thus strengthening the overall magnetic flux density in accordance with Eq. (2.1). The magnetization, **M**, is defined as the magnetic moment per unit volume. In situations where the magnetization can be approximated as linearly dependent on **H**, the above equation can be given as:

$$\mathbf{B} = \mu_0 \mu_r \mathbf{H}, \tag{2.2}$$

where μ_r is the material specific *relative permeability*.

The *magnetic flux*, Φ, is given by:

$$\Phi = \int \mathbf{B} \bullet \hat{n} \, dA, \tag{2.3}$$

where A is the area through which the flux passes and $\hat{n}$ is the outward normal vector of the area. From Eq. (2.2) it is apparent that the flux through a material is highly dependent on its relative permeability, μ_r.

2.1.2 Maxwell's equations

The fundamental theory of electromagnetism, which gives the relationship between electric and magnetic fields, is described by Maxwell's equations:

$$\nabla \times \mathbf{E} = -\frac{\partial \mathbf{B}}{\partial t} \tag{2.4}$$

$$\nabla \times \mathbf{H} = \mathbf{J}_f + \frac{\partial \mathbf{D}}{\partial t} \tag{2.5}$$

$$\nabla \bullet \mathbf{D} = \rho_f \tag{2.6}$$

$$\nabla \bullet \mathbf{B} = 0 \tag{2.7}$$

B and **H** are the magnetic flux density and magnetizing field described above, **E** is the electric field, **D** is the electric displacement field, ρ_f is the free charge density, and $\mathbf{J}_f$ is the free current density. The first equation, Eq. (2.4), is called Faradays law and in the specific case of a generator it describes how currents are induced by changing magnetic fields. The second equation, Eq. (2.5), is called Ampere's law and describes how currents create magnetic fields. The third equation, Eq. (2.6), called Gauss's law, describes how electric fields are created from electric charges. Finally, the fourth equation, Eq. (2.7), describes
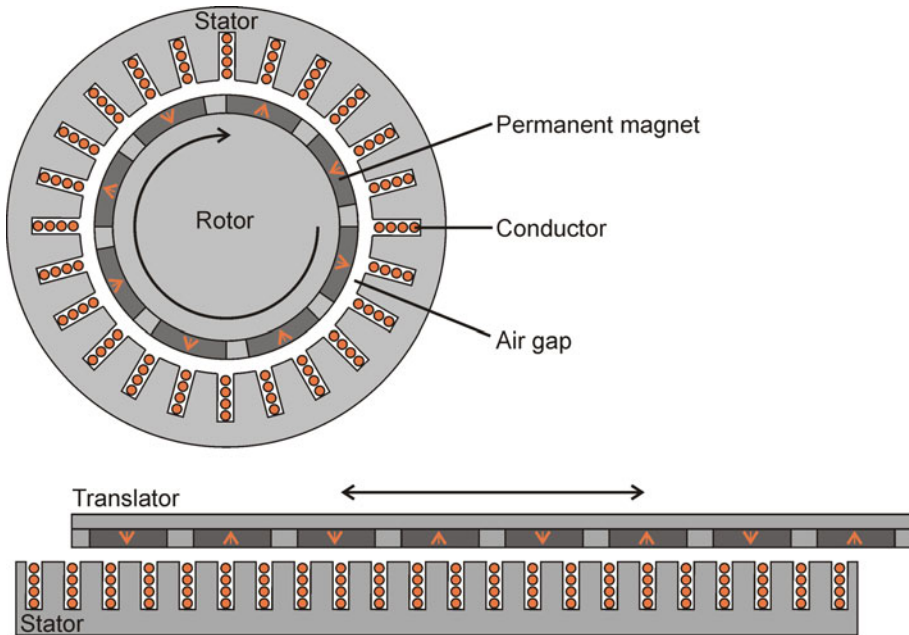
Figure 2.1: The basic components of a round and a linear permanent magnet generator. Permanent magnets are mounted on the moving rotor/translator. The stator holds cables in which voltages are induced from the movement of the rotor/translator. The air gap separates the static and moving parts.

the non-existence of magnetic monopoles, i.e. that magnetic field lines always form closed paths.

2.1.3 Magnetic materials

The magnetic materials are carefully chosen in the design of a generator. Because ferromagnetic materials in general have a high relative permeability, they are used to control the path of the magnetic flux, the importance of which will be described further in Section 2.1.6. These ferromagnetic materials, which are used in the stators of generators, are an example of soft magnetic materials. In permanent magnet generators, the magnets themselves are composed of what is called hard magnetic materials and they have properties that are very different from that of the soft magnetic materials. Figure 2.1 shows the basic components of a round and a linear permanent magnet generator. The properties of a magnetic material is best illustrated in a B-H diagram, see Figure 2.2.

Starting from a non-magnetic material, the origin in Figure 2.2, the B-field in the material follows the dotted path as and external magnetic field, $\mathbf{H}$, is applied and increased in strength. A large part of the increase in B-field is attributed to the magnetization, $\mathbf{M}$, which is dependent on $\mathbf{H}$ and increases with it in a non-linear fashion. Eventually, however, all of the microscopic magnetic dipoles in the material are aligned with the externally applied field
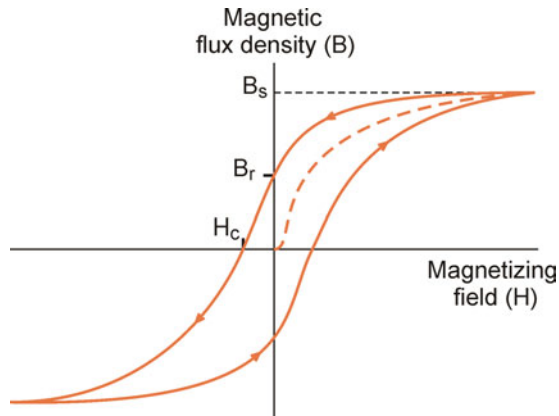
Figure 2.2: A B-H diagram showing saturation (B_s), remanent induction flux density (B_r), coercive field strength (H_c) and a trail up from the unmagnetized material.
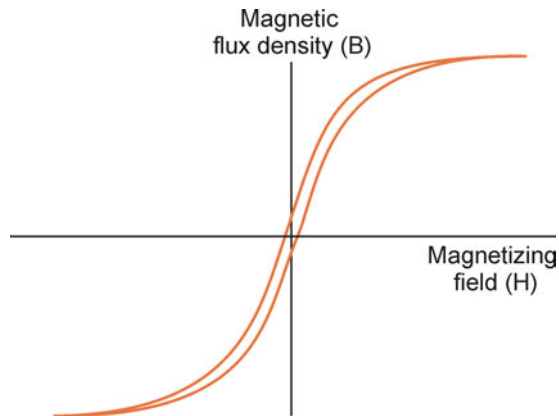

Figure 2.3: A typical B-H curve for a soft magnetic material, a small area and a large saturation flux density.

and the magnetization has reached a constant level. The material is saturated, B_s. Even if the magnetizing field decreases to zero from this point, some of the magnetic dipoles will not turn back to point in their original directions but will remain in their new positions. The material will thus remain magnetized despite the absence of **H** and this is called the *remanent induction*, B_r. In order to push the B-field back to zero from this point, the external field has to be applied in the opposite direction. The strength of the magnetizing field needed to do this is called the *coercive field strength*, H_c. This process can be repeated in both directions and the loop created in this way, see Figure 2.2, is called the *hysteresis loop*. The area of the hysteresis loop corresponds to the energy that is lost, as heat, in the process of changing the directions of the magnetic dipoles of the material.

Characteristic of soft magnetic material is that the area of its hysteresis loop, and thus its heat losses, is small and that the saturation flux density, B_s, is very high, see Figure 2.3. The material in a generator generating electricity
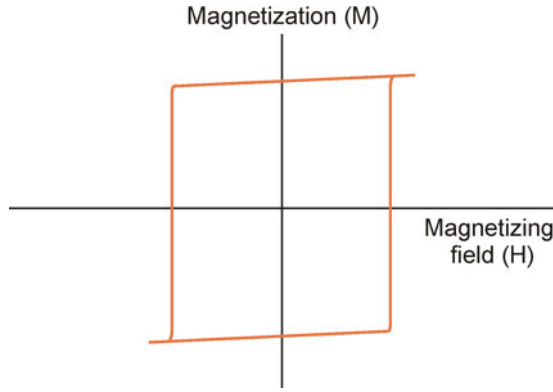
Figure 2.4: A M-H curve for a hard magnetic material. Once magnetized the magnetization varies little with the external H-field.

with a frequency of 50 Hz will go through 50 hysteresis cycles per second, thus potentially leading to large heat losses. Hence a small hysteresis loop is desired, and since high flux is also desired to induce a high voltage, see Sections 2.1.6 and 4.1.1, so is a high relative permeability.

The permanent magnets used in the wave energy converter constructed as a part of this thesis are made of hard magnetic material. As such they have a very high coercive field strength, H_c, a high remanent induction, B_r, and a magnetization which varies very little during normal working conditions of the generator i.e. it is almost constant in regard to the external H-field, see Figure 2.4. A magnet of this sort has the potential to create high levels of flux in the generator and will not become demagnetized easily.

2.1.4 Generator losses

The most important energy losses in a generator can be divided into three parts: mechanical, iron and copper losses. Other sources of energy loss, such as ventilation losses and losses due to eddy currents in the magnets are considered small enough to neglect here. Mechanical losses are due to the friction between various moving mechanical parts. These losses have not been measured on the studied wave energy converter and all simulations and measurements have ignored them.

Iron losses are associated with the varying magnetic fields in the stator and, in the case of linear PM generators, in the magnet back iron. The losses can be attributed to three different frequency dependent sources; the hysteresis, the eddy currents, and excess losses:

$$p_{Fe} = k_{hysteresis}B_{max}^2 f + k_{eddy}\left(B_{max}f\right)^2 + k_{excess}\left(B_{max}f\right)^{3/2}, \qquad (2.8)$$

where $k_{hysteresis}$, k_{eddy} and k_{excess} are material and geometry dependent constants, B_{max} is the amplitude of the varying magnetic flux density, and f is
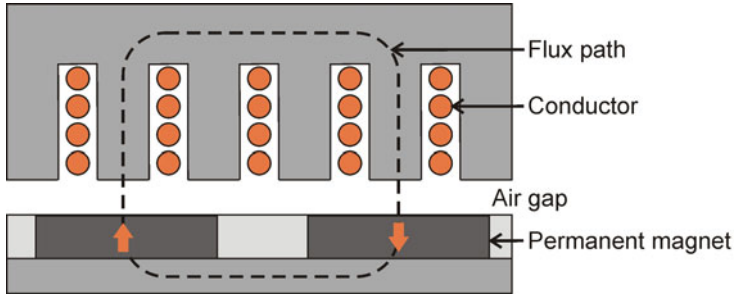
Figure 2.5: Magnetic circuit.

the frequency of the varying flux. The first part of the equation is due to the previously mentioned *hysteresis*, the energy lost in the process of changing the directions of the magnetic dipoles. The second source of iron losses represents losses due to *eddy currents*. These are current loops in the iron that are induced by changing flux densities in the iron, e.g. due to the passing of permanent magnets on a translator. The circulating currents induce a magnetic flux density themselves that opposes the changing flux density resulting from the external source. This action and reaction is referred to as *Lenz's law*. The larger the area of the eddy current loops, the larger the losses and because of this the stators in generators are not made of a solid block of iron, but rather a stack of very thin iron plates isolated from each other. The third source of iron losses are called *excess losses*. These represent losses due to changes in the magnetic materials other than the hysteresis or eddy current losses.

Copper losses are associated with the current carrying cable windings in the generator. There are two types of copper losses. The first are losses due to eddy currents. However, because of the relatively low frequency of the magnetic flux of the considered generator, and the many strands in the used cables, these losses have been ignored throughout this thesis. The second type of copper loss can be given directly for macroscopic conductors and is given by:

$$P_{Cu} = RI^2,\tag{2.9}$$

where R is the resistance of the cable windings and I is the current.

2.1.5   Flux density in the air gap

The sensors described in Chapter 5, and that Paper IX is based on, measures the *magnetic flux density* in the air gap of a generator. A simplified theoretical derivation of the field can be found by studying the magnetic circuit of the generator, see Figure 2.5. Furthermore, some general operating principles of a permanent magnet generator, such as the one designed and constructed as a part of this thesis work, can be understood by studying its magnetic circuit.

For the considered magnetic circuit, Ampère's law, Eq. (2.5), can be written as:

34

$$\oint \mathbf{H}d\mathbf{l} = \int \mathbf{H}_{Pm}d\mathbf{l}_{Pm} + \int \mathbf{H}_{Air}d\mathbf{l}_{Air} + \int \mathbf{H}_{Fe}d\mathbf{l}_{Fe} = NI, \qquad (2.10)$$

where the circuit is divided into three parts corresponding to the three materials in the magnetic flux path: permanent magnet – Pm, air gap – Air, and iron – Fe. N is the enclosed number of current carrying cables and I is the current. We now consider the static case where we do not have an induced current in the conductors, i.e. $NI = 0$. Furthermore we assume that the iron is not saturated and that there is no leakage flux, i.e. $\Phi = constant$, an assumption which is fair if the air gap is small and the permeability of the iron is large. We also assume that the magnetization, $\mathbf{M}$, in the iron is linearly dependent on the magnetizing field, $\mathbf{H}$, as in Eq. (2.2), and that the magnetization in the magnet is constant, see hard magnetic materials in Section 2.1.3 and Figure 2.4. Recalling the definition of the magnetic flux density, Eq. (2.2), we can now rewrite Eq. (2.10) as:

$$\left(\frac{B_{Pm} - B_r}{\mu_0}\right) l_{Pm} + \frac{B_{Air}}{\mu_0} l_{Air} + \frac{B_{Fe}}{\mu_0 \mu_{Fe}} l_{Fe} = 0, \qquad (2.11)$$

where we, according to Eq. (2.1) and Figures 2.2 and 2.4 have made the approximation $M = B_r/\mu_0$. Recalling Eq. (2.3), and because the magnetic flux, Φ, is constant in all parts of the circuit, the following holds:

$$B_{Pm} = \frac{B_{Air} A_{Air}}{A_{Pm}}, \quad B_{Fe} = \frac{B_{Air} A_{Air}}{A_{Fe}}. \qquad (2.12)$$

The sought air gap magnetic flux density can now be expressed as:

$$B_{Air} = \frac{B_r l_{Pm}}{l_{air} + \frac{A_{Air}}{A_{Pm}} l_{Pm} + \frac{A_{Air}}{A_{Fe} \mu_{Fe}} l_{Fe}}. \qquad (2.13)$$

2.1.6 Fundamental equations

A few more equations will be helpful in describing the material presented in the following chapters. Faraday's law, Eq. (2.4), is often given in a more simplified form:

$$V = -N \frac{d\Phi}{dt}. \qquad (2.14)$$

Here Faraday's law states that the induced voltage, V, in a coil equals the number of coil turns, N, times the change in magnetic flux over time. The flux that contributes to this induced voltage is that which encloses the coil. Flux will always prefer the easiest path through a magnetic circuit, i.e. the path with the lowest *reluctance*. Materials with high permeability exhibit a low reluctance to flux, and because of this soft magnetic materials are often used to control

the path of the flux so that it encloses the coil. Through this simple equation many fundamental aspects of generator operation can be understood. For example, if the goal is to achieve a high induced voltage there are at least three ways to go about it; a large number of coil turns, large flux in the magnetic circuit, or a fast change of the flux over time e.g. a fast motion of the rotor or translator.

The operating principle of the air gap sensor in Chapter 5 functions according to Faraday's law, Eq. (2.14), but is best described by the Lorentz force equation. This equation describes the force on an electrically charged particle passing through electric and magnetic fields. An expression can be derived from the Lorentz force equation which describes the voltage induced in a straight conductor passing through a B-field with its length perpendicular to the motion:

$$V = \int (\mathbf{v} \times \mathbf{B}) \bullet d\mathbf{l}, \quad (2.15)$$

where $\mathbf{v}$ is the speed and the integral is calculated over the length of the conductor. The air gap sensor is easily seen as being made up of many straight conductors, see Figure 5.2.

In a linear isotropic conducting media the free current of Maxwell's second equation, Eq. (2.5), can be related to the electric field through the conductivity, σ, according to:

$$\mathbf{J}_f = \sigma \mathbf{E}. \quad (2.16)$$

The conductivity is material specific and the inverse of the conductivity is the resistivity. The above equation is the equivalent of Ohm's law for electric circuits.

2.1.7 Noise in electric circuits

All electronic circuits add noise to the signals passing through them. Depending on the magnitude of the noise compared the signal, this may or may not represent a problem. A noise source is generally described by its power density spectrum, PDS, denoted $S(f)$. The total noise voltage is given by:

$$V_{noise} = \sqrt{\int_{f_1}^{f_2} S(f) df}, \quad (2.17)$$

where the frequency, f, is integrated over the bandwidth of the circuit.

Thermal noise, or white noise, is produced by the temperature dependent movement of atoms and is present in all circuits that have a resistance. It has equal power density at all frequencies and is consequently characterized by a constant PDS:

$$S_{white}(f) = 4k_BTR, \tag{2.18}$$

where k_B is Boltzmann's constant, T the absolute temperature, and R the resistance.

2.2   Linear theory of ocean waves

For a thorough description of ocean wave theory see [23].

The linear theory for ocean waves is based on two fundamental equations, the *continuity equation*:

$$\frac{\partial \rho}{\partial t} + \nabla \bullet (\rho \bar{v}) = 0, \tag{2.19}$$

and *Navier-Stokes equation*:

$$\frac{\partial \bar{v}}{\partial t} + (\bar{v} \cdot \nabla) \bar{v} = -\frac{1}{\rho} \nabla p + \nu \nabla^2 \bar{v} + \frac{1}{\rho} \bar{f}. \tag{2.20}$$

ρ is the density of a fluid, $\bar{v}$ is its velocity vector, ν its kinematic viscosity, and $\bar{f}$ is an external force on the fluid.

The continuity equation, or the conservation of mass, basically states that the change in density of a fluid within a volume equals the flow of mass into or out of the volume.

Navier-Stokes equation is basically Newtons second law stating that force equals mass times acceleration, $F = ma$. The left side of the equation represents the acceleration of the fluid, and the right side represents the force per mass where the three components represent forces associated with the pressure gradient, the viscosity, and external forces.

In the first step these equations are subjected to five assumptions:

1. Incompressible fluid. $\rho = constant$.

2. Irrotational fluid. $\nabla \times \bar{v} = 0$.

3. Viscosity can be neglected. $\nu = 0$.

4. Gravity, where g is the gravitational constant, is the only external force. $\bar{f} = -g\rho\hat{z}$.

5. Small velocity. Velocity terms of second order, v^2, and higher can be neglected.
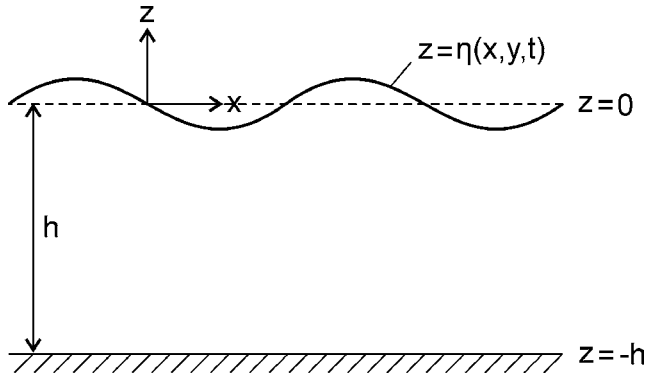
Figure 2.6: Definitions for surface waves.

If a *velocity potential*, ϕ, is defined so that $\bar{v} = \nabla\phi$ then with the aid of the assumptions the continuity equation reduces to Laplace's equation:

$$\nabla^2\phi = 0. \tag{2.21}$$

The Navier-Stokes equation, subjected to the assumptions, reduces to the linearized Bernoulli's equation:

$$\frac{\partial\phi}{\partial t} + \frac{1}{\rho}p + gz = b, \tag{2.22}$$

where b is a constant.

Boundary conditions are required in order to solve Laplace's equation. Figure 2.6 presents definitions used in this special case of ocean waves. p is pressure and p_0 is the atmospheric pressure at sea level, h is the water depth, $z = 0$ is the mean water level or the water level at calm sea when there are no waves. The free surface elevation, η, will be a function of surface coordinates and time, $\eta(x,y,t)$. A McLaurin expansion of the vertical speed of the water surface yields:

$$\frac{\partial\eta}{\partial t} = v_z\Big|_{z=\eta} = \frac{\partial\phi}{\partial z}\Big|_{z=\eta} = \frac{\partial\phi}{\partial z}\Big|_{z=0} + \frac{\partial^2\phi}{\partial z^2}\Big|_{z=0} \cdot \eta + \frac{1}{2}\frac{\partial^3\phi}{\partial z^3}\Big|_{z=0} \cdot \eta^2 + \dots. \tag{2.23}$$

If the values of η are small then the higher order terms can be ignored. This leaves us with the linear approximation of the sea surface movement, hence the *linear theory of ocean waves*:

$$\frac{\partial\eta}{\partial t} = \frac{\partial\phi}{\partial z}\Big|_{z=0}. \tag{2.24}$$

Since there is no vertical movement of the water at the seabed, the *sea floor boundary condition* is acquired:

$$\frac{\partial \phi}{\partial z}\bigg|_{z=-h} = 0. \tag{2.25}$$

Bernoulli's equation for the surface becomes:

$$\frac{\partial \phi}{\partial t}\bigg|_{z=\eta} + \frac{p_0}{\rho} - b = -g\eta \Rightarrow [\text{for small } \eta] \Rightarrow \frac{\partial \phi}{\partial t}\bigg|_{z=0} + \frac{p_0}{\rho} - b = -g\eta. \tag{2.26}$$

At calm sea, i.e. no surface motion, we find that:

$$\frac{\partial \phi}{\partial t} = \eta = 0 \Rightarrow b = \frac{p_0}{\rho} \Rightarrow \frac{\partial \phi}{\partial t}\bigg|_{z=0} = -g\eta,$$

and we thus have:

$$\eta = -\frac{1}{g}\frac{\partial \phi}{\partial t}\bigg|_{z=0}, \tag{2.27}$$

which, in combination with Eq. (2.24), yields the *surface boundary condition*:

$$\left[\frac{\partial^2 \phi}{\partial t^2} + g\frac{\partial \phi}{\partial z}\right]_{z=0} = 0. \tag{2.28}$$

Now, if the Laplace's equation, Eq. (2.21), is solved together with the boundary conditions, Eqs. (2.25) and (2.28), and with Eq. (2.27), then the following particular solutions can be found:

$$\phi = \frac{gH}{2\omega}e^{kz}\sin(kx - \omega t) \tag{2.29}$$

$$\eta = \frac{H}{2}\cos(kx - \omega t) \tag{2.30}$$

$$\omega^2 = gk\tanh(kh) \tag{2.31}$$

Eq. (2.29) is a solution to the Laplace equation, Eq. (2.30) is the vertical movement of the surface, and Eq. (2.31) is known as the *dispersion relation*. $k = 2\pi/\lambda$ is called the wave number, λ is the wave length, $\omega = 2\pi f$ is the angular frequency, $f = 1/T$ is frequency, T is the wave period, g is the gravitational constant, and H is the wave height defined as the vertical distance from crest to trough.
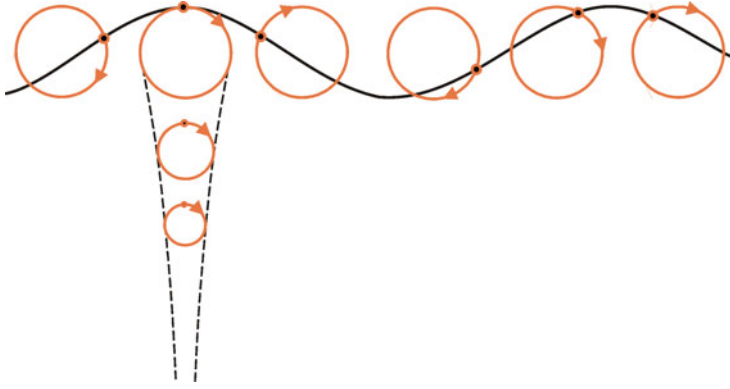
Figure 2.7: The water in waves, at deep water, moves is circular orbits and the motion decreases exponentially with depth.

2.2.1 Harmonic waves on deep water

In order to simplify theoretical treatment it is common to consider waves only on very deep water where the waves are not affected by the seabed. In such cases the dispersion relation reduces to:

$$\omega^2 = gk. \tag{2.32}$$

The motion of the water, or "water particles", in a wave and how it varies with depth can now be derived using the deep water dispersion relation and by recalling the definition of the velocity potential, $\bar{v} = \nabla\phi$:

$$\bar{v} = \nabla\phi = \frac{\omega H}{2} e^{kz} \left(\cos\left(kx - \omega t\right), 0, \sin\left(kx - \omega t\right)\right). \tag{2.33}$$

The above equation states that water in waves moves in circular orbits and that the motion decreases exponentially with depth as illustrated in Figure 2.7.

The deep water dispersion relation can also be used to find a relationship between the wave length and the period of a wave. The speed, c, of a harmonic wave is:

$$c \equiv \frac{\lambda}{T} = \frac{\omega}{k} = [\text{Deep water}] = \frac{g}{\omega} = \frac{g}{2\pi}T \approx 1.56T. \tag{2.34}$$

The speed of harmonic ocean waves are thus linearly dependent on the period. A consequence of this is that bigger waves, which in general have a longer period, travel faster then smaller waves as described earlier in Section 1.1.

Real ocean waves are not harmonic but are made up of a combination, or group, of harmonic components. The speed with which a group of waves travel, called the group speed c_g, is defined as:

$$c_g \equiv \frac{\partial\omega}{\partial k}, \tag{2.35}$$

which for deep water reduces to:

$$c_g \equiv \frac{\partial \omega}{\partial k} = [\text{Deep water}] = \frac{\partial}{\partial k}\sqrt{gk} = \frac{c}{2}. \qquad (2.36)$$

The group speed is also the speed with which the energy in waves travel across the ocean.

2.2.2   Energy flux of harmonic waves

The energy flux, [W/m^2], is described by pressure times velocity. If we integrate over the depth we will be left with an expression for the flux per meter of wave crest:

$$J = \int_{-\infty}^{0} p \cdot v_x dz \quad [\text{W/m}], \qquad (2.37)$$

where the integral goes from the surface down to infinitely deep water. The pressure, p, if given by Bernoulli's equation, Eq. (2.22), and the speed from Eq. (2.29), resulting in:

$$J = \frac{\rho g^2}{32\pi} T H^2. \qquad (2.38)$$

Usually, the constant $\rho g^2 / 32\pi$ is denoted k, not to be confused with the wave number defined earlier.

If the group speed c_g, Eq. (2.35), and the total energy density E_{tot}, Eq. (2.42) below, is known, then the energy flux is also described by:

$$J = E_{tot} c_g. \qquad (2.39)$$

2.2.3   Energy density of harmonic waves

The average potential energy in a wave per unit area of ocean surface is:

$$E_p = \frac{1}{S}\int g \cdot \frac{1}{2}\eta \cdot \rho \eta dS = \frac{H^2}{16}\rho g \quad [\text{J/m}^2], \qquad (2.40)$$

where S is the surface area over which the integration is performed. This is basically the know formula for potential energy, $E_p = mgh$, where $\rho \eta dS = dm$ is the mass, and $\eta/2$ is the distance from the center of mass to the calm surface level.

The average kinetic energy below a square meter of ocean surface is:

$$E_k = \frac{1}{S}\int \frac{1}{2}v^2 \rho dV = \frac{H^2}{16}\rho g, \qquad (2.41)$$

where v is the speed calculated from the velocity potential, Eq. (2.29), and V is volume. The equation is basically the formula for kinetic energy known from mechanics: $E_k = mv^2/2$.

The average total energy below a square meter of ocean surface is thus:

$$E_{tot} = E_p + E_k = \frac{H^2}{8}\rho g \approx 1.26 \cdot 10^3 H^2 \quad \left[\text{J/m}^2\right]. \tag{2.42}$$

Because the kinetic energy is equal to the potential energy, the average total energy can also be written as:

$$E_{tot} = \frac{\rho g}{S} \int \eta^2 dS, \tag{2.43}$$

which means that the energy per unit area of ocean surface is proportional to the variance of the sea-surface displacement. Now, consider a point on the ocean surface, its vertical position given by:

$$\zeta(t) = \eta(x_0, y_0, t). \tag{2.44}$$

The *variance* of ζ around the calm surface level, $\eta = 0$, becomes:

$$\langle \zeta(t)^2 \rangle = \frac{1}{T_0} \int_0^{T_0} \zeta^2(t) dt = \frac{1}{T_0} \int_0^{T_0} \frac{H^2}{4} \cos^2(\omega t) dt = \frac{H^2}{8}, \tag{2.45}$$

and the average total energy density, Eq. (2.42), can thus also be written as:

$$E_{tot} = \rho g \frac{H^2}{8} = \rho g \langle \zeta(t)^2 \rangle. \tag{2.46}$$

The space average of Eq. (2.43) is thus given as a time average instead. This will allow the description of ocean waves by means of spectra.

2.2.4   Real ocean waves on deep water

Most ocean waves, not being harmonic but possible to consider as a combination of harmonic components, can be described by a Fourier series. In discrete complex notation the sea surface displacement is given by:

$$\zeta(t) = \sum_{n=-\infty}^{\infty} z_n e^{in\omega_0 t}, \tag{2.47}$$

where

$$z_n = \frac{1}{T_0} \int_{-T_0/2}^{T_0/2} \zeta(t) e^{in\omega_0 t} dt, \tag{2.48}$$
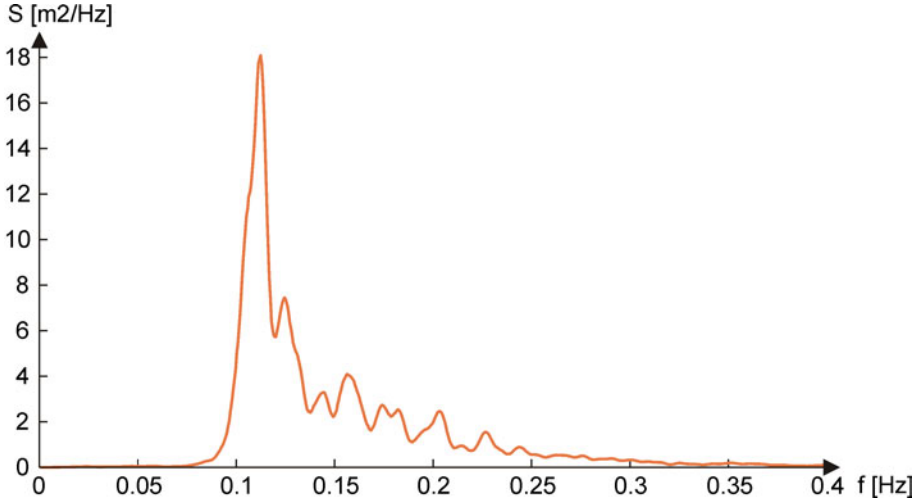
Figure 2.8: Example wave spectra from the Lysekil research site. The spectra contains information on the significant wave height, H_{m0}, which is 3.1 m, the energy period, T_{m0-1}, which is 7.7 s, and the energy flux, J, which is 35 kW/m.

are the coefficients, and ω_0 is the fundamental frequency. Taking the variance of Eq. (2.47) around $\eta = \zeta = 0$ yields:

$$\langle \zeta(t)^2 \rangle = \langle \zeta \zeta^* \rangle = \sum_{n=0}^{\infty} 2 z_n z_n^*, \qquad (2.49)$$

which represents a transfer from time to frequency-space. Now, a *spectral density function*, or *wave spectrum*, is defined:

$$S(n\omega_0)\,\omega_0 = 2 z_n z_n^*, \qquad (2.50)$$

so that the variance, in discrete and continuous from, can be written as:

$$\langle \zeta(t)^2 \rangle = \sum_{n=0}^{\infty} S(n\omega_0)\,\omega_0, \quad \int_0^{\infty} S(\omega) d\omega. \qquad (2.51)$$

Furthermore, we define *spectral moments*, in discrete and continuous form, as:

$$m_j = 2 f_0^j \sum_{n=0}^{\infty} n^j z_n z_n^*, \quad m_n = 2\pi \int_0^{\infty} f^n S(f) df. \qquad (2.52)$$

Now, the average total energy of Eqs. (2.42) and (2.46), can be given as a constant times the integral of the spectral density function, see Figure 2.8, and in terms of the zeroth spectral moment:

$$E_{tot} = \rho g \langle \zeta(t)^2 \rangle = \rho g \int_0^\infty S(\omega) d\omega = \rho g m_0. \qquad (2.53)$$

From spectral analysis the *significant wave height*, H_{m0} or sometimes denoted H_s, is defined as:

$$H_{m0} = 4\sqrt{m_0}, \qquad (2.54)$$

and the *energy period*, T_e or T_{m0-1}, is defined as:

$$T_{m0-1} = \frac{m_{-1}}{m_0}. \qquad (2.55)$$

In an earlier definition of significant wave height, $H_{1/3}$, it was defined as the average height of the 1/3 highest waves during a chosen period of time. The definition of H_{m0}, coming from spectral analysis of a chosen sea state, was defined to be approximately the same as $H_{1/3}$.

As noted in Section 2.2.2 the energy flux is given by $J = E_{tot} c_g$ which, using the derived formula of E_{tot} for real ocean waves, Eq. (2.53), gives the energy flux for real waves:

$$J = \frac{\rho g^2}{64\pi} T_{m0-1} H_{m0}^2 \quad [\text{W/m}] \quad \approx 500 \, T_{m0-1} H_{m0}^2 \quad [\text{W/m}], \qquad (2.56)$$

which is half of the energy flux of a harmonic wave of height H. It must be remembered, however, that H and H_{m0} cannot be compared directly.

Thus, if the spectral density function, also known as the wave spectra, is known for a certain cite, then a lot of information, such as the significant wave height, the energy period, and the energy flux, is also known. There are various methods of attaining wave spectra, for example wave measuring buoys, satellite altimeter measurements, and hindcast methods where computer models simulate wave spectra from measured wind data. There are, however, also a number of empirical spectra, based on various assumptions, that have been developed from experiments. The number of input parameters needed in these spectra, as well as their complexity and reliability, varies. Two common spectra with few input parameters are the *Pierson-Moskowitz* spectra which only requires the input of wind speed at 19.5 m above sea level, and the *JONSWAP* spectra which requires the input of wind speed ten meters above sea level as well as the *fetch*, i.e. the distance of ocean over which the wind has blown.

The derivation of wave spectra from buoy measurements, as well as the calculation of sea state specific parameters from wave spectra, such as the energy flux, has been an important part of many of the papers, i.e. Papers II – VIII and X – XIV.

2.3 Extreme waves

Knowledge of the extreme waves that may occur at a particular site is of great importance in the design of offshore structures. These so called design waves are used to estimate the forces that a structure is required to withstand without being damaged. The design wave is often chosen to be the highest singular wave that occurs once per 50 or 100 years, and because there are no, or very few, recorded data series of these lengths, the work of finding design waves is a statistical process based on measured or modeled wave data from much shorter time periods. More information on the calculation of extreme waves can be found in [44–46], and a description of extreme waves heights in the North Atlantic is given in [47].

2.3.1 Data selection

The data used in extreme wave analysis is usually recorded or modeled values of significant wave height, H_{m0}. It is also possible to use real time series of waves, but this is more calculation intensive and sufficiently long time series for a good analysis are rare. In the following it will be assumed that the available data is in the form of significant wave heights.

Good data selection is the foundation for good extreme wave analysis and in general it is not a good approach to use all of the available wave height data. For good statistical analysis, the data should be *stationary* and *uncorrelated*. This means that the values of H_{m0} should not be dependent on cyclical trends such as seasonal variations, and they should not be to close to each other in time. The recommended method for choosing a good data set for the analysis is the *Peaks Over Threshold* method (*POT*) [44]. Other methods are the *Initial Distribution* method, and the *Annual Maxima* method, which are described in [44]. The POT method considers local maxima, i.e. peak storm values of H_{m0}, above some chosen threshold wave height, $H_{threshold}$. The value of $H_{threshold}$ should be chosen to achieve the best possible results (see Q-Q plots and goodness of fit tests below). Choosing peaks over some threshold in this way removes most of the non-stationary aspects of the data. In order to make the data uncorrelated a restriction is placed on the minimum time allowed between two subsequent values of H_{m0}. Between two and four days is recommended.

2.3.2 Probability distributions

Following the above step, which results in a data set of significant wave heights of relatively high amplitudes, these data are to be fitted to a *cumulative distribution function* (*CDF*). Before this is done the chosen values of H_{m0} must be sorted in ascending order. There are many probability distributions that have been used in extreme wave analysis, some of the most important ones are given in [45]. According to [45] the data set should be fitted to all distributions and compared qualitatively using *quantile-quantile*

(*Q-Q*) plots. The chosen distribution is the one which produces the best fit. If only one distribution is to be used then [44] recommends the *three parameter Weibull distribution* because this distribution "seems to provide an acceptable fit to significant wave height data for most oceans". The CDF for the three parameter Weibull distribution is given by:

$$p = F(x) = 1 - e^{-\left(\frac{x-a}{b}\right)^c} \qquad (2.57)$$

where p is probability and $F(x)$ is the probability of the wave height x, a ($a<x$) is the so called location parameter, b the so called scale parameter, and c the so called shape parameter. However, because the POT method results in a data set that is a truncated version of the full set, it is recommended that the *truncated three parameter Weibull distribution* be primarily used:

$$p = F(x) = \frac{[F(x) - F(x_0)]}{[1 - F(x_0)]} = 1 - \exp\left[-\left(\frac{x-a}{b}\right)^c + \left(\frac{x_0-a}{b}\right)^c\right] \qquad (2.58)$$

where x_0 is the threshold wave height.

2.3.3 Fitting methods

There are numerous types of fitting methods, i.e. the mathematics used to compute the unknown parameters a, b, and c, of the CDFs above in order to achieve a good fit. *Maximum Likelihood*, the *Method of Moments*, and *Least Squares* are three commonly used fitting methods, but the only recommended method for extreme wave analysis is the maximum likelihood method [44]. The maximum likelihood method maximizes the following equation in terms of the parameters a, b, and c:

$$L(x_1,...,x_n;a,b,c) = \prod_{i=1}^{n} f(x_i;a,b,c), \qquad (2.59)$$

where x_i are the significant wave heights resulting from the POT method, and $f(x)$ is the *probability density function* (PDF), i.e. the derivative of the CDF.

2.3.4 Quantile-quantile plots

Quantile-quantile, or Q-Q, plots are used for qualitative evaluation of the goodness of a performed fit. These plots can be made after a CDF has been fitted to the wave height data as described above. To create a Q-Q plot one must calculate the inverse CDF, i.e. $x = G(p)$ where x is the statistical significant wave height, $H_{m0,statistic}$, corresponding to a certain probability, p. The goal of the Q-Q plot is to plot the "real" H_{m0} from the POT against the calculated $H_{m0,statistic}$ that are predicted by the fitted distribution, see Figure 2.9. The probability values, p, plugged into the inverse CDF are calculated in the following way:
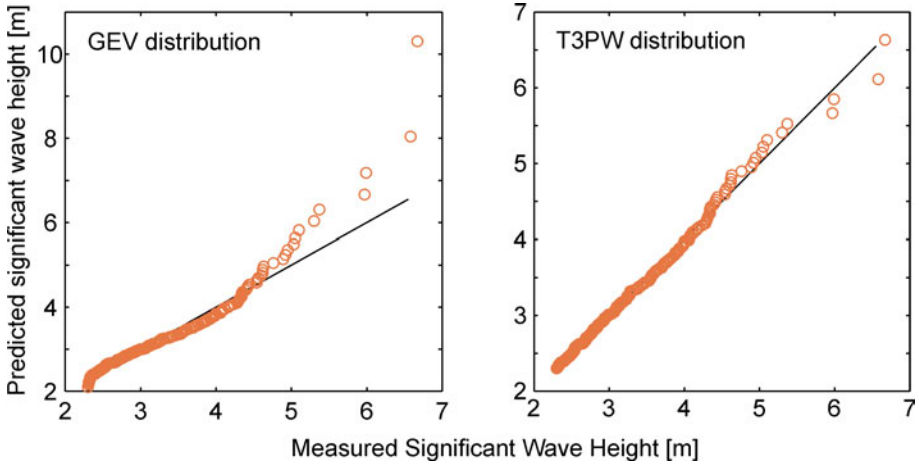
Figure 2.9: Two examples of Q-Q plots, used to qualitatively evaluate the fit between data and distributions. The measured values, x-axis, are plotted against the corresponding values predicted by the distributions, y-axis. The data represents eight years of wave heights from site 4 of Paper X. The threshold has been chosen to 2.3 m. The left plot illustrates the maximum likelihood fit to the *Generalized extreme values distribution (GEV)* and the right plot illustrates the maximum likelihood fit to the *truncated three parameter Weibull distribution (T3PW)*. The circles represent data points remaining after POT has been applied. The data is clearly better described by the T3PW distribution. The GEV distribution overestimates the extreme wave heights in this example.

$$p = \frac{n_i - 0.5}{n}, \qquad (2.60)$$

where n is the number of H_{m0}-values resulting from the POT. The inverse CDF of the truncated three parameter Weibull distribution is:

$$H_{m0,statistic} = x = G(p) = b \left[\left(\frac{x_0 - a}{b} \right)^c - \ln(1 - p) \right]^{1/c} + a \qquad (2.61)$$

To visualize the quality of the fit it is helpful to plot a line x=y. The plot of H_{m0} against $H_{m0,statistic}$ should be as close to this line as possible for a good fit. See Figure 2.9 for an example of a good and a bad fit, where the bad fit in the given example would result in an overestimation of the extreme wave heights.

2.3.5   Goodness of fit tests

While Q-Q plots are used for qualitative evaluations of how good a distribution has been fitted to the input data, *goodness of fit* tests are used to give a quantitative measure of the fit. In other words, when the unknown parame-

ters of a distribution have been found through the chosen fitting method, then goodness of fit tests can be performed to evaluate the fit. The quality of the fit is determined by the resulting significance level of the test, measured in percent. Two common goodness of fit tests are the *Chi-square* test and the *Kolmogorov-Smirnov* test. In Paper X a significance level of 95% or more was aimed for.

2.3.6 Return value

The desired return value, $H_{m0,max}$, i.e. the statistical hundred (or fifty etc.) year significant wave height, is at last calculated by plugging the following probability, p_R into the fitted inverse CDF, e.g. Eq. (2.61), above:

$$p_R = 1 - \frac{\tau}{R}. \tag{2.62}$$

R is the wanted return period, e.g. 100 for a statistical hundred year wave, and τ is the average time, in years, between the significant wave heights, H_{m0}, of the data set resulting from the POT.

2.3.7 Statistical extreme waves

The calculated return value, $H_{m0,max}$, above is a significant wave height that represents a time period of equal length as that represented by the values of H_{m0} that went in to the calculation of the extreme waves. It is thus not the single highest wave during the return period. The single highest wave, H_{max}, is found by assuming that the wave amplitudes in any given record of waves will be Rayleigh distributed, [45]. In this case H_{max} can be calculated as:

$$H_{max} = H_{m0,max} \sqrt{\frac{\ln(N)}{2}} \tag{2.63}$$

where N is the total number of zero-crossing waves in the record, i.e. approximately the number of wave periods in the record.

3. The Lysekil project

All of the work that has been performed throughout this thesis has been conducted within or closely linked to the Lysekil project. The Lysekil project was started in 2002 with the goal of researching a concept for wave energy based on a holistic perspective and with an electrical approach to wave energy conversion, an approach that has been uncommon in the wave energy field where the focus has often been on the hydrodynamics. The project is based at the division for Electricity at the Ångström laboratory of Uppsala University, but since 2004 it has also encompassed a wave energy research site close to the city of Lysekil on the Swedish west coast, and a measuring station on the small island of Härmanö approximately three kilometers from the research site, see Figure 3.1. Several institutions have helped fund the project through the years, these are: The Swedish Energy Agency (STEM), Vattenfall AB, Statkraft AB, Fortum AB, the Gothenburg Energy Research Foundation, Draka Cable AB, the Göran Gustafsson Research Foundation, Vargöns Research Foundation, Falkenberg Energy AB, the Wallenius Foundation, Ångpanneföreningen AB, the Olle Engquist Foundation, J. Gust. Richert Foundation, and Seabased AB.

The Lysekil project has, since 2004, been part of the Swedish Centre for Renewable Electric Energy Conversion (CFE). The centre supports PhD-students in renewable energy, seminars, and international exchange programs in the subject. The research that is conducted within the centre is expected to result in increased knowledge in energy extraction from renewable energy sources, as well as a number of technical solutions and their commercialization. The centre is supported by STEM and the Swedish Governmental Agency for Innovation Systems (VINNOVA).

Most of the papers presented in this thesis deal with this wave energy project in one way or another. Paper I presents results from the first laboratory prototype; Papers II – VIII present the first complete wave energy converter (WEC) that was deployed off the Swedish west coast in the spring of 2006 and many of the studies performed on it; Paper IX presents a passive sensor for measuring the generator air gap; and Paper X presents a thorough study of the wave climate off the Swedish west coast. Furthermore, Paper XI gives an updated overview over what has been achieved so far in terms of experiments, and Paper XII introduces the underlying ideas that the presented concept for wave energy conversion rests upon. Papers XV – XVI present a non-technical study that discusses the concept of utilization. Utilization was briefly introduced in Chapter 1, but the content of these two papers is, due to the recentness of them, otherwise only discussed in the discussion and conclusion chapters of this thesis, Chapters 7 and 8. Finally, Papers XIII –
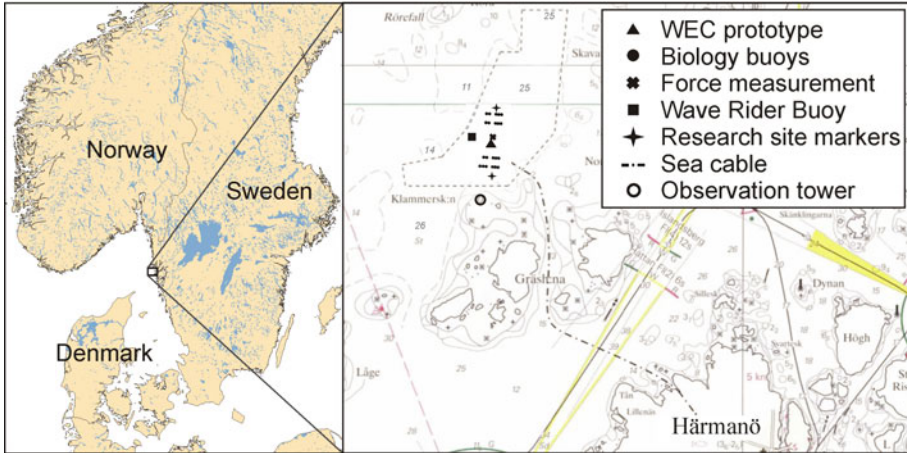
Figure 3.1: Map of Sweden showing the location of the research site and a sea chart with the locations of the objects that are currently at the site.

XIV present studies within the Lysekil project in which the author has only played a minor role. Except for the papers presented in this thesis, a large number of articles [20, 29, 30, 48–73] and a number of theses, from masters to PhD, [34, 35, 74–78] have been produced through the course of studying this wave energy concept. These papers discuss the wave energy conversion concept from many perspectives, e.g. economic considerations, generator and electrical system design and hydrodynamic interactions between converter and waves.

3.1 The wave energy research site

The area drawn by the dashed line in Figure 3.1 marks the wave energy research site of the Lysekil project. The county of Västra Götaland has given the project permission to use the site for wave power research until 2014. A north and a south marker, indicated in the figure, identify the region chosen for the actual research. There are no plans to extend past these.

The water depth of the site is approximately 25 m although, depending on tides and air pressure, this has been seen to vary in the interval of -0.7 – +0.46 m. The seabed is relatively flat and is composed of sand. Basically all of the waves entering the site come straight from the west. Since the site is close to shore no waves, save waves reflected on the cliffs, come from the east. The average energy flux of the site is 2.6 kW/m as shown in Paper X.

3.2 The wave energy technology

The wave energy converter is composed of a buoy on the ocean surface, an encapsulated linear generator on the seabed, and a line in between, see Fig-
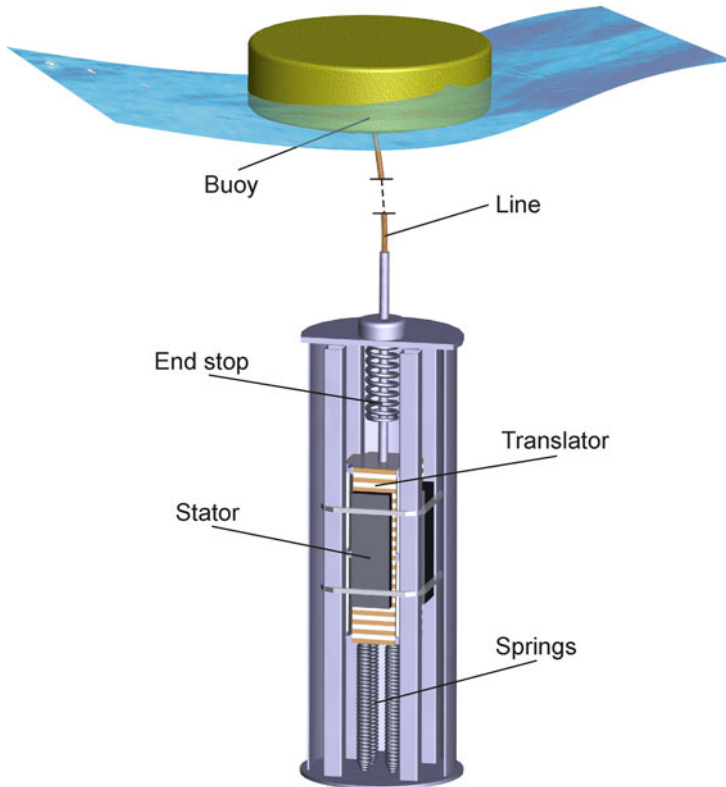
Figure 3.2: Conceptual drawing of the wave energy converter.

ure 3.2. Extension springs are connected to the bottom of the translator so that, after a wave has lifted the buoy, the springs pull it back down in the wave trough. Two stop springs are part of the construction, one is attached to the bottom and one to the top of the capsule, the purpose of the springs is to limit the motion of the generator in particularly large waves. Either a cone, or four long cylindrical bearings set in a square formation are mounted on the top of the WEC. These are used to guide the line so that the force from the buoy is applied vertically to the generator. The electricity is transmitted to shore via a sea cable. Because the buoy, although a few meters in diameter, is very small in relation to the length of the waves from which it captures energy, it is sometimes called a *point absorber* as noted in the introduction, Section 1.3.2.

There are no energy conversion steps, neither mechanical, hydraulic or other between the buoy and generator. The resulting mechanical system is thus very simple in that is has few moving parts, and it is expected to require little maintenance and to have a high survivability. The direct coupling between buoy and generator means that the motion of the buoy is mimicked by the generator in both speed and direction. The effect of this is a relatively large, slow moving generator and generated electricity that varies in both frequency, amplitude and phase order, see Figure 3.3. The simple mechanical system
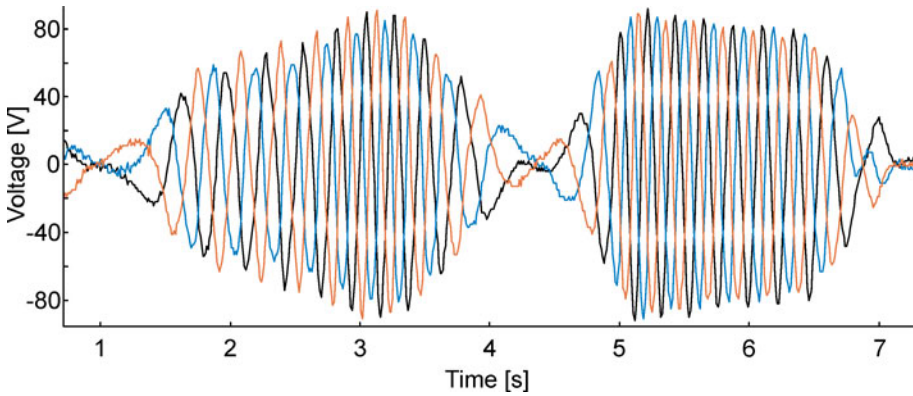
Figure 3.3: The output voltage varies in both frequency, amplitude and phase order. A consequence of the simple mechanical system with a buoy directly coupled to a linear generator.

thus has consequences on the electrical side. This is, however, believed to be a much smaller problem and more easily solved than the problems associated with complex and maintenance heavy mechanical systems. Conventional generators, for example, are rotating rather than linear, and they are typically designed for high rotational speeds. The use of this type of generator thus necessitates the conversion of the relatively slow motion of waves to a high speed rotating motion, which is a big challenge for a mechanical system in the harsh ocean climate. A comparative study of linear generators and hydraulic systems, in favor of linear generators, is given in [79]. The use of linear generators in wave energy applications is also suggested by [80–84].

For the generated electricity to be of use for the electric grid it has to be converted from its original form, Figure 3.3, to the suitable frequency and amplitude. This is done with standard power electronic components by first rectifying the generated alternating voltage, and then inverting it back to AC of the desired frequency. Thereafter the voltage needs to be transformed to the grid voltage before the power can be supplied to the grid. This can be done in many different ways [66]. In the simplest case the generated electricity is transmitted to shore directly via a sea cable. On shore it is then converted to the suitable form. This alternative, because of the low voltage-level of the generated power, inevitably leads to high transmission losses.

An alternative is to convert the power close to the generators. In such a scenario the WECs would be connected to a marine substation in the close vicinity of the WECs. In the marine substation the electricity would be converted to the desired frequency and transformed to a higher voltage level before being transmitted to shore.

Although all of the WECs within the Lysekil project will be installed at the depth of 25 m, the range of depths that are considered possible for installation, at the current stage of the technology, are from 20 to at least 100 m.

3.3   Project goal

The goal of the Lysekil project is to thoroughly study the discussed Swedish concept for wave energy conversion. In real conditions and over several years a research park of wave energy converters will be constructed and connected to the electric grid. Some of the research areas that are being studied within the project are: the ability of the wave energy converters to capture the energy of the ocean waves; the design of an electrical system required to collect and convert the generated electricity to a form suitable for the electric grid; the detailed interactions between buoy and wave; the study of sea states and wave climates; and not least the mechanical challenge involved in the construction of a wave energy converter that can survive the harsh conditions of the ocean.

The goal for the wave energy research site is to install 10 complete WECs together with one or more marine substations. In addition, up to 30 buoys, called *biology buoys*, will be installed for ecological impact studies. These biology buoys are comprised of a buoy connected via a line to a concrete foundation. They are thus similar to the WECs with the main difference being the missing generator. All together the research park will serve as a model of a large wave energy park, both in terms of handling the non-coordinated energy production of several units as well as to study the ecological impact. Furthermore, an observation tower is needed to monitor the site and to observe the interactions between the buoys and the waves during different sea states.

3.4   Project achievements

The most important achievement so far is the level to which the wave energy research site has been developed. At the time of writing the first offshore wave energy converter of the presented technology has been in operation for a total of over 12 months. Throughout this time its generated power has been continually measured and recorded. Furthermore, a total of 26 biology buoys have been installed during different time periods and today 15 of them remain at the site. The mentioned observation tower has been built and is equipped with a camera that can be run by solar panels, a small wind power plant and a battery backup. A *wave rider*™ wave measurement buoy has been installed since the spring of 2004 and hourly values of significant wave height can be seen online [85]. Finally, the measuring station has been operational since the installation of the first wave energy converter in the spring of 2006. Through the years it has been continually upgraded and modified and today the output from the WEC can be rectified and filtered so that the power output is continuous with only slow variations in power, see Paper VIII. The generated energy has thus far been consumed by dump loads. Figure 3.4 gives an illustration of the different objects that are currently installed in the Lysekil wave energy research site.

A more detailed time line of the achievements is given in the following. This is, however, still only a brief outline of the work that has been done.
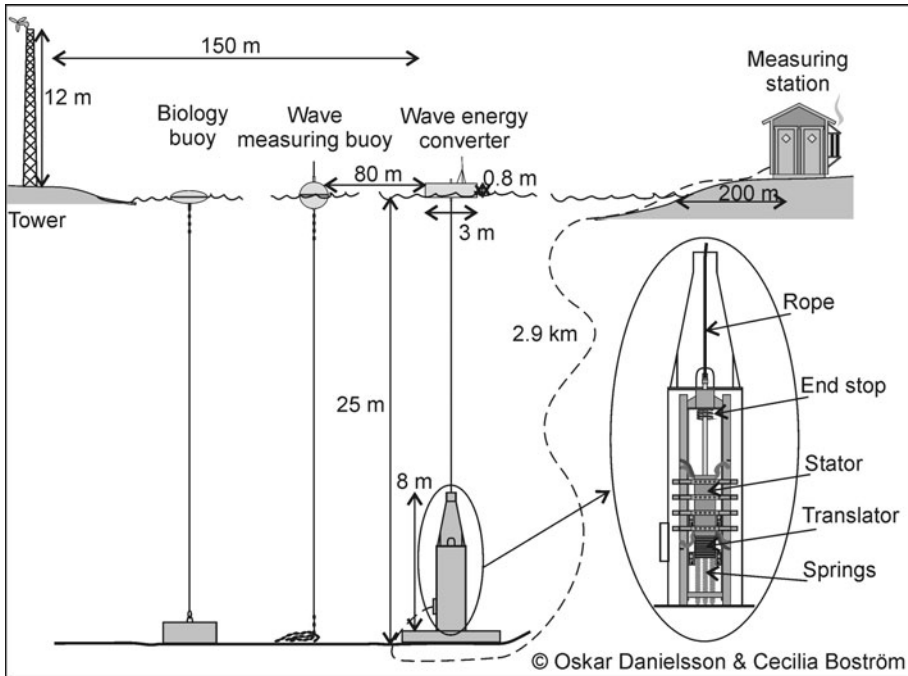
Figure 3.4: The different components currently installed at the wave energy research site.

Figure 3.5, at the end of this chapter, presents a collage of pictures from the Lysekil project.

2002

- The project that later became known as the Lysekil project was started during the spring.

2003

- Preliminary studies of the seabed on the Swedish west coast is started in the search for a good location for the wave energy research site.
- The construction of the first prototype *laboratory generator* is completed. At this time it can only be driven at low speeds by the laboratory overhead crane.

2004

- The first permits for the research site are approved by the county of Västra Götaland. The project is given permission to perform wave energy research on the site until 2014.

- The marine infauna of the Lysekil research site is studied through soil samples.
- A wave measurement buoy is installed at the Lysekil research site and measurements are begun in April.
- In September the Swedish Energy Agency (STEM), and the Swedish Governmental Agency for Innovation Systems (VINNOVA), approve the formation of the Swedish Centre for Renewable Electric Energy Conversion, centered at the division for Electricity at the Ångström laboratory of Uppsala University. The center is preliminarily intended to run from the first of July 2004 to the 30th of June 2008.

2005

- The laboratory generator is connected to a motor that can drive the generator at high speeds.
- A buoy with a force sensor, connected via a line to a collection of springs and a concrete foundation on the sea floor, is installed at the research site.
- One larger, 3 m in diameter, and four smaller, 1.5 m in diameter biology buoys are installed at the site.
- Design and construction of the first wave energy converter, named *Lysekil 1* or simply the *L1*, intended for real offshore testing at the Lysekil research site has begun.

2006

- The measuring station, located at the island of Härmanö, is built during February and March.
- In the end of February the underwater cable, intended for the first wave energy converter, is drawn from the measuring station to the research site. A signal cable, intended for later WECs is submerged together with the cable.
- On the 13th of March the first offshore prototype WEC is installed at the research site.
- On the 24th of May, roughly two and a half month after the installation, the line to the buoy breaks due to bending movements and insufficient cooling of the isolated fiber core.
- The Geological Survey of Sweden (SGU), performs tests on the nature of the seabed.

2007

- On the 3rd of March, after 9 months of standstill at the bottom of the ocean, the buoy is reconnected to the generator via a new line. The line is of the same type as the previous line, but a change has been made to the top of the generator to decrease the bending movements.
- A total of 21 biology buoys are installed during March and May.

- In the beginning of April the WEC is run against a DC-load for the first time. Previously all the loads were purely resistive AC-loads.
- An observation tower is installed on an islet in the close vicinity of the research site.
- On the 27th of July, after almost five months, the line between the WEC and the buoy breaks once again and for the same reason as the previous time.

2008

- Biology buoys come loose during the year due to a design problem in the mooring system.
- On the 21st of May, after another ten months of standstill at the bottom of the ocean, a new, ring shaped buoy, is connected to the wave energy converter, which again starts to operate similarly to when it was first installed in 2006.
- Biological studies are performed at the research site during the summer months.
- The marine substation is designed and constructed, and is simultaneously and successfully tested against a wind generator and a marine current generator in the lab at the division for Electricity.
- Another two WECs, similar to the first, are being prepared for installation at the wave energy research site.

Figure 3.5: Some pictures of different objects in the Lysekil project. From top to bottom: A view over the research site; the buoy used during the first two operational periods; the measuring station; the wave measurement buoy; the observation tower; the buoy used during the third operational period; a diver under a biology buoy, and a biology buoy on the surface.

4. The construction of a Wave Energy Converter

The first offshore wave energy converter of the technology presented in this thesis, described earlier in Chapter 3, was installed at the Lysekil wave energy research site on the 13th of March 2006. The work involved in the design and construction of this wave energy converter, as well as all other WECs, spans over many disciplines, e.g. hydrodynamics, electromagnetism, mechanics, power electronics, electric circuit theory and measurement. The WEC installed at Lysekil is a result of the combined effort of many at the division for Electricity at Uppsala University.

As noted in the introduction, Section 1.4, the ocean is a difficult place to work. Compared to construction on land, sea based structures are more difficult and sometimes impossible to access. A productive site for wave energy naturally has a lot of good size waves, and some work, such as diving, is only possible during relatively mild sea states. Thus, if something breaks during a stormy part of the year, it may take months before the sea has calmed down enough to repair the equipment. Because of this, high demands are placed on the offshore structure in terms of survivability and the need for maintenance. In the end, the design of a WEC is a delicate balance between economy and the amount of materials needed for survivability. If the technology is going to have a chance to be successful, the price of the produced electricity has to be competitive.

4.1 Basic design considerations

This section starts with a basic description of generator design considerations, the generator being the heart of the wave energy converter. Thereafter some mechanical challenges are discussed that have to be taken into account in the design of a structure that aims to survive for years in the harsh ocean climate.

4.1.1 Generator

The generator used in the wave energy converter has been designed using a detailed finite element simulation tool custom built for the purpose of designing generators. A more thorough description of the simulation tool can be found in [75]. Although the details and methodology of the design tool will not be given here, some fundamental properties of the generator can easily be

discerned in the description of the generators magnetic circuit, illustrated in Figure 2.5 of Section 2.1.5, and by recalling Faraday's law, Eq. (2.14).

Although there is no simple rule for designing generators, as long as there is no danger of electrical breakdown during the operation of the generator, it is often beneficial to generate electricity of a given power at high voltage when this leads to lower copper losses, Eq. (2.9). From Faraday's law we know that there are three alternative ways to affect the generated voltage: a faster variation of flux, e.g. a faster motion of the translator; a high magnetic flux in the circuit; or a large number of conductors.

Speed

In the case of the direct driven linear generator considered in this thesis, the speed of the translator will never be high compared to standard electrical machines. The speed can, to some degree, be affected by the chosen buoy, and it is also very much affected by the electrical load that the generator is subjected to. All the same, the generator will always be considered a slow moving one.

Another way to affect the speed of the change in flux over time is to control the *pole width* of the magnetic circuit. The pole width of a surface mounted permanent magnet synchronous machine, e.g. the Lysekil generator, is the length from the middle of one magnet to the middle of the next. In the most simple case there are six cable slots in the stator per two magnets on the translator. Since the two magnets have alternating direction of magnetization, **M**, the motion from the middle of one magnet to the middle of the next completes one half period of variation in flux. More complicated variations of the number of cable slots per pole and phase are used to decrease cogging forces in the machines at the cost of a decrease in voltage. The smaller a pole width is, the shorter the distance that the translator has to move to complete one magnetic period. Hence, at a given translator speed, smaller pole widths will lead to a faster change in flux and thus a higher voltage. There is, however, a limit to how small the poles can get. Figure 4.1 shows the magnetic flux density, B, as well as the corresponding flux lines in two magnetic circuits. The iron in the stator is needed to lead the flux around the cables and if the iron is saturated, see Figure 2.2, then the flux will pass through the air close to the air gap instead, this is called *leakage flux*. This leakage flux will not contribute to the flux that induce voltage through Faraday's law. A higher flux frequency will lead to higher iron losses, Eq. (2.8), but the frequency of the studied generator is still relatively small compared to standard machines and these losses have not, because of this, been considered in the research presented here.

Flux

The second way to achieve high voltage is to design a magnetic circuit where the amplitude of the magnetic flux is high. This can in part be achieved with strong magnets, such as the Neodymium-Iron-Boron magnets (Nd-Fe-B) that are used in the generators in the Lysekil project. Moreover, the geometry of the magnetic circuit is essential. The flux path should be fitted to the magnet with stator teeth that are wide enough to let the flux pass without saturating the
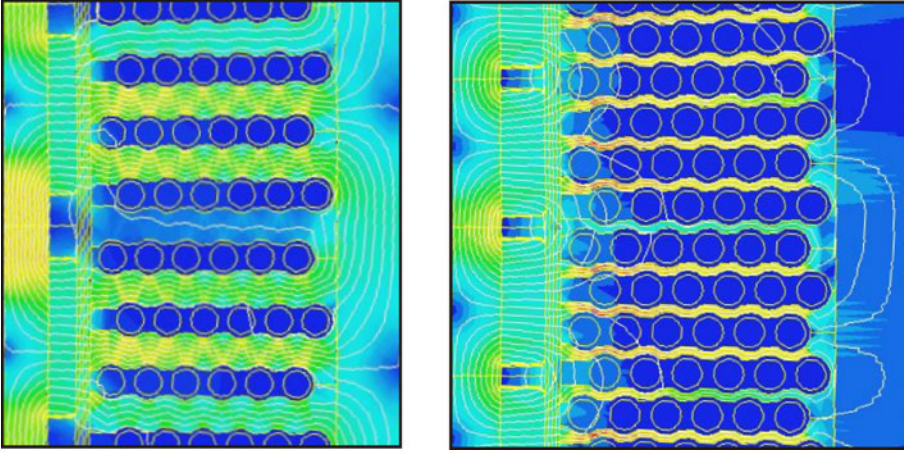
Figure 4.1: Two examples of magnetic circuits from finite element simulations. The left picture illustrates a well-dimensioned circuit where most of the flux, as seen from the flux lines, circles the conductors. The right picture shows an ill-dimensioned circuit with very large leakage flux.

iron. As above, saturating the iron will lead to increasing levels of leakage flux. Furthermore, a high saturation means a large hysteresis loop, see Figure 2.2 of Section 2.1.3, which in turn means larger losses as given by Eq. (2.8). Large heat losses within the stator can lead to problems with the insulation of the cables.

The amount of flux in a magnetic circuit is strongly affected by the size of the air gap as seen in Eq. (2.13). It is thus of great interest to keep the air gap as small as possible, but with powerful permanent magnets mounted close to the iron stator the attractive forces can become very large, as high as 10 tonnes per square meter or more. This places high demands on the structure of the generator.

Finally, the flux amplitude can be raised by increasing the area of the cable loop, i.e. the magnetic circuit, since $\Phi = B \cdot A$ as given in Eq. (2.3). In the linear generator case, the area of the loop can be increased by making the stator longer. Furthermore, the width of the stator, called the *stack length*, can be increased with the same effect. The width is the third dimension of the stator which is not visible in the cross section views of Figure 4.1.

Cables

The parameter, N, in Faraday's law, Eq. (2.14) represents the number of coil turns, or cables in the case of Figure 4.1, per phase. The generated voltage is linearly dependent on the number of coil turns and it is therefore tempting to increase their number. In terms of the magnetic circuit, this can be achieved by decreasing the conductor area so that more conductors may fit in the slots of the stator. The downside of this is a higher resistance and reactance of the winding. A high reactance has a limiting effect on the generated voltage, an effect that increases with the amplitude of the current. This is an important

aspect for the direct drive generator used in the studied WEC since the generated voltage needs to be higher than the DC-level of the DC-bus in order for the bridge rectifier to conduct. This has to work during all sea states, i.e. also during powerful sea states when the generated currents will be high. The size of the stator slots can also be increased in order to fit more conductors. This will have the same effect but will also lead to a longer flux path. The longer the flux path gets, the larger the reluctance of the circuit and the larger the leakage flux will get, see the right circuit of Figure 4.1 for an illustration of a magnetic circuit with high reluctance and large leakage flux.

Overall, the magnetic circuit is thus a matter of optimization, and the design of its geometry is essential and often limited by the saturation of the stator iron, the structural limitation of the air gap width, and by the leakage flux.

Peak powers

Due to the nature of ocean waves, the power available for a wave energy converter is impossible to control. The designers of wave energy converters have to engineer their creations to control the power captured instead. In the case of the WECs in the Lysekil project the generator is designed to hold for power levels more than an order of magnitude higher than the rated power. This is because the speed and force with which the translator is set in motion is decided by the buoy and the wave, and the generator must be designed to survive long time periods with extreme waves. The current density in the stator winding during average power production is, for this reason, designed to be very low so that the generator will not be damaged when very energetic sea states occur.

4.1.2   Mechanical challenges

Stress

All WECs will be subjected to mechanical stress, this is inescapable, but depending on technology the location and magnitude of the applied stress will vary. Some of this stress is good since the forces from the waves are needed to drive the power take-off of the converter. For the discussed technology, forces induced by ocean waves are apparent throughout the construction, and a large part of the design phase was dedicated to finding out the magnitude of the stresses, where they are located, how much material is needed to endure them, and how all of these factors change with different design solutions.

The magnitude and the locations of the stress can be found out through calculation, physical simulations, through experience or as a last resort by guesswork. As mentioned previously, in Section 2.3, a common practice for structures that are intended for long stays in the ocean is to design them to survive a 50 or 100 year wave. In the case of the first WEC for the Lysekil research site, the forces between the translator and stator are relatively easy to find, see [54]. The wave forces on the buoy, some of which is transferred via the line to the generator, was measured with a full scale buoy connected to a collection of springs as noted in Section 3.4.
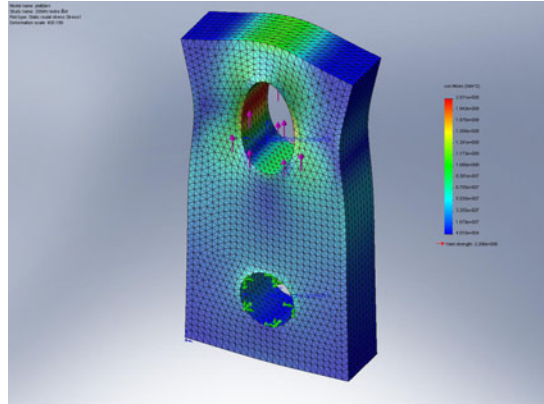
Figure 4.2: An example of a finite element simulation of stress on a mechanical component.

For simple geometries, stress calculations can be performed by hand. Soon, however, the geometries get very complicated and a common approach is to use one of the many available programs for finite element simulations, e.g. Solidworks, ANSYS, Pro Engineer, Comsol Multiphysics etc., to perform stress simulations that mimic the loads on the intended structure, see e.g. Figure 4.2.

Fatigue

Once the offshore structure has been designed to withstand the stresses that it is subjected to from the ocean, the structure will endure for a while. Due to the cyclic nature of waves, however, fatigue may become a significant problem. In the design work of the discussed WEC, manufacturers of some components would, when asked about the fatigue endurance of their product, reply that the component would survive an infinite number of load cycles. According to standard definitions, however, infinity in this case usually means 10^7, i.e. 10 million, load cycles. The problem with this definition and ocean waves is that the offshore structure may be exposed to a few million waves per year, and each wave will induce many load cycles in the generator, for example due to cogging.

Different materials show very different characteristics when it comes to durability against fatigue. These characteristics are illustrated in *S-N curves* where various stress levels are plotted against the number of load cycles to failure, see e.g. Figure 4.3 [86]. In a design it is therefore critical to know the places where the structure is fatigue sensitive and where it will experience high amplitude load cycles. Furthermore, one will need to choose a material that will do the job, or redesign the structure, if possible, to reduce or avoid the problem.
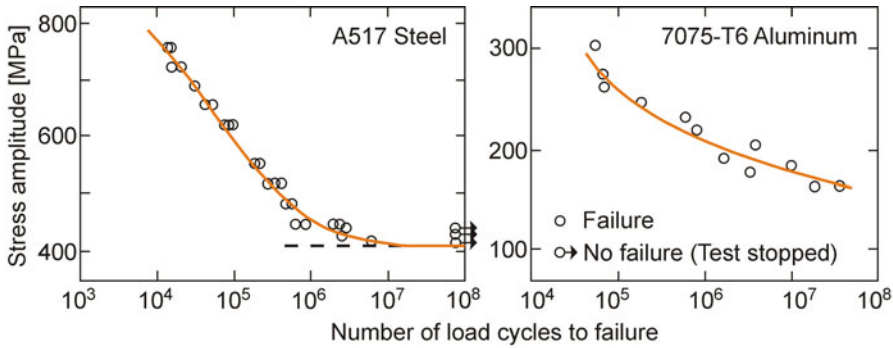
Figure 4.3: Material specific fatigue curves, or S-N curves, for steel and aluminum [86]. The diagrams show the number of load cycles to failure as a function of stress level. The steel is the more fatigue tolerant of the two examples. The curve eventually levels out indicating that for a certain level of stress the steel will survive an "infinite" number of load cycles. By contrast, the S-N curve for the aluminum does not show any sign of leveling out even at low stress levels. The illustrated curves are material specific, and there are many different types of steel and aluminum that have characteristics that are very different from those shown above.

Tolerances

At first glance it may seem strange that technical handbooks recommend several different standard hole sizes for each bolt diameter, and a range of choices in the specifications of the diameter of an axle, see e.g. [87, 88]. It would seem more natural to assume that as long as the hole diameter is larger than that of the bolt or axle, it should be fine. Tolerances can seem like one of the easiest things to manage since they always work perfectly on the drawing board. Reality, however, is quite the opposite. This is one of the fields where the difference between the drawing board and reality is most obvious.

Although the precision of machines and techniques that are used in shaping material components varies considerably, no material component in a structure is perfect in its dimensions. They may be bent, twisted, or in some other way slightly off in their dimensions, and it is not uncommon that these defects are not discernible to the naked eye. See Figure 4.4 which points out the tolerance properties of a standard square steel profile [89]. When many of these slightly imperfect components are put together the imperfections add up and it is crucial to keep this in mind so that the machine, in case of generators, will work properly in the end. In case of the bolt example; although a bolt at one end of a machine may fit perfectly, with all of the structure in-between, a bolt on the other side of the machine may not.

In the discussed WEC an example of an important area is the size of the air gap. In the first generator of the Lysekil research site the stator is 1265 mm long, 400 mm wide, and the air gap is 3 mm. The attractive forces between stator and translator are very large at this distance and they increase exponentially with smaller distances as seen in [54]. It is thus important that the four
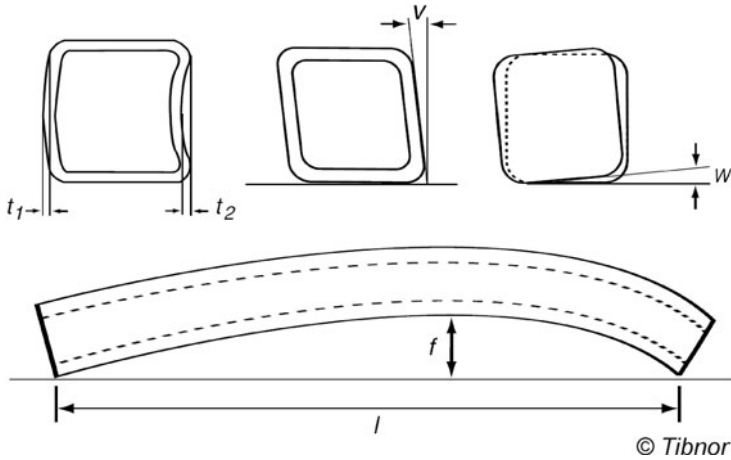
Figure 4.4: The properties of a standard square profile of construction steel that are subject to imprecisions. The profile is likely to be buckled, skewed, twisted and bent to some degree, and the given tolerance values give the maximum allowed deviations from a perfect geometry.

sided translator is positioned with great precision and with the same air gap width on all sides to avoid imbalances in the total force on the structure.

Corrosion

Common types of steel, although relatively cheap, strong, and fatigue tolerant, are highly sensitive to corrosion. One type of corrosion is the oxidation of iron which happens when the iron is exposed to moisture and oxygen. In the ocean this effect is particularly strong around the surface where there is plenty of both humidity and oxygen, sometimes called the splash zone. The near surface areas are also particularly exposed since the corrosive process increases with water speed.

Another type of corrosion occurs when two different metals are in galvanic contact through sea water. This is called *galvanic corrosion* and is caused by a difference in the electric potential between the two metals which generates a current that oxidates one of the metals, the *anode*, and reduces the other, the *cathode*. In the process the anode is solved in the water. Galvanic corrosion can really speed up the corrosive process and it is therefore important to try to avoid mixing materials in the same underwater construction, or to choose materials between which there is only a small or no electrical potential. Sensitive and exposed metal parts can generally be protected by means of *cathodic protection*. This means that metals that are much more easily corroded, called *sacrificial anodes*, are attached to the structure that needs protection. This alters the electric potential so that the attached sacrificial anodes are oxidated rather than the steel. For the protection of steel, the sacrificial anodes are commonly made of zink or aluminum.

Although part of the corrosion is oxygen dependent, and the corrosion effect is thus strongest in the limit between surface and air and lowest in the

Figure 4.5: A pack of heavily corroded steel springs after having been used in force measurements during one of the earliest experiments at the Lysekil research site. The springs were placed openly and without cathodic protection in the corrosive sea water.

deep ocean, it still has significant effects on relatively deep water. See e.g. Figure 4.5 which shows an early lesson learned in the Lysekil project where the springs used in force measurements eventually broke due to corrosion. There are many steel alloys that are very resistant to corrosion, but these are generally more expensive and sometimes difficult to work with. Oftentimes a less expensive steel is chosen instead in combination with sacrificial anodes.

4.2   The laboratory generator

Before anything was installed at sea a first linear generator for laboratory experiments was built. The purpose of it was to test the electromagnetic finite element simulations of the generator that had previously been made, and to make sure that the process of designing generators was accurate and under control in advance of future offshore installations.

At first the laboratory overhead crane was used to move the translator of the generator. This only allowed for very slow translator speeds and correspondingly low induced voltages. In order to test the generator at higher power outputs it was connected to a motor [76]. This was achieved during 2005 and some results from the first test runs at higher speeds are given in Paper I. The laboratory generator is four-sided and has two extension springs attached to the bottom of the translator. The springs act as a restoring force similarly to the real case described in Section 3.2. Table 4.1 presents the general features of the generator and Figure 4.6 shows a picture of the set-up.

Another reason for building the laboratory generator was to gain experience from an engineering point of view, e.g. to test how the powerful magnets could be handled and if winding the stator was going to be difficult. It turned out that
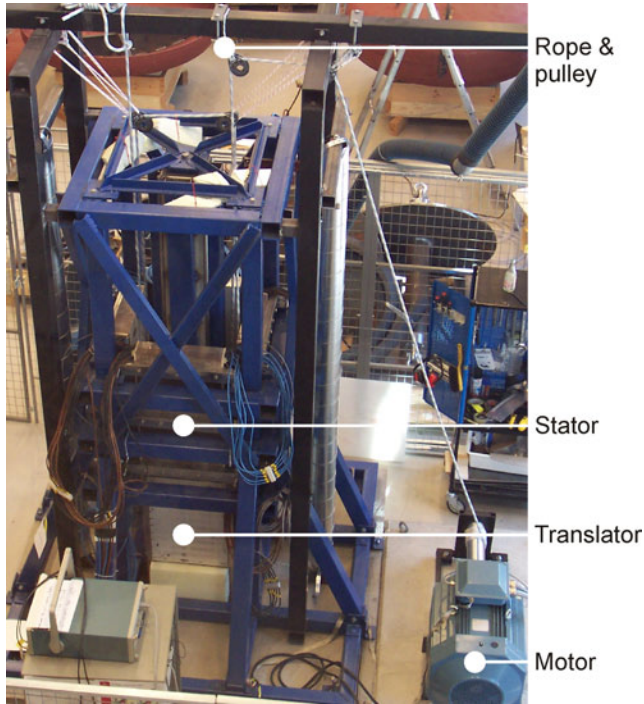
Figure 4.6: The laboratory generator.

forces between the stator and translator, mentioned in Section 4.1.2, became a problem due to an ill-designed concrete pillar in the middle of the generator, the purpose of which was to guide the translator. Because this pillar was too weak the smallest safe air gap width was approximately 7 mm, and even at this distance the air gap was not constant during the motion of the translator. This weakness was problematic for the experiments performed with the air gap sensor of Paper IX, described in Chapter 5. It is probable that the correlation

Stator length	700 mm
Translator length	650 mm
Stator/Translator width	400 mm
Pitch length	± 800 mm
Air gap width	7 mm
Pole width	50 mm
Slots per pole & phase	6/5
Max experimental speed	0.86 m/s
Max experimental power	1.6 kW

Table 4.1: *General features of the laboratory generator.*

between theory and measurements of the sensor would have been even better had it not been for the instability of the translator.

4.3 First offshore WEC of the Lysekil research site

A natural next step after the laboratory generator had been constructed and the permits for the wave energy research site were in place, was to go ahead and design, construct, install and evaluate the first complete offshore wave energy converter. Most of the work presented in this thesis is concerned with

Figure 4.7: Pictures taken from different stages during the construction of the first wave energy converter for the Lysekil wave energy research site.

this. Paper XI illustrates how the WEC was installed, Paper XII presents the general underlying design strategy, and Papers II – VIII present experiments and studies that have served to increase the knowledge and understanding of the operation of the WEC.

The WEC was deployed on the 13th of March 2006. Since then it has been running during three time periods and measurements have been continually recorded during all of that time. Initially, during the first two and a half months after its installation, and then during five months of 2007. It was started up for the third time on the 21st of May 2008 and was run for another five months. Figure 4.7 shows a collage of pictures taken from different stages in the construction of the WEC.

4.3.1   Mechanical design specifications

Although isolated parts were made earlier, the design work of the WEC really picked up in the fall of 2005. The linear generator of this converter is very similar to the laboratory generator. It is four-sided, uses magnets of the same dimension, and the stator has been wound in the same pattern and with the same type of cable. There are, however, some important differences. The translator and stator have been made longer, the air gap smaller, the pitch length has been slightly increased, and the generator is fitted with end stop springs in both ends in order to limit the motion of the translator during particularly high waves. Instead of having two extension springs attached to the bottom of the translator, there are now eight. Furthermore, the bearing problems of the laboratory generator have been solved. See Figure 3.2 in Chapter 3

Buoy diameter	3 m
Buoy height	0.8 m
Buoy mass	$\sim$1000 kg
Buoy draft	$\sim$0.4 m
Stator length	1867 mm
Translator length	1264 mm
Stator/Translator width	400 mm
Free pitch length	$\pm$900 mm
Upper end stop length	250 mm
Lower end stop length	140 mm
Static spring force	10 kN
Spring constant	6.2 kN/m
Upper end stop spring constant	243 kN/m
Lower end stop spring constant	215 kN/m

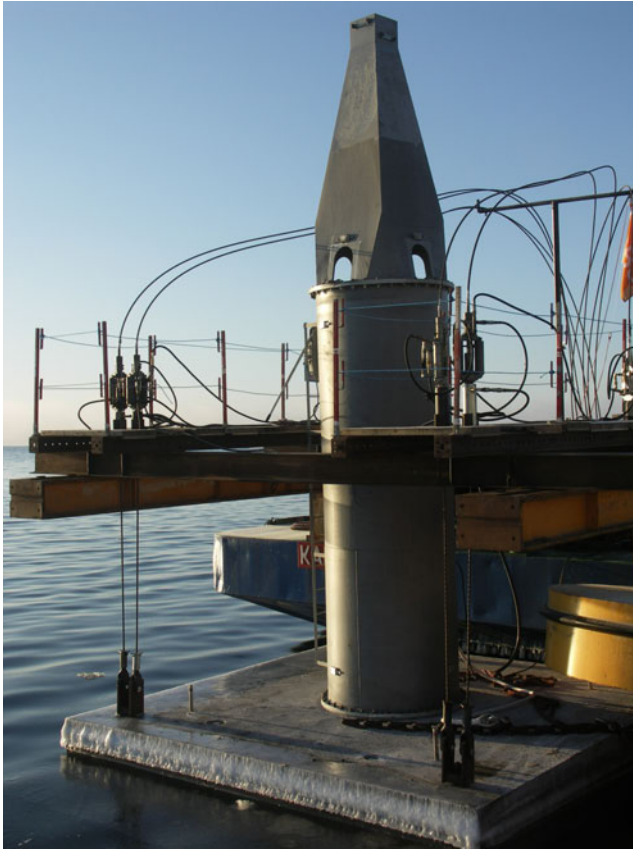Table 4.2: *Physical features of the first Lysekil WEC.*

Figure 4.8: The first WEC of the Lysekil project that was installed at the wave energy research site. Here it is mounted at the end of a barge on the day before its installation.

for a drawing of the interior of the WEC. Table 4.2 presents a list of physical features of the WEC.

The generator is placed in a water-tight casing that is pressurized to the surrounding water pressure at 25 m depth, see Figure 4.8 for a picture of the WEC the day before it was launched in 2006. A sealed piston connects the dry generator to the line outside the casing. The line connects to a steel buoy which, during the first two operational periods had the shape of a cylinder. When the WEC was taken into operation again in 2008 the buoy was changed to a ring shaped buoy with 6 m in diameter, made up of six cylindrical sections with a diameter of 710 mm. Both buoys can be seen in Figure 3.5 of Chapter 3. During the first two test periods, the line consisted of a Vectran™ core and a Dynema™ (first trial), or polyester (second trial), outer casing. During the third trial period this was changed to a steel wire with a plastic coating of the type used on sea cables.

4.3.2 Electrical design specifications

The generator was designed to produce an average power of 10 kW at a certain load and speed of the translator. As noted earlier however, in Section 4.1.1, the wave climate cannot be controlled and the WEC has to be able to handle any wave that descends upon it. Because of this, the generator was designed to effortlessly survive extreme overloads, and so far it has momentarily generated a maximum of 87 kW. See Table 4.3 for list of general electric features of the WEC system.

   The generator is connected via a 2.9 km sea cable to a measuring station on the island Hermanö. During the earliest experimental stages, the generator was connected to a purely resistive delta coupled dump load located at the measuring station, see Figure 4.9 A. Results based on experiments with this type of loading are presented in Papers II – VII.

   As described in Section 3.2, before the generated energy can be supplied to the electric grid, the voltage has to be converted to the correct amplitude and frequency. A first step in achieving this is to rectify and filter the generated highly fluctuating voltage and this was first accomplished in the beginning of April of 2007. The electric circuit of this configuration is given in Figure 4.9 B. Results from experiments with this type of loading are given in Paper VIII. The size of the filter determines the level of smoothing of the output power. With more WECs connected together in the future, the size of the

Air gap width	3 mm
Pole width	50 mm
Slots per pole & phase	6/5
Nominal speed	0.67 m/s
Nominal power	10 kW
Nominal voltage (line-line)	200 V
Generator phase resistance	0.44 Ω
Generator phase inductance	7.8 mH
Sea cable phase resistance	0.54 Ω
Sea cable capacitance	145 μF
First operational period	
Delta coupled dump load resistance	2.2/4.9/10 Ω
Damping factors (corresponding to loads)	12.7/8.53/5.23 kNs/m
Second and third operational period	
Capacitive filter (C_+, C_-)	24.34 F
Resistance (R_+, R_-)	9.2/13.8/27.5

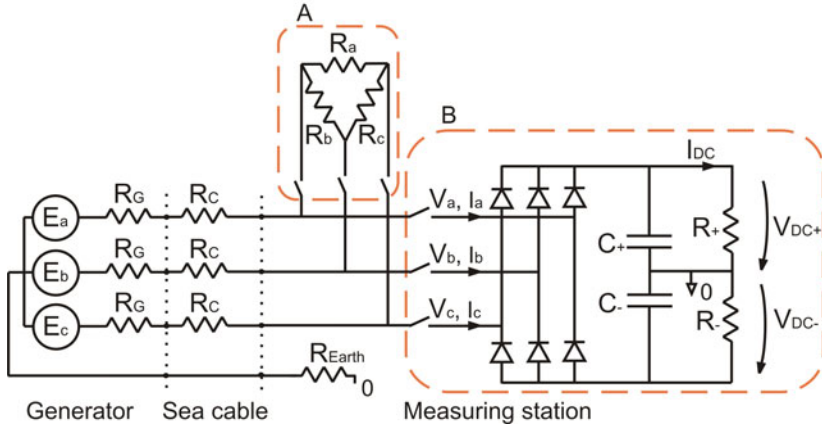Table 4.3: *Electrical features of the first Lysekil WEC.*

Figure 4.9: Electric circuit. A – Resistive delta coupled load. B – Rectification, filter and resistive dump load

filter required to achieve a wanted smoothing level is anticipated to decrease due to the overlapping of the power generated by the WECs [49].

For current and future developments at the Lysekil wave energy research site that are not included in this thesis, see Chapter 9.

4.3.3 Installation

The wave energy converter was assembled in the workshop of the division for Electricity at Uppsala University. Some smaller parts and last minute fixes were made in the workshop, but for most of the parts comprising the WEC the blueprints were made at the division but the parts were ordered from nearby machine shops. When fully assembled, the finished WEC was transported via truck to the Lysekil harbor on the west coast. There the WEC was mounted on a concrete gravity foundation that is needed to ensure that the WEC will not move or tip over during operation. In fact, when in the steel casing, the WEC's density is less than water and it would thus float without the foundation. The complete set-up was hung via eight hydraulic wire jacks at the end of a barge and the line from the generator was attached to the buoy, see Figure 4.8. On a calm day the WEC was transported out to the research site and slowly lowered the 25 m to the seabed. As it was lowered, it was pressurized to the surrounding water pressure. The descent using the 8 wire jacks took hours, much longer then expected, and lessons were learned for future installations.

The buoy was tied down to the WEC during the installation. This was done because there could not be any generated voltage in the end of the cable attached to the generator when it was joined to the land side of the cable. The cable from the research site to the measuring station had been laid out a few weeks before the installation of the WEC, and when the WEC had been lowered to the bottom, both loose ends were brought to the surface and spliced together. When this was completed and the cable was lowered to the sea floor,

the buoy was released and the wave energy converter was in operation for the first time. At that moment the first voltage signals, showing that the generator had survived the transportation to the west coast and the descent to the seabed, were measured at the measuring station. The installation of the converter is presented in greater detail in Paper XI.

4.3.4 A sample of results

A lot of experience has been gained from the experiments performed on the WEC through the years. The general behavior of the generator is seen in Fig-
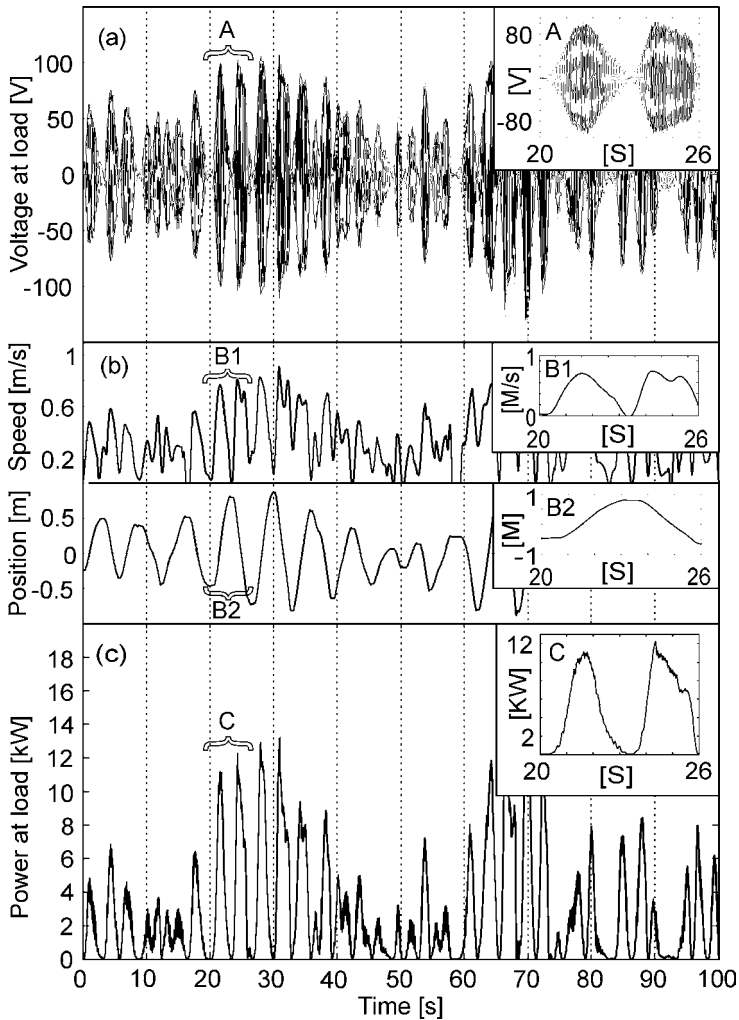

Figure 4.10: Experimental results. Generated voltage, translator speed and position, and generated power from the wave energy converter. The small pictures within show a closeup of a time window of a few second representing one whole wave, wave crest and wave trough. Paper II.

ure 4.10. In these experimental measurements it is clear how the amplitude and frequency of the generated voltage varies as the translator moves at various speeds and alternating directions. The generated power is a direct consequence, i.e. the faster the movement, the higher the generated power, and since the translator has to stop in order to change direction the power drops to zero at the top of every wave crest and at the bottom of every wave trough.

During the first operational period, which has been the main focus in the papers presented in this thesis, the generator was subjected to a large variety of loads. In particular, delta coupled resistive loads of 2.2, 4.9, or 10 Ω were used during long periods of time and consequently in many different sea states. The average power absorption during various sea states and these three loadings is given in Figure 4.11. In the figure, each mark represents one half hour average of absorbed power and the corresponding sea state given in energy flux per meter. Because the frequency of the generated voltage is relatively low, and because the mechanical losses were not measured before installation at the wave energy research site; iron losses and mechanical losses of the generator have been ignored as a rule. The absorption values of Figure 4.11 thus only represent the copper losses in the generator and sea cable, and the energy dissipated in the dump load at the measuring station.

Describing the load on the generator in terms of resistance values can be a bit ambiguous. A better way of describing this is to translate the loads into *damping factors*. The damping factor is here defined as force per speed:
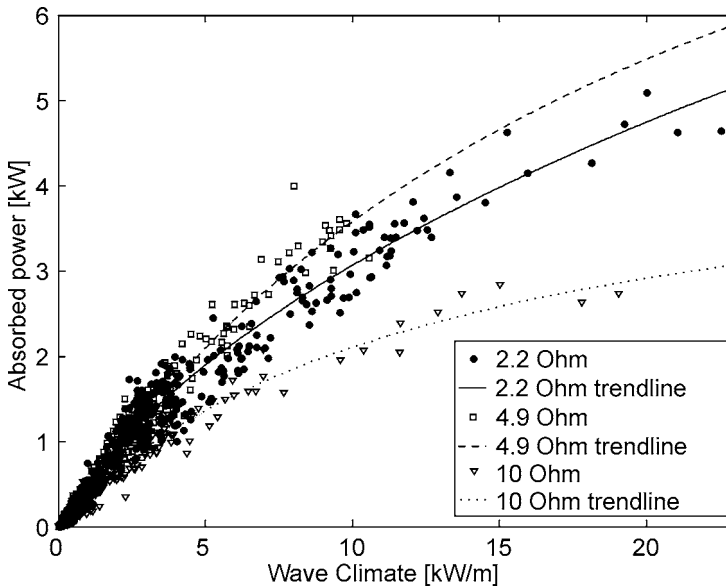

Figure 4.11: Absorption results over a long time period as a function of sea state. Each mark represents a half hour average of absorbed power (copper losses and dump load only, i.e. no iron or mechanical losses). Paper II.
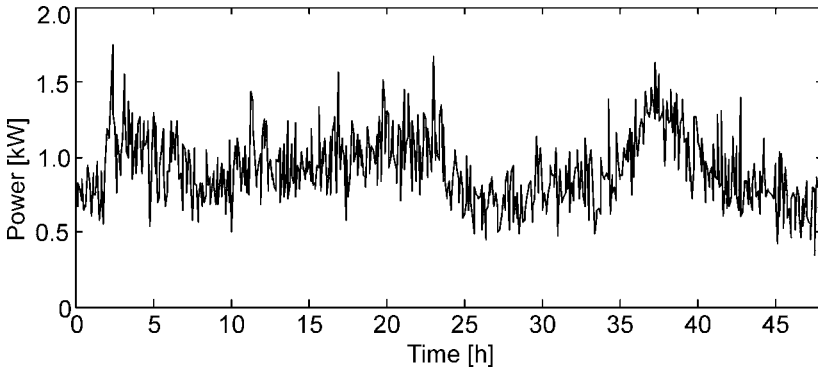
Figure 4.12: The variation of power output over several hours. Paper VIII.

$$k_{damping} = \frac{F}{v} = \frac{P}{v^2} \tag{4.1}$$

where F is force, v is speed, and where the known relation that power, P, equals force times speed has been used. The lower the resistance value, the higher the induced currents and the stronger the retarding force from the stator on the translator. This definition was used in Paper III instead of the ohmic values. From experimental measurements of speed and generated power it was found that 2.2, 4.9 and 10 Ω expressed as damping factors become 12.7, 8.53 and 5.23 kNs/m respectively.

A sample of the generated power output, after it has been rectified and filtered with a high capacitive filter, is given in Figure 4.12. This figure is also presented in Paper VIII and shows how the strongly fluctuating power input can be converted to a significantly smoother power output, which is a first step toward grid connection.

Much has been learned regarding the operation of the WEC. For example: It has been found that for purely resistive loads, the optimal load, or damping factor, does not vary with wave climate. Moreover, the absorption of the energy in the waves, disregarding absorption to cover for iron losses and mechanical losses, reached at most a half hour average of 24% for one of the buoy-generator-load configurations of the first operational period. Furthermore, maximum translator speed and standard deviation of generated power were shown to decrease as the damping factor is increased. The knowledge that has been gained through the studies that have been performed can be used to apply loading strategies on the WECs in order to control their operation, e.g. if it is desired to decrease physical stress levels on a machine during particularly high waves, see Paper III.

4.4 Impact on and from the environment

The ocean is a harsh environment for constructions, and some of the challenges faced, such as the problems with corrosion, have previously been discussed in Sections 1.4 and 4.1.2. Another challenge is the interaction between biological life and the survivability and operation of offshore structures, and this can take different shapes, positive or negative, depending on technology and organism. The interaction between wave energy devices and the marine environment is described in [50, 90, 91].

Wave energy converter technologies may contain potentially harmful components, e.g. hydraulic oil or poisonous paints, that can get released to the environment. Great care has to be taken in order to avoid the risk of these potentially negative environmental impacts. It would be truly sad if wave energy, the purpose of which is to provide a positive contribution to the world's societies by providing clean energy, had adverse environmental effects.

The occurrence of unwanted biological growth on constructions at sea is called *biofouling*. In this case, organisms have found a place to live on the construction, but in a way that may be negative to the operation or survivability of the structure. Since most wave energy converters have moving parts they are particularly vulnerable compared to rigid structures. Especially hard organisms, such as barnacles, may be damaging to the moving parts of the converter, and they are often not easily removed. Figure 4.13 shows organisms growing on one of the biology buoys mentioned in Section 3.3. The types of organisms that can cause problems to the WECs will vary with location in the world and with depth. The greater the depth, the smaller the problems of biofouling are likely to become. Figure 4.14 shows how the abundance of some organisms vary with depth around Sweden.

On the positive side, wave energy converters may provide habitats for organisms in a way that is not harmful to the converters operation. In this case

Figure 4.13: Example of biofouling on one of the *biology buoys* at the Lysekil wave energy research site.
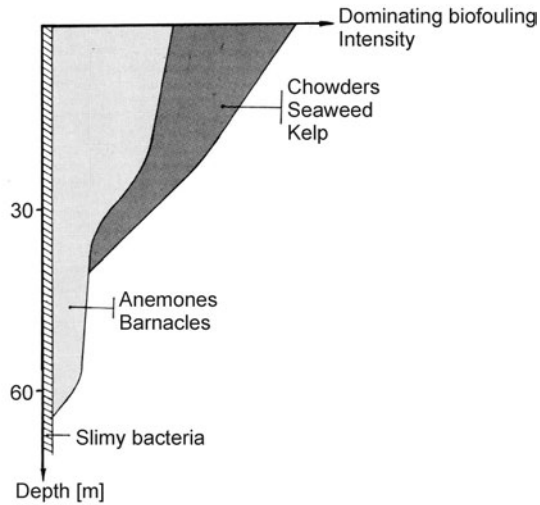
Figure 4.14: Illustration of how the abundance of some common organisms around Sweden vary with depth [14].

the WECs serve as artificial reefs, making the local environment more diverse, complex, and a protected home for many more species than resided there before the construction. A park of WECs is likely to be off grounds for some types of fishing, e.g. trawling, and the park may consequentially become a spawning area for fish. Figure 4.15, next page, shows a collage of organisms found living on or around the wave energy converter in Lysekil.

Figure 4.15: A sample of the biological life on the wave energy converter.

5. Generator air gap measurements

The distance between the moving translator (or rotor in a conventional machine) and the static stator is called the *air gap*, see Figure 5.1. The air gap is a critical design feature in an electrical machine since the translator and stator cannot be allowed to connect, which places high demands on the tolerances and the strength of the construction. In the linear generator discussed in this thesis it is particularly challenging because of the large forces between the translator and stator due to the powerful permanent magnets on the translator. At the same time, however, a small distance is beneficial because it reduces the required size of the relatively expensive permanent magnets, as seen in Eq. 2.13.

5.1 Sensor design

Because of the large forces in the linear generator it was decided that a sensor be designed for the purpose of monitoring the air gap, potentially over the course of many years on the seabed. High demands were placed on the sensors because there will be no means of reaching them for reparation and maintenance once they are on the seabed. A single coil etched on a printed circuit board, PCB, was chosen as the basis for the sensor for a number of reasons. This type of sensor does not need an active power supply since it functions
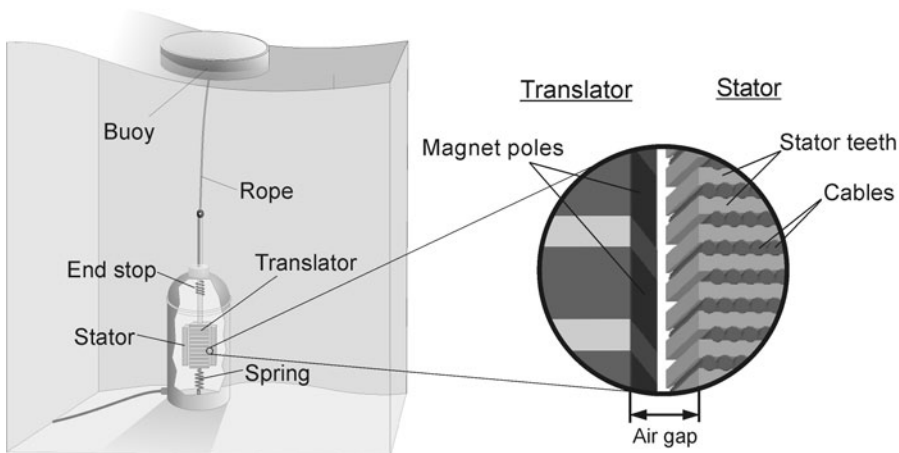
Figure 5.1: Conceptual drawing of the wave energy converter together with a detailed view of the air gap.
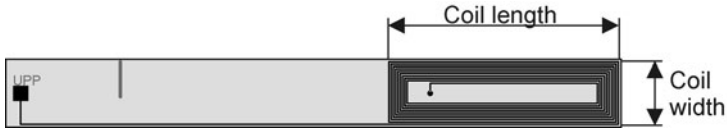
Figure 5.2: One side of the search coil sensor used to measure the air gap width of the linear generator.

through induction. Furthermore, it is a simple device as well as cheap and robust. Etching the coil on a printed circuit board also allows for the manufacturing of very precise and thin coils, thin enough to fit inside the air gap.

The resulting sensor is made of a rectangular coil etched on a two sided PCB with ten coil turns on each side. The coil has a maximum length of 30.3 mm and maximum width of 8.1 mm. The PCB is 0.36 mm thick. The sensors are glued to the front of stator teeth in the air gap, facing the magnets. Figure 5.2 shows one side of the sensor. Paper IX is based on experiments performed with the sensors on the laboratory generator.
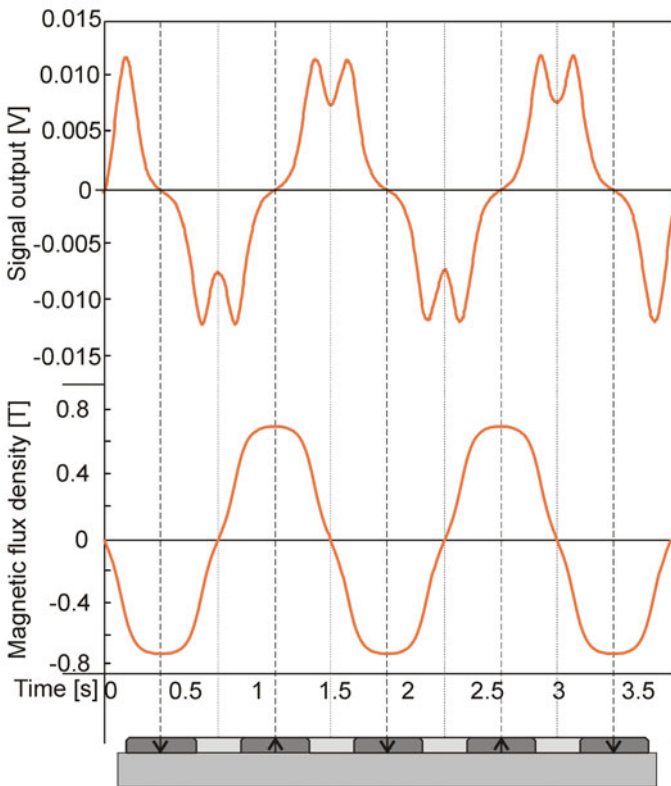
Figure 5.3: An illustration of how the search coil signal is created from the passing of translator mounted permanent magnets of alternating polarity.

80

5.2   Sensor operation

As the translator moves the sensors experience a change in the magnetic flux passing through the coil and this induces a voltage in accordance with Faraday's law, Eq. (2.14). Figure 5.3 illustrates how the sensor signal is generated from the magnetic flux density, **B**, produced by the permanent magnets. In the theoretical simulations of the sensor, however, Faraday's law was not used directly. Instead, Eq. (2.15) was used on each individual straight section of the rectangular coils and their individual contributions to the sensor signal were summed. This allowed for a more detailed and accurate simulation of the sensors. The purpose of these experiments was to test and verify the theoretical sensor simulations to facilitate the interpretation of the signals of sensors mounted on generators at sea.

The manner in which the magnetic flux density in the air gap changes as a function of its width was derived in Section 2.1.5. This derivation shows that the amplitude of the induced sensor signal is affected by the size of the air gap in addition to the speed of the translator.

5.3   Interpretation of data

There are various ways in which the experimental and simulated sensor signals can be compared. The method decided upon was to calculate the definite integral over a time interval of an experimental signal, and compare the result to the definite integral over the corresponding time interval of a theoretical signal. The region between two zero crossings was the chosen interval. In other words, the areas between the signal and zero were calculated, see Figure 5.4. The resulting positive areas from the experimental signals were compared to the positive areas from the theoretical signals and, accordingly, the negative
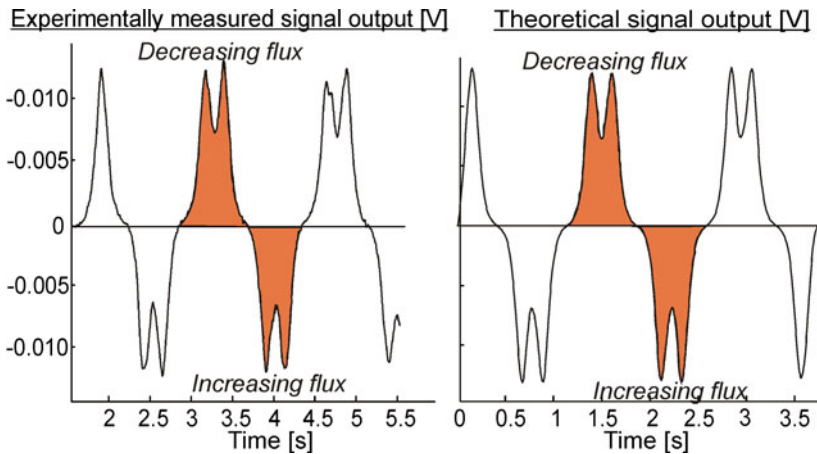

Figure 5.4: An illustration of the integrated signals, and their corresponding areas, used to compare theoretical and simulated sensor signals.

areas from the experimental signals were compared to the negative areas from the theoretical signals. The results of the comparison and the evaluation of the sensor is given in Paper IX.

The main benefit of the chosen method is that as the signal is integrated over time it removes the time dependence of the resulting value. This means that the translator speed, at which the signal was collected, is of no importance. From observing Figure 5.3 and recalling Faraday's law, Eq. (2.14), one sees that the positive areas are equivalent to the value of decreasing flux from the middle of one row of magnets to the middle of the next row. Similarly, the negative areas are equivalent to the value of increasing flux from the middle of one row to the middle of the next. An example of an experimental signal compared to the corresponding simulated signal is provided in Figure 5.5. The experiment was somewhat disturbed by the cement pillar used to guide the translator, as noted in Section 4.2. The results are likely to have been much more accurate had it not been for the weakness of the pillar and its inability to maintain a constant air gap. Still, the resulting sensor can, based on the performed experiments, measure the air gap width with an accuracy of ± 0.4 mm at a confidence level of 95%.

As described in Chapter 9, two more WECs are currently under construction and will soon be installed at the research site. The search coil sensors have been installed in the generators of these WECs.
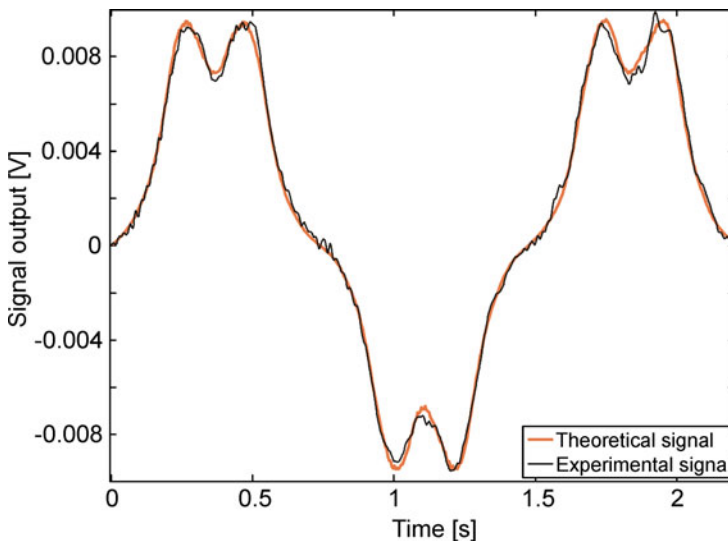

Figure 5.5: Comparison of theoretical and experimental signals at 7.0 mm air gap. Paper IX.

6. Wave climate studies

A wave energy converter needs to be dimensioned to its intended wave climate just as the generator of a hydro power plant is dimensioned with regard to the head of its dam. Knowledge of the average sea states and extreme waves are vital, and a natural and important step in designing a wave energy converter for a particular location is therefore to determine the wave climate of the site. This is important, not only to ensure that the WEC will survive, but also to optimize its economical competitiveness.

During Sweden's previous high period of wave energy research, in the late 70s and 80s, several studies were performed that aimed at describing the wave climate of the waters surrounding Sweden; the Baltic sea, Kattegatt and Skagerrak. Actual measurements were performed at some sites using devices such as echo sounders or wave measuring buoys [92]. The first wave measuring station was started in 1978 near the lighthouse Trubaduren outside Gothenburg on the Swedish west coast [93]. In later years three other stations were started, at Fladen and Näsö near Trubaduren, and one station further north at the island Väderöarna. Other than at these stations no other wave measurements were conducted on the west coast. Although the measurements of these sites were used to calibrate hindcast models, i.e. simulations of wave climates based on wind measurements, it was felt, within the Lysekil project, that a newer and more detailed study was motivated that focused on the Swedish west coast wave climate. A sample of wave climate studies in other parts of the world is given in [94–96], and studies on the Baltic Sea, off the east coast of Sweden, are found in [29, 30, 97, 98].

6.1 Describing wave climates

A particular *sea state*, i.e. the waves appearing at a location over a relatively short period of time, is generally described by its significant wave height and energy period (or sometimes average period), see Section 2.2.4 for the definitions. If the deep water approximation can be used then this information not only gives the values of wave height and period, but also the average energy flux. The long term wave characteristic of the same location, called the *wave climate*, is generally given only in terms of the average energy flux. The reason for this is that values of significant wave height and energy period become more and more ambiguous with time. They are average values derived from wave spectra, and the spectra represents sea states with waves ranging from no waves at all during calm days to extreme waves in storms.
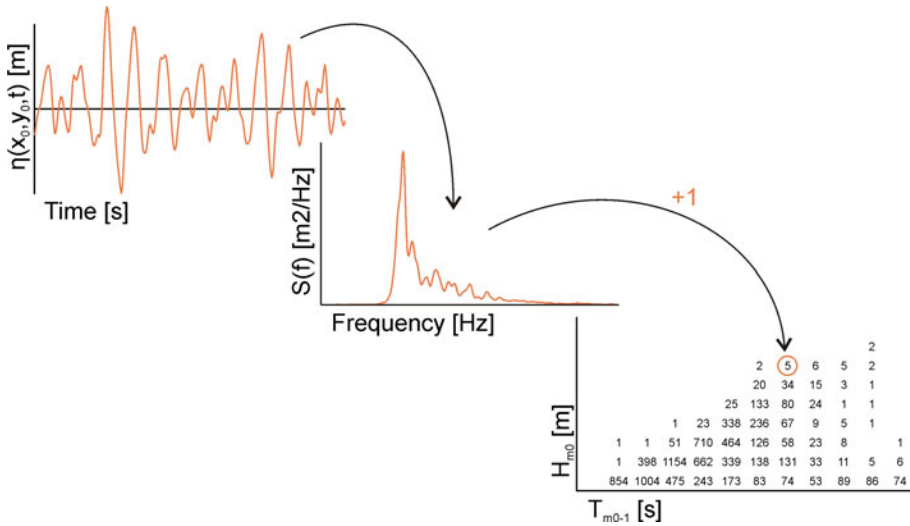
Figure 6.1: Illustration of how a scatter diagram is created. Measurements from a wave measurement buoy are converted to wave spectra, and the wave spectra is used to determine the sea state in terms of the significant wave height and energy period.

The above parameters used to describe sea states and wave climates can be found through several methods. Direct buoy measurements and hindcast modeling were mentioned above, and another common method is to use satellites placed in circular orbits which measure the sea state of a particular location each time it passes over it. The linear wave theory presented in Chapter 2 can be used to derive the wave parameters from raw surface elevation measurements of wave measurement buoys. The wave elevations are converted to wave spectra, $S(\omega)$, through Fourier transforms, and the parameters are calculated from the spectra using the definitions provided in Section 2.2.4, See Figure 6.1 for an illustration of the process. Common time intervals for sea states is one half hour or one hour.

The picture to the far right in Figure 6.1 is called a *scatter diagram*. Scatter diagrams give a much more detailed picture of the wave climate of a particular site compared to the previously mentioned single value all-time average energy flux. Each number in the above example represents the number of hours per year that a certain sea state, in terms of wave height and period, appears. The diagram clearly shows the most powerful sea states, the calmest sea states, and how often they occur. Due to lack of data or lack of publishing space, however, the overall average energy flux is usually the only information given, and scatter diagrams are rarely presented.

6.2   The Lysekil research site

Although known among locals as being a rough spot with high waves, the Lysekil wave energy research site is relatively close to shore and the depth is
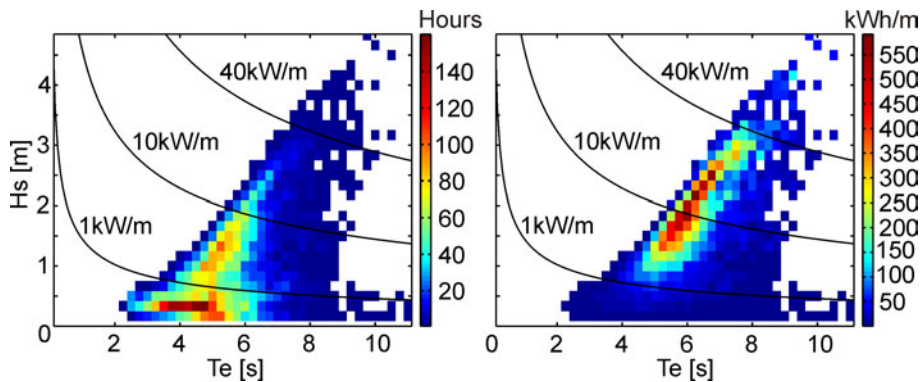
Figure 6.2: The occurrence of sea states measured in hours (left picture), and cumulated energy measured in kWh/m (right picture) as a function of significant wave height and energy period at the Lysekil wave energy research site. The data covers all of 2007, excluding August. Paper XI.

only about 25 m. Due to this and the bathymetry of the seabed surrounding the research site, the predominant direction of the waves that enter the site is directly from the west, and the average energy flux is relatively low, even compared to Swedish west coast standards a short distance further offshore.

A wave measurement buoy was installed at the research site in 2004. Since then it has been in continuous operation with only short breaks for the changing of batteries. Its measurements have been used to study the wave climate of the site in the way illustrated in Figure 6.1. Scatter diagrams resulting from measurements over all of 2007 excluding August is given in Figure 6.2. The average energy flux during this time period was 3.4 kW/m.

Figure 6.2 shows an alternative to the basic scatter diagram described above. The scatter diagram of Figure 6.1 shows the distribution and the prevalence of the different sea states. It does not immediately show where the energy is found, which, in wave power applications, is among the most interesting things to know about a potential site. In Figure 6.2 the previous scatter diagram is combined with a different type that focuses on the energy. The diagram presents the accumulated total energy appearing at the site as a function of sea states. It is seen that most sea states have very small waves and that the total energy contained in them over a year is very little. Instead, most of the energy is contained in the sea states with much higher waves. At the research site, during this year, most of the energy was found in sea states with wave heights of around 2 m and energy periods of around 6 s.

6.3 The Swedish west coast

In order to get a detailed understanding of the wave climate of the Swedish west coast a more thorough study was performed that included another 12 sites in addition to the research site. The location of these sites are spread out over
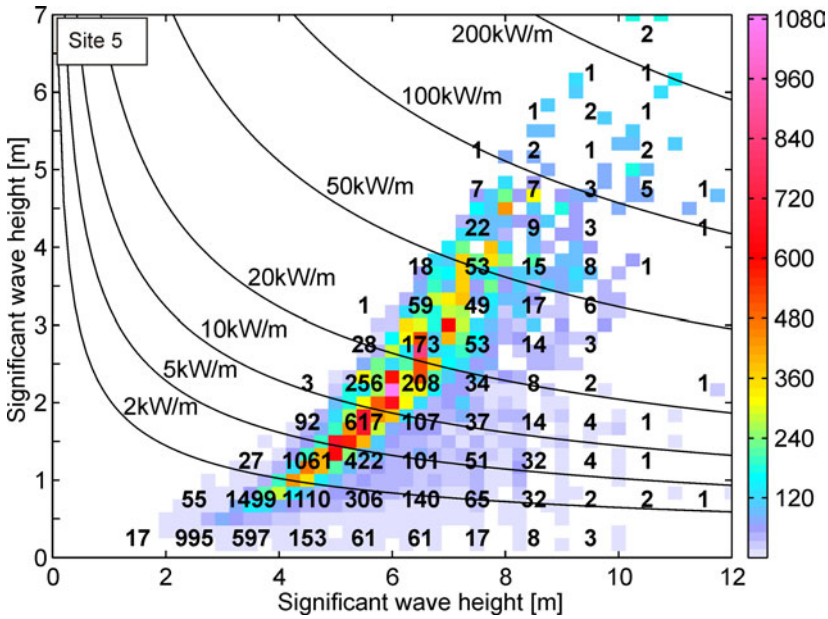
Figure 6.3: Combined scatter and energy diagram for an offshore site on the west coast, i.e. site 5 of Paper X. Colors show annual energy transport per meter of wave crest [kWh/(m·year)]. Numbers give average occurrence of sea states in hours per year. Isolines present the energy flux according to Eq. (2.56). Results are based on an eight year average. Paper X.

the west coast from north to south and from near shore to offshore. The location of the sites and the results of the study is given in Paper X. The wave data that this study was based on was purchased from Fugro OCEANOR of Norway. The data consists of time series of relevant wave parameters representing one half hour of every six-hour time period during the years 1997 to 2004. The data has been collected through the combined information from on-site wave-buoys, satellites, and a wave and wind model, called WAM, run by the European Centre for Medium-range Weather Forecast [99]. The information from the wave-buoys are used to calibrate the satellite altimeter data, and the satellite data is, in turn, used to calibrate the WAM model. At near shore sites and other sites where the waves are affected by the geography of the sea floor and coast line, a model called SWAN was used on the WAM data in order to further improve the accuracy of the results. A short description of the SWAN model is given in [100].

The results indicate that the average energy flux of northern parts of the coast, i.e. the part that is not shaded by Denmark and is called the *Skagerrak*, is approximately 5.2 kW/m offshore and 2.8 kW/m near shore. For the southern parts of the coast, called the *Kattegatt*, the average flux was found to be around 2.4 kW/m. The study also showed that the most frequent wave direction is from the south west, not surprisingly the same as the most frequent wind direction. Using the theory described in Chapter 2, statistical hundred
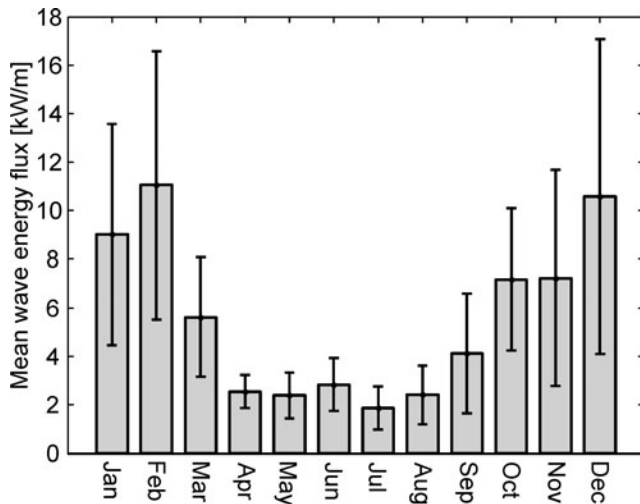
Figure 6.4: Eight year averages of energy flux on a monthly basis together with standard deviations. The site is the same as in Figure 6.3. Paper X.

year extreme waves were calculated from the wave parameters. A scatter diagram combining the corresponding information of the two scatter diagrams of Figure 6.2 for the site furthest offshore is given in Figure 6.3. The difference compared to the milder wave climate of the Lysekil wave energy research site is clearly seen. Figure 6.4 presents how the energy flux varies over the year for the same site. As expected, in the Nordic countries, the summers exhibit relatively small levels of energy flux while the winter half of the year is much more energetic.

When comparing these new results of average energy flux to values presented during the 70s and 80s it is seen that the new values are somewhat lower. These older publications indicate that the average energy flux is 6 kW/m in the Skagerrak and 3 kW/m in the Kattegatt. [14] One source even indicates that the average energy flux of a particular area of the coast is as high as 12 kW/m [93].

6.4 Dimensioning wave energy converters

Deciding which wave climate parameters of a particular site that should be used as the base for the design of a wave energy converter, and the accompanying electrical system to which the WEC is integrated, is no obvious and simple task. On the one hand the entire system should be designed to survive extreme waves, e.g. a fifty or hundred year wave, which can be found through the statistics described in the theory section, Chapter 2. On the other hand, if the system is optimized for these extreme waves then it will operate at power levels more than an order of magnitude lower than its potential most of the time. Such a wave energy converter system would hardly be viable from an
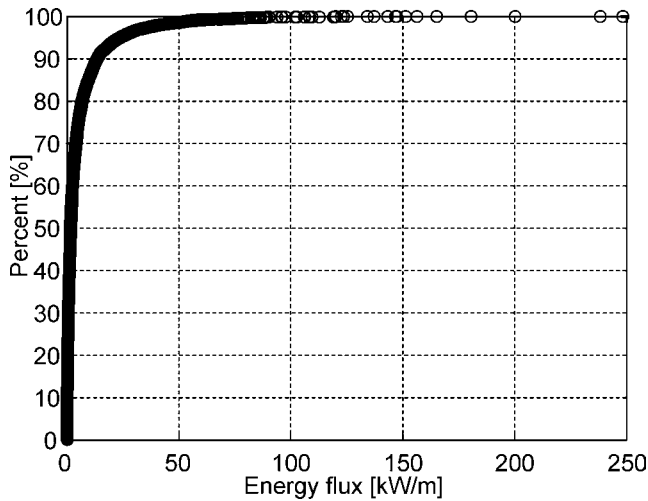
Figure 6.5: Cumulative appearance of sea states as a function of time. The 11688 data points cover eight years. Each circle represents the average energy flux over six hours. Paper X.

economic standpoint. Figure 6.5 presents the cumulative appearance of sea states as a function of time for the same offshore site described in Figures 6.3 and 6.4. The figure shows that although the most extreme energy flux found is close to 250 kW/m, 90% of the time exhibits levels of energy flux lower than 10 kW/m. A possible solution to this problem is to build the system robust or smart enough so that it will survive extreme waves, though at the same time limit the generator and the electrical system so that its optimal power production is placed at a level corresponding to a much more moderate sea state.

Another tempting design point is to optimize the power generation of the WEC system to the average energy flux of the site. However, Figure 6.2 clearly shows that most of the energy is found around sea states with an energy flux much higher than the average, 3.4 kW/m, of that site.

Scatter diagrams in combination with estimations of extreme waves may constitute the best basis for the design of a WEC system. Scatter diagrams provide a large amount of information and also show the distribution of energy over the sea states, see Figures 6.2 and 6.3, in a transparent and enlightening way.

7. Discussion

Although some results have been given in the previous chapters, much of the focus has been on providing a thorough background and surrounding information to the performed research that has not been included in the papers. The previous chapters aim, together with the papers, at providing a full picture of the research that has been performed within the scope of this thesis. The current chapter as well as the next chapter, the conclusion, are based on this full picture.

The Lysekil wave energy project is based at the Centre for Renewable Electric Energy Conversion (CFE) at the Division for Electricity at Uppsala University. Wave energy research at the university began in 2002, and in 2004 the wave energy research site off the Swedish west coast was started. The research site currently has permission to run until 2014, and during this time up to 10 grid-connected wave energy converters and 30 buoys for environmental impact studies will be installed. To date the research area holds one wave energy converter connected to a measuring station on shore via a sea cable, a wave measurement buoy, 15 buoys for environmental impact studies, and an observation tower.

   The experimental data that has been used in the performed studies have been collected with the installations at the research site. The measurements have been carried out simultaneously in order to allow scientific studies. Descriptions of the observed sea states in terms of energy flux, significant wave height, and energy period have been gained through the wave measurement buoy. Force and vertical buoy movement measurements have been collected by force sensors and accelerometers installed on the buoys. The measuring station has recorded the generator's output of voltage and current through which additional parameters, such as generator motion and variance in generated power, have been derived. The wave energy converter has been submerged at the research site for over two and a half years. It has been taken into operation during three time periods over a total of 12 months, the latest being during five months of 2008. During the first two operational periods, a total of seven and a half months, a cylinder shaped buoy with a diameter of three meters was used. During the latest period this buoy was changed to a ring shaped buoy of six meters in diameter. The only problematic area in the operation of the converter that has been seen so far is that the line between the buoy and the generator has broken. Since the start in 2002, four theses have been presented on the wave energy concept: *Simulation of Linear Permanent Magnet Octagonal Generator for Sea Wave Energy Conversion* by Irina Ivanova (licentiate thesis); *Electric Energy Conversion Systems: Wave Energy and Hydropower*

by Karin Thorburn, *Wave Energy Conversion, Linear Synchronous Permanent Magnet Generator* by Oskar Danielsson, and *Modeling and Experimental Verification of Direct Drive Wave Energy Conversion. Buoy-Generator Dynamics* by Mikael Eriksson (doctoral theses).

The present thesis can be divided into four main areas. Most important is the first wave energy converter (WEC) of the concept for wave energy conversion studied at Uppsala University. It has been designed, constructed, and installed offshore, and its function has been successfully verified. To date more than 12 months of data has been recorded from the WECs operation at sea. The work incorporated in this has represented the bulk of the work performed throughout this thesis. The three other areas discussed are the design and verification of a sensor for measuring the air gap of the WECs generator, a detailed study of the wave climate off the west coast of Sweden, and how energy technologies may be compared through the concept of utilization.

7.1 The wave energy converter

Much knowledge has been gained through the extensive work performed on the WEC at the Lysekil research site and the numerous studies performed and published on various aspects of the device and on the wave energy concept as a whole, see e.g. Papers I – VIII and XI – XIV. These experiences and observations have served to move this technology on the path toward a renewable energy technology that may become an integrated part of the energy system. The experiences gained also function as a platform and guidance for future research on this ocean wave energy concept. The papers presented in this thesis illustrate the function of the studied and constructed wave energy converter, these discoveries are summarized below.

7.1.1 General behavior – AC

The motion of the WECs generator mimics the motion of the ocean waves and this results in a direct coupling of the motion of the point absorber to the dynamics of the electromagnetic energy converter. This direct drive system reduces the mechanical complexity of the converter since no mechanical energy conversion steps are required between the buoy and the generator. However, the mechanical simplicity has repercussions on the electrical system.

Unlike conventional generators running at constant speed, the motion of a linear generator will vary in speed and direction, and the generated voltage and current will have varying amplitude, frequency, and phase order as a result of this, see Figure 3.3 in Section 3.2. The output from the generator will vary with the speed of the point absorber, leading to large fluctuations of power on the second scale and power peaks that will reach levels several times higher than the average power production. This has implications on both the individual generator and on the system as a whole. A lesson learned from this is that the

generators have to be dimensioned with the ability to handle large variations in power in relation to the average generated power.

No direct measurements were performed on the position or motion of the translator. The position of the translator can, however, be calculated from the generator pole configuration and the phase order of the windings. A change in phase order of the generated voltage signifies a change in its direction of motion. Furthermore, every voltage period represents a movement of two pole widths in length, i.e. 0.1 m. This has been used to calculate the speed and position of the translator, which is an important aspect in the understanding of the WEC operation. See Figure 4.10 in Section 4.3.3.

7.1.2 General behavior – DC

The highly fluctuating output generated by the WEC needs to be converted before it is transmitted to the electric grid. The general strategy for this is to first rectify the electricity and then invert it to the desired constant frequency and transform it to the desired voltage level, as described in Section 3.2 and Paper VIII. The first step, rectification with a filter for power smoothening, was achieved in the spring of 2007. This allows the WEC to generate electricity against a DC load, which has several fundamental consequences for the operation of the WEC.

During shorter periods of time, approximately 10 s, the ultra capacitors of the filter will, due to its large energy storage capacity, give a similar effect as if the generator was connected to a DC bus with a constant voltage level. This changes the dynamics of the WEC in at least two ways: First, the rectifier will only conduct when the voltage of the generator is slightly higher than that of the DC bus. Second, when the rectifier conducts, the damping factor will vary in a nonlinear fashion as a result of the DC bus acting as a varying resistance. By contrast, in the AC load case the damping factor is constant.

The DC bus voltage determines the speed with which the translator has to move in order to deliver energy to the load. A consequence of a high DC bus voltage is thus that the translator must have a high speed in order to produce energy to the system, and no energy is being generated at all if the speed is to low. Unlike the AC load where power is continually being generated and the translator motion dampened correspondingly, in the DC case the translator will be allowed to accelerate unhindered until it reaches the voltage level of the DC bus. Because of this, the speed curve corresponding to a DC load, see Figure 3 in Paper VIII, will be more rectangular compared to the corresponding AC curve, see Figure 2 in Paper II.

A difference in the operation of the generator can also be seen in the voltage and current pulses. By comparing Figure 3 to Figure 2, in the above papers, it is seen that the voltage pulses in the second figure are somewhat rounder, which is a direct consequence of the linear load. The linear load also leads to the shape of the generated current, which has more or less the same shape as the voltage. Conversely, as seen in Figure 7.1, the level of the DC bus voltage will limit the amplitude of the generators phase voltage. The current, on the
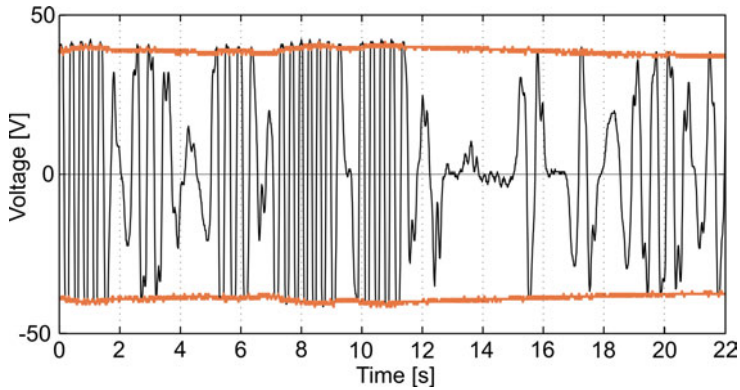
Figure 7.1: The DC bus voltage (orange line) limits the amplitude of the generated voltage. Paper XI.

other hand, will vary to a great extent and its curve form will be very different from that of the voltage, see Figure 3 in Paper VIII.

With the current experimental set-up it has been shown that long term, slowly varying, power generation is possible, see Figure 4 in Paper VIII. In the future, several WECs will be interconnected at the Lysekil wave energy research site, and the power from all of the generators will be rectified and fed into a common DC bus.

7.1.3 Control

The hydrodynamic behavior of the point absorber depends, to a large extent, on the damping of the generator. The damping, in turn, can be controlled remotely by changing the load. In Paper III load control strategies, and how these may influence the dimensioning criteria of the electrical system, were studied.

There are many factors that influence the design of a WEC. The peak power levels submitted to the generator affect the overload capacity that the electrical system needs to be designed for. The speed of the generator not only determines the generated voltage level, but also the dimensioning of the end stops since the kinetic energy of the translator is directly related to the stress level that the end stops and the WEC structure need to be designed to handle. Moreover, the variance of the generated power of one WEC will have an impact on the farm system behavior in terms of the overlapping power pulses of many interconnected WECs. This will also determine the required size of the capacitive filter.

In Paper II it was found that, among the three tested loads, the highest average power was achieved with the 4.9 Ω load. Paper III showed that, for the AC load case, the delta coupled resistive dump load with resistance values of 2.2, 4.9 and 10 Ωs, corresponded to constant damping factors of 12.7, 8.53, and 5.23 kNs/m, respectively. The study showed that the peak power level is approximately proportional to the average power, and that maximum transla-

92
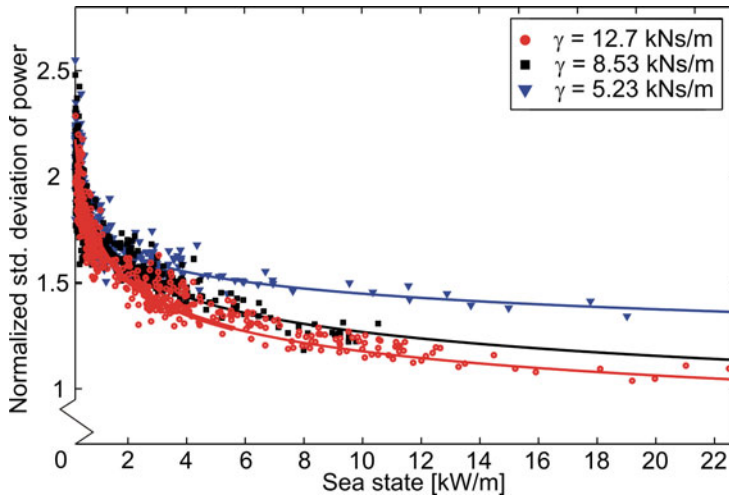
Figure 7.2: The variance of power as a function of damping factor. The lines are least square fits. Paper III.

tor speed and the variance of the generated power decrease as the damping factor is increased, see Figure 7.2. Hence, during the most energetic sea states when the translator reaches the end stops and the peak instantaneous powers are very high, a suboptimal damping factor can be chosen. In this case a large damping factor should be chosen in order to reduce both the maximum instantaneous power levels and the maximum translator speeds.

As for the DC load case, by regulating the DC level the speed of the translator and the generated current can be controlled, and this control of the DC bus voltage will be a key parameter for the wave energy concept, e.g. when the power output is to be maximized. So far the DC level has not been actively controlled but has been a slowly varying consequence of the sea state and the dump load connected in parallel with the capacitive filter. When the DC level can be controlled it may be kept at a relatively lower level, thus allowing the generator to deliver energy during a larger portion of the time and increasing the overall produced energy.

7.1.4   Survivability

The generator is located on the ocean floor to avoid the direct impact of the large powers of the ocean. The buoy point absorber on the surface is a relatively cheap and insensitive component. Furthermore, a directly driven generator circumvents the need for gearboxes, a component in need of regular maintenance and with a relatively high risk of failure, something which has been learned the hard way in the wind industry [101].

The force and buoy acceleration data in Figure 8 of Paper XI and Figure 7.3 provide detailed information on the operation of the WEC. The measurements have been used to study maximum line forces, which also cause maximum material stress in parts of the structure. The knowledge gained from these
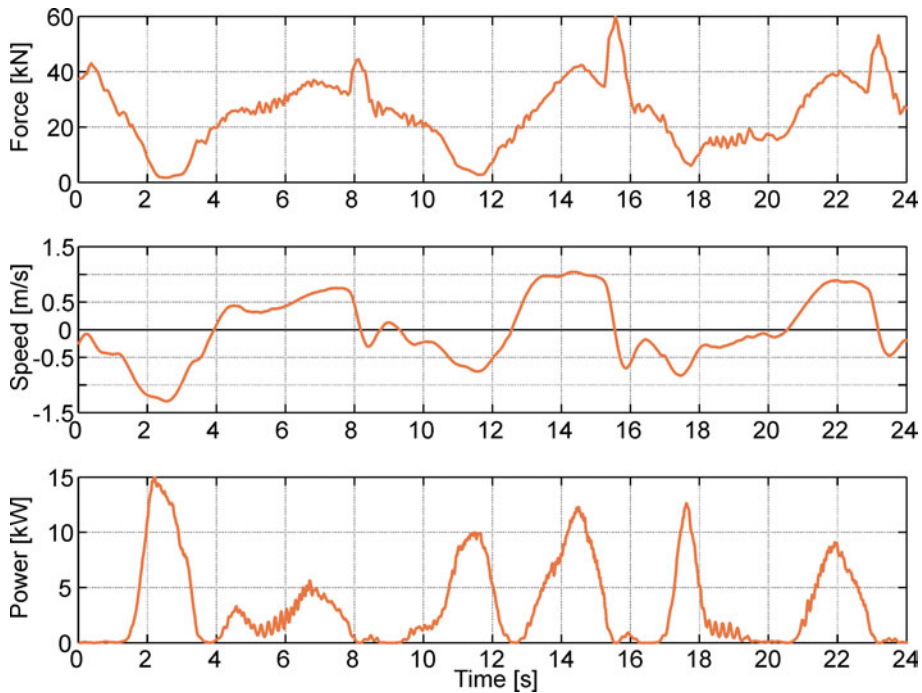
Figure 7.3: The force, as measured by a force sensor mounted between the line and the buoy, the speed of the translator, and the power generated by the WEC. Peaks in the force, where a corresponding peak in speed and power is not seen, correspond to the linear generator hitting the upper end stop.

types of measurements can be used to find stress levels to be used in fatigue calculations, and for material optimization in general. As noted in the control section above, an energy-wise suboptimal damping factor can be chosen to decrease the movement of the translator and the corresponding stress subjected to the WEC. Figure 7.3 shows simultaneous force, speed and power measurements where force peaks indicate that the linear generator has connected with the upper end stop.

Wave energy conversion demands robust technology that can handle the many challenges, e.g. large peak powers and corrosion, associated with ocean waves, see Section 1.4. The presented concept for wave energy conversion aims at handling overloads electrically instead of mechanically. This is believed to increase the survivability of the plant since electrical components are known to be reliable, relatively insensitive to wear, and much cheaper to dimension against extreme loads compared to mechanical parts.

7.1.5 Energy absorption

The optimal load for maximum energy absorption will, off course, vary with each specific configuration of generator, buoy, and electrical system. In Pa-
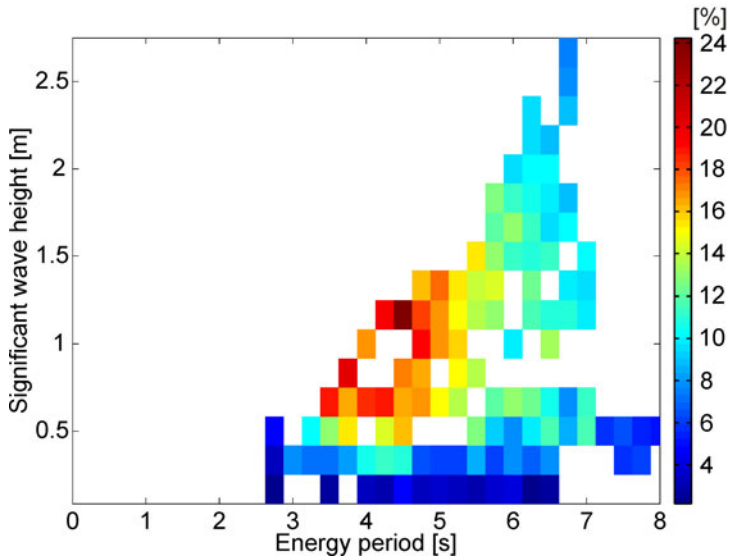
Figure 7.4: The absorption, in percent of the total energy flux, as a function of significant wave height and energy period.

per IV it was shown that linear potential wave theory could successfully be used to model the absorption of this wave energy converter.

Paper II presents the first published results on the absorption of the WEC for different damping factors. The results, encompassing 2386 half hour averages of recorded absorption, implies that the optimal load in the AC load case is independent on wave climate, see Figure 3 in that paper. An important trend, presented in the same paper, is a decrease in relative power absorption for more energetic sea states. Although the absolute value of absorbed power continues to increase with the energy level of the sea states, the trend is evident, see Figure 3 again. This effect is likely due to the longer wave periods of more energetic sea states and their impact on the translator speed. A secondary cause may be the finite lengths of the translator and stator. During long stroke lengths part of the stator will be left inactive during part of the wave period, and this effect increases with the stroke length, i.e. the wave height.

A more detailed study of wave energy absorption is presented in Paper V. Here, the absorption, in percent, as well as the total absorbed power was plotted as a function of wave height and energy period. The data used was from the first months of operation in 2006 when the buoy used had a diameter of 3 m. The study showed that the absorption has a clear and relatively flat peak over a range of wave heights and energy periods centered around a wave height of 1 m and an energy period of 4.5 s. The location of this peak did not vary between the three damping factors applied to the generator. The absorption reached a maximum of approximately 24% excluding iron and mechanical losses, see Figure 7.4.

Due to the finite lengths of the translator and stator it was anticipated that the WEC would be sensitive to changes in mean water level. When the trans-

lators middle position is shifted away from the center of the stator, relatively small waves will cause the translator to begin to leave the stator, rendering part of it inactive. A study of this is presented in Paper VI. The study shows that the WEC clearly is sensitive to changing water levels, but only for deviations larger than 25 cm. Since approximately 85% of the year exhibits water level deviations that are smaller than 25 cm this does not compose a problem at the current site. This is also believed to be the case for the Swedish west coast in general.

The sensitivity to water levels as well as part of the decrease in relative power absorption at more energetic sea states are due to the finite lengths of the translator and stator. Increasing the length of these components would improve the absorption at locations where these factors would present a problem. The associated costs of building a longer machine, however, have to be considered and evaluated against the increase in energy absorption.

As for the overall energy absorption, a larger buoy would capture more energy and, as indicated by [59] a correspondingly higher damping factor of the generator would enable the generator to produce more power. There are many parameters that contribute to the wave energy system as a whole, the potential is large and as the research continues there are a number of areas that will see improvement.

7.2   Air gap measurements

The very low speed of the linear generator has consequences on the size of the machine. The generator has to be large in order to achieve a high power output. Moreover, since the translator is covered with powerful permanent magnets and with an air gap of only 3 mm, the forces between the translator and stator become large. The WECs are intended for years of uninterrupted operation on the sea floor and, for the purpose of monitoring the stability of the air gap during this time, a sensor was designed. The sensor, called a search coil sensor, is composed of a coil etched on a printed circuit board. It measures the air gap through induction caused by the dynamic magnetic fields between the translator and stator. The sensor is presented in Paper IX.

Chapter 5 together with Paper IX give a detailed description of the operation of the sensor and the results from the experimental verification of the theoretical results. The study showed that whereas the theoretical signal was symmetric, the second peaks of the experimental "double peaks" were systematically 5% – 10% higher than the first, see Figure 6 in Paper IX. A probable explanation for this asymmetry is the magnetic hysteresis of the stator and translator steel, which dampens the rate of change of the flux at the beginning of the cycle and accelerates the rate of change towards the end. Hysteresis is ignored in the numerical model, hence the symmetri of the theoretical signal.

A method for handling and evaluating the signals was developed. It studied the definite integral over each part of the signal separated by two zero crossings. This approach has many advantages. Integration evades the time

dependence of the signal, meaning that the speed with which the translator is moving as the signal is picked up is of no consequence if eddy currents are negligible. Integration also decreases errors due to high frequency noise. The influence of hysteresis is also avoided since the integral gives the difference in peak flux between two adjacent magnets, which is unaffected by hysteresis. Moreover, a definite integral yields a single value, which can be compared directly to a matrix of collected theoretical or experimental integral values corresponding to different known air gaps and load conditions.

There were a number of things that made the study more difficult: The cement pillar used to guide the translator was unstable, making the measurements less accurate; the effect of the longitudinal ends was not included in the finite element simulation tool; and a better instrument for measuring the air gap width should have been used. However, in spite of these obstacles the experimentally measured and theoretically calculated sensor signals showed very good agreement, see Figures 7 & 8 of Paper IX. The set-up had a sensitivity of ± 0.4 mm in the range of $4 - 9.5$ mm air gap.

The potential for future improvements of the sensitivity is believed to be considerable. The most important being:

1. The air gap measurements should be taking place simultaneously with the collection of the sensor signal, and with an instrument of high accuracy.
2. Longitudinal end effects of the translator and stator should be included in the simulation tool.

7.3   The Swedish west coast wave climate

The information that the wave climate studies have been based upon have come from two sources: A wave measuring buoy installed at the Lysekil wave energy research site in 2004, and purchased data covering eight years, 1997 – 2004, for 13 locations off the Swedish west coast.

The WEC results presented in Papers II – VII are based on the data gained from the first operational period of the converter, in the spring of 2006. During this time period the average energy flux at the research site was only 1.37 kW/m, and the most energetic half hour exhibited an energy flux of 40 kW/m. This is very little compared to most coastlines in the world but also compared to the general case in Sweden.

In Paper XI almost a full year of research site wave data was studied. The eleven month average was 3.4 kW/m which was not surprising considering it being a near-shore site and that one of the milder months had been excluded due to missing data. The study showed that most of the energy appearing over the studied period, year 2007, was contained in significant wave heights in the interval of $1.2 - 2.7$ m, and energy periods in the interval of $5 - 7$ s, see Figure 7 of Paper XI. These intervals represent the sea states that are the most interesting in the design of a wave energy converter for this site. Comparing this information to Figure 2 of Paper V gives a hint of how the design of the WEC could be changed in order to increase the energy captured overall.

A detailed study of the west coast wave climate is presented in Paper X. The average energy flux of the studied offshore sites of Skagerrak was found to be approximately 5.2 kW/m. The decreasing water depths closer to shore have a dampening effect on the longer waves, and the result is a decrease in energy flux by half for the near-shore sites. Other important contributing factors are to some extent refraction due to the bathymetry and that winds from the inland do not give rise to waves at these locations. From Figures 3 – 7 of Paper X it is seen that the majority of the highest energy carrying sea states, on a yearly basis in Skagerrak, are found in wave heights in the interval of 1 – 3 m, and energy periods in the interval of 4 – 7 s. At the near-shore sites the corresponding intervals are approximately 1 – 2.5 m and 4.5 – 7 s. In Kattegatt the waves are smaller on average as well as in extremes. The average energy flux is approximately 2.4 kW/m with a higher flux toward the north. For all sites not shaded by Denmark, the dominant wave direction is nearly identical and from the south-west.

The seasonal trend is seen in Figure 8 in the paper. As expected, the winter half of the year exhibits more powerful sea states than the summer half. In a closer study of site 5 in Paper X, out of the studied eight years 33 days had seen average levels of energy flux over 55 kW/m, i.e. ten times the overall average. Seven days out of the studied eight years, exhibited levels of energy flux exceeding 100 kW/m, and the most powerful flux reached a half-hour average of 250 kW/m, a full 45 times higher than the overall average. This clearly illustrates the very large variability in the energy flux of ocean waves.

The statistical study of extreme wave heights estimates that the hundred year, half hour, significant wave height is 6.5 – 8 m at the offshore sites and 4 – 5 m at the near-shore sites of Skagerrak, and 4 – 6 m in Kattegatt. The single highest hundred year waves are estimated to 10 – 13 m for offshore and 6 – 8 m for near-shore Skagerrak, and 6.5 – 9.5 m for Kattegatt. The extreme waves presented here are believed to be biased toward lower wave heights due to the limited record lengths of the available wave data. On the other hand, water depth has not been included in the extreme wave calculations, and this will limit the possible wave heights at some locations.

In the case of site 5 as much as 79% of the annual energy was found in sea states with a higher energy flux than the average 5.5 kW/m. This indicates that WECs optimized to the average energy flux, or sea state, of a site will not capture much of the ocean energy on a yearly basis. Although single parameter studies never tell the whole truth and should be regarded with caution in general, the performed wave climate study illustrates which west coast sea states carry most of the energy. This should be of interest to designers of WECs intended for this area.

7.4   Utilization

The market for renewable energy technologies is hot today due to the efforts of many societies to combat climate change. An ever-increasing number of

technical solutions are suggested by inventors and companies, and sorting out the better solutions from the worse is a difficult task for investors and governmental institutions. Papers XV and XVI discuss the concept of utilization, which can be helpful in these analyses. It is a method that compares renewable energy technologies based on the physics of the energy source and the technology suggested to harvest the energy.

Utilization evaluates renewable energy technologies in terms of their impact on the stability of the electric grid and their energy production or average power in relation to rated power. As long as there is no large scale solution for storing electric energy it has to be produced simultaneously with its consumption. When these start to come out of phase with each other the frequency and amplitude of the grid voltage changes, and large fluctuations are potentially damaging to electric equipment. The best energy source for a stable grid is, because of this, non-fluctuating and controllable, i.e. the opposite of intermittent renewable energy technologies as mentioned in Chapter 1. If the combined rated power, of technologies with low utilization, is high, then the grid needs to have a correspondingly high level of spare capacity in order to fill in the gap between production and consumption at times when the intermittent energy technologies generate less than their rated power. A high utilization thus implies a more stable grid and a smaller need for spare capacity.

The difference between energy and power is particularly important for renewable energy technologies; the rated power drives the cost of the power plant while the produced energy gives the return on investment to the power utility. When dealing with investments in renewable energy technologies the most cost-effective method is thus to energy optimize rather than power optimize. The utilization describes the amount of energy that is produced in relation to the rated power of a technology, hence it is helpful in determining the economics of an investment.

The energy source plays a large role in determining the degree of utilization of a technology. For example, since the sun does not shine during the night the utilization of solar energy installations can never reach a utilization higher than 50%, and probably much less than that since the power from the sun is at its highest only during a small part of the day. Furthermore, since it on average is more windy at sea compared on land, it follows that the utilization for sea based wind power is potentially higher than corresponding land based wind power. However, technology also plays a large part in the utilization. One can choose to match the technology to the energy source, for example by choosing the rated power, rated wind speed, or rated wave climate relative to the available energy at a site, and in this way control the degree of utilization to some degree, see e.g. Figure 7.5. In the end, although being informatory for only part of the basis for a decision, utilization is a helpful tool in the evaluation of energy technologies in terms of grid stability and the return on investment relative the cost of installation.
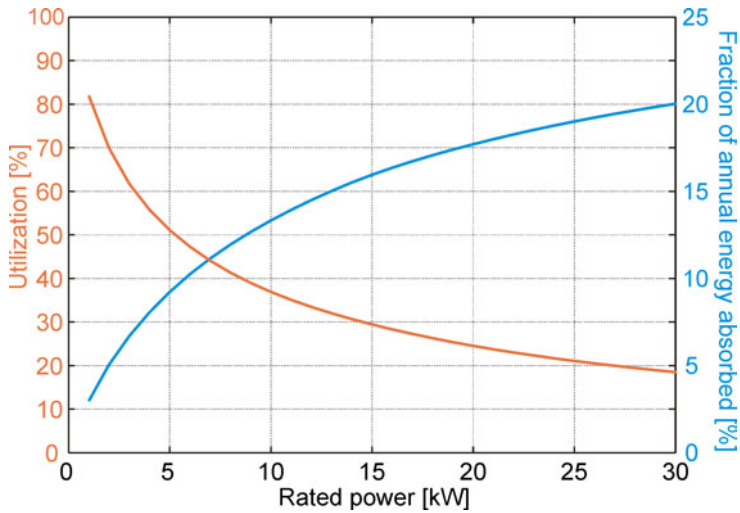
Figure 7.5: An illustration of the impact of the choice of rated power (the capital investment cost) on the utilization (the number of full loading hours) of a WEC. The plot shows utilization as a function of rated power, and the fraction of available energy that is captured by the WEC on an annual basis as a function of rated power. The theoretical WEC has a five meter diameter buoy and captures 25% of the incident energy in a sea state, but no more than the rated power. The wave climate is that of site 5 in Paper X with corresponding sea states given in Figure 9 in the same paper.

8. Conclusion

A wave energy converter has been constructed and its function and operational characteristics have been thoroughly investigated and published, see Papers II – VIII and XI – XIV. The wave energy converter (WEC) was installed in March of 2006 approximately two kilometers off the Swedish west coast in the proximity of the city of Lysekil, about 70 km north of Gothenburg. Since then the WEC has been in operation during three time periods and for a total of 12 months. Throughout this time the generated electricity has been transmitted to shore and operational data has been recorded. The WEC and its connected electrical system has been continually upgraded and each of the three operational periods have researched more advanced stages in the progression toward grid connection in the near future.

The research performed on this wave energy concept aims to understand and evaluate it thoroughly from a physical, technological, ecological, as well as economical point of view. The WEC system has faced the challenges of the ocean and initial results and insights have been reached, most important being that the overall wave energy concept has been verified. With the current experimental set-up it has been shown that long term, slowly varying, power generation from ocean waves, using the presented technology, is possible.

A holistic perspective is strived after in each step in the development of the wave energy concept. In other words, the implications for the entire system, from ocean wave to the electric grid, is taken into consideration in each detail of the system design. This is combined with an effort to keep the mechanics as simple as possible and a desire to handle overloads electrically rather than mechanically. The simple design of the wave energy converter exemplifies this effort. The WEC is based on a linear permanent magnet synchronous generator located in a water tight casing on the seabed, a buoy (acting as a point absorber) on the surface, and a line in between. The generator is directly driven and its motion mimics the motion of the ocean surface. No gearbox or other mechanical or hydraulic energy conversion system is thus needed, and this is believed to reduce maintenance and increase survivability. Furthermore, electrical components are known to be reliable, relatively insensitive to wear, and much cheaper to dimension against extreme loads compared to mechanical parts, which is why an electrical handling of overloads in the system design is beneficial.

Unlike conventional rotating generators the motion of a linear generator will vary in speed and direction, and the generated voltage and current will have varying amplitude, frequency, and phase order as a result of this. For the presented concept the output from the generator will vary with the speed of

the point absorber, leading to large fluctuations of power on the second scale and power peaks that will reach levels several times higher than the average power production. This has implications on both the individual generator and on the system as a whole. The general strategy to handle this is to first rectify and filter the electricity and then invert it to the desired constant frequency and transform it to the desired voltage level.

Experiences from the first two operational periods are presented in this thesis. During the first period, in the spring of 2006, the generator was connected to a purely resistive dump load. This load was varied and the impact of the load on the system behavior was studied. During the second period, five months of 2007, the generator was connected to a DC bridge and a capacitive filter which served to rectify the generated, highly fluctuating AC voltage and smoothen the variations of the DC voltage. During relatively short periods of time, in the order of tens of seconds, the generated DC level was near constant, and during time periods of several hours the DC voltage would vary relatively slowly, following the slow variations of the sea state. A sample of the experiences that has been gained on the presented concept for wave energy conversion is given below.

- For purely resistive loads, the optimal load, or damping factor, does not vary with wave climate.
- The direct drive nature of the generators and the intermittent nature of ocean waves require that the generators be dimensioned to handle large variations in power. By consequence, the average generated power will be much smaller than the peak power levels. The highest recorded power peak so far is 87 kW.
- The average energy absorption over half an hour, in relation to the incident energy flux in the waves, reached at most approximately 24% for the first buoy-generator-load configurations. This does not include absorption to cover for iron losses and mechanical losses.
- A flat region of optimal absorption for the first buoy-generator-load configurations is located around a 4.5 s wave period and 1 m wave height.
- Maximum power levels are approximately proportional to the average power levels.
- Maximum translator speed and standard deviation of generated power decrease as the damping factor is increased.
- Loading strategies can be applied during energetic sea states in order to limit the physical stress on the WEC.
- The WEC is sensitive to variations in mean water levels over a certain level, but because of the predominantly small variations at the research site it is not expected that the concept's sensitivity to mean water level changes will constitute a problem at the studied site, nor at most other locations on the Swedish west coast.
- The DC level of the electrical system will play a significant role when the power production is to be optimized in the future.
- Running the WEC against a DC bus will change the dynamics compared to the AC case in at least two ways: First, the rectifier will only conduct

when the voltage of the generator is slightly higher than that of the DC bus. Second, when the rectifier conducts, the damping factor will vary in a nonlinear fashion as a result of the DC bus acting as a varying resistance.

The combined efforts within the Lysekil project has resulted in experiences and observations that have served to move this technology on the path toward a renewable energy technology that has the potential to become an integrated part of the energy system in the near future. The experiences gained serve as a platform and guidance for the research that is being and will be performed. There are many parameters that contribute to the wave energy system as a whole. The potential is large and as the research continues there are a number of areas that will see improvement in the endeavor to produce an inexpensive, robust technology for the generation of renewable energy from the oceans.

A sensor, intended to monitor the stability of the air gap of the WECs generator during years on the seabed, was developed, see Paper IX. It is composed of a coil etched on a printed circuit board. The *search coil* sensor measures the air gap through the means of the sensed dynamic magnetic fields between the translator and stator. The sensor has been tested on the laboratory generator and the results have been compared with calculations based on finite element simulations. The results show that the air gap width can be determined to a 95% certainty with an accuracy of ± 0.4 mm in the range of $4 - 9.5$ mm air gap. The potential for improvement of the sensor is considerable.

The wave climate off the west coast of Sweden has been presented based on 8 years of wave data from 13 studied sites in the Skagerrak and Kattegat and buoy measurements at the Lysekil wave energy research site, see Papers VII, X, and XI. The mean energy flux was found to be approximately 5.2 kW/m in offshore Skagerrak, 2.8 kW/m in near shore Skagerrak, and 2.4 kW/m in the Kattegat. The highest energy carrying sea states, on a yearly basis, for the offshore Skagerrak are found in wave heights in the interval of $1 - 3$ m, and energy periods in the interval of $4 - 7$ s. At the near shore sites the corresponding intervals are approximately $1 - 2.5$ m and $4.5 - 7$ s. Statistical hundred-year waves have been estimated to range from approximately $10 - 13$ m in offshore Skagerrak, $6 - 8$ m in near shore Skagerrak, and $6.5 - 9.5$ m in the Kattegat. Discussions on WECs conclude that the design sea state should be chosen with awareness of the fraction of available energy in the sea states that is made obtainable to the WEC, which is a consequence of the chosen WEC system design.

A method for evaluating renewable energy technologies (RETs) in terms of economy and engineering solutions, by studying the fundamental physics of renewable energy sources and how it matches with the RETs, has been investigated, see Papers XV – XVI. This match is described by the "Degree of Utilization". It is argued that, if competitive RETs are to be developed, engineers need to match the technology to the physics of the renewable energy source,

resulting in a high degree of utilization. The findings from an extensive review of published material indicate that new innovations should focus on a possible full loading hours, and that this would lead to more economically viable RETs. This, in turn, would enable a faster, cheaper and more long-term sustainable integration of environmentally friendly renewable energy solutions into society.

9. Current and future work

Currently, another two WECs are in the finishing stages of being constructed. They are similar to the first WEC, electrically in particular, but some mechanical details have been changed in response to the lessons learned during the construction of the first WEC. Moreover, a marine substation has been designed and constructed. It will be installed together with and in the close vicinity of the two new WECs, and all three WECs will be connected to it. The substation will rectify, combine, invert and transform the generated electricity, and transmit it to the measuring station at a frequency of 50 Hz and a voltage of 1 kV. This will be an important step toward grid connection.

The buoy used in all experiments that this thesis is based upon has been a 3 m in diameter and 0.8 m high cylinder. The third operational period, not reported here, has performed experiments on a torus, or ring, shaped buoy with a diameter of 6 m. Another three cylinders are waiting to be installed, each with different diameters and volumes. Furthermore, the observation tower has been equipped with a camera that today enables observation of the research site but will, in the future, be used to study the detailed motions of the buoys.

Although the generator has been functioning as planned there is still much that remains to be studied. The effect of the linear generator's longitudinal ends was introduced in [75], but the study could be significantly expanded. Also, as noted earlier, the accuracy of the air gap sensor may be much improved by redoing the experiments with a stable test rig and better measuring equipment.

In the future development of the project, on the road toward expanding the park to include 10 WECs and an accompanying electrical system, there are numerous areas that will need research. Some of these are: energy optimizing the DC level; determining the detailed function and required size of the gravity foundation; describing the interactions between waves and the point absorbers in greater detail; studying the interconnection of several WEC units; and overall improving the combined system characteristics, from the buoy's ability to capture the energy of the waves to the operation of the electric system. Wave energy research spans over many areas of physics, and a successful attempt to harness the energy of ocean waves relies on the interaction between all of these areas.

10. Summary of papers

All of the papers included in this thesis deal with wave energy in one way or another. Paper I describes the linear generator constructed for laboratory experiments prior to experiments at the Lysekil research site. Papers II – VIII and XI – XIV present studies on the first offshore wave energy converter installed at the Lysekil research site. Paper IX introduces a sensor for measuring the air gap of the linear generators used in the WECs. Paper X presents a detailed study of the wave climate of the Swedish west coast. Finally, Papers XV – XVI discuss the evaluation of renewable energy technologies by means of the degree of utilization.

PAPER I

Full-Scale Testing of PM Linear Generator for Point Absorber WEC

The paper describes the laboratory generator that was constructed prior to the first offshore WEC described in later papers. The generator was constructed and tested in order to verify the accuracy of finite element simulations prior to constructing generators for offshore installations. It also gave the opportunity, from an engineering point of view, to test how the very powerful magnets could be handled and if the winding of the stator was going to be difficult. A test rig, with a motor and hoisting rope, was built to simulate the force and motion of a buoy, and a resistive load was connected to the generator. Experimental results show a peak voltage of 64.3 V and a peak power of 1.6 kW.

The paper was presented by Magnus Stålberg at the *6th European Wave and Tidal Energy Conference* and is published in the corresponding conference proceedings.

The author participated in the design and construction of the generator, as well as in the writing of the paper.

PAPER II

Experimental results from sea trials of an offshore wave energy system

This is the first paper that was published on the results of the first WEC of the Lysekil research site. The information covers two and a half month of data from the WECs operation in a range of sea states and with various loads connected to the generator. The paper was the first to verify the studied concept for wave energy conversion. It showed energy absorption dependency on load

and demonstrated voltage and power output. The results indicate that optimal load does not vary with wave climate.

The paper is published in *Applied Physics Letters*.

The author played one of the leading roles in the design and construction of the wave energy converter. He performed the simulations and most of the work in the writing of this paper.

Paper III

Influence of Generator Damping on Peak Power and Variance of Power for a Direct Drive Wave Energy Converter

The hydrodynamic behavior of the point absorber/buoy, depends, to a large extent, on the damping of the generator. The damping, in turn, can be remotely controlled by changing the load resistance. This paper investigated the peak power, the translator speed, and the variance of the power at different sea states and for different levels of damping. The aim was to analyze whether load control strategies could influence the dimensioning criteria for the electric system and the generator. In the study, it was found that maximum generated power is approximately proportional to the average power, while the maximum translator speed and standard deviation of power decrease as the damping factor is increased.

The peer-reviewed conference paper was presented by the author at the *26th international conference on Offshore Mechanics and Arctic Engineering*. It was later published in *Journal of Offshore Mechanics and Arctic Engineering*.

The author performed the simulations, created the resulting figures and participated in the writing of the paper.

Paper IV

Wave power absorption: Experiments in open sea and simulation

In this paper, experimentally collected data of energy absorption for different electrical loads were used to verify a model of the wave power plant that includes the interactions of wave, buoy, generator, and the external load circuit. The wave-buoy interaction was modeled with linear potential wave theory. The generator was modeled as a non-linear mechanical damping function that is dependent on piston velocity and electric load. The results showed good agreement between experiments and simulations and potential wave theory was found to be well suited for the modeling of this point absorber in normal operation as well as for the design of future converters. Moreover, the simulations were fast, which opens up for simulations of wave farms.

The paper is published in *Journal of Applied Physics*.

The author played one of the leading roles in the design and construction of the wave energy converter and the experiments at sea. He is also responsible

for the experimental results in the paper and has participated in the writing of it.

PAPER V

Power Absorption of a Wave Energy Converter

The ability of the wave energy converter to capture the energy of ocean waves was studied in this paper. The absorption is presented as a function of significant wave height, energy period, and electrical load. The study showed that the absorption, in percent, has a clear region of more optimal absorption and that the power generated overall increases with wave height. In the study the absorption reached a maximum of approximately 24% at certain sea states and at a certain combination of buoy, generator, and load. The presented values did not take absorption to cover for iron losses and mechanical losses into account, and the actual absorption is thus somewhat higher than presented in the paper.

The paper is submitted to *IEEE Journal of Oceanic Engineering*.

The author performed the simulations and most of the work in the writing of this paper.

PAPER VI

On the influence of water levels on wave power absorption: experimental results

This paper investigates the sensitivity of the studied wave energy system to variations in mean water levels. Changing water levels are expected to affect the energy absorption, since they will displace the equilibrium position of the translator which, in some cases, will result in a smaller active area of the stator. In the study, measurements of absorbed energy were correlated to measurements of sea states and water levels at the site. During the time of measurements, the water levels were in the range of -70 – +46 cm. The results show a decline in absorption for water levels that make the translator deviate more than ±25 cm from its center position. However, this was not considered to be much of a problem at the research site since these water levels only make up approximately 15% of the time.

The paper is submitted to *IEEE Journal of Oceanic Engineering*.

The author performed the simulations leading to the WEC absorption values of Figures 4 & 5, contributed with Figure 1, and participated in the writing of the paper.

Paper VII

Offshore experiments on a direct-driven Wave Energy Converter

The paper provided an update on the research performed at Uppsala University and near Lysekil. In addition, it showed the wave climate of the Lysekil wave energy research site during the three first months of operation of the installed WEC, and how the absorbed power had varied as a function of significant wave height. The average energy flux during the first test period was 1.4 kW/m and the relative absorption for the current system configuration was shown to be higher in the lower range of the wave spectrum.

The peer-reviewed paper was presented by Jens Engström at the *7th European Wave and Tidal Energy Conference*.

The author participated in the writing of the paper and is responsible for the simulations leading to the experimental data used in Figures 3 and 4.

Paper VIII

Wave energy conversion system - experimental results from offshore operation

This paper presents experimental results from the second operational period of the wave energy converter. At this time the electrical system had been expanded, and the power from the generator was now being rectified with a diode bridge and filtered using a capacitive filter. Performance of the whole conversion system was studied using resistive loads connected across the filter. The aim was to investigate the operational characteristics of the generator when it was connected to a non-linear load. By changing the value of the resistive load, the speed of the translator can be changed and also the damping of the generator. The power absorbed by the generator was studied at different sea states as well. The observations presented in the paper provide important information on how the WECs will behave when they are connected to the electric grid in the future and on how the electrical system should be designed.

The paper is conditionally accepted to *IEEE Journal of Oceanic Engineering*.

The author participated in the writing of the paper. He also wrote the basic programs used to perform the simulations leading to the data given i Figure 5.

Paper IX

Measuring air gap width of permanent magnet linear generators using search coil sensor

Critical for the survival of the generator is that the air gap between the moving and static parts of the generator is constantly fixed at the designed width to prevent the moving and static parts from connecting during operation. This paper shows the design and evaluation of an inductive sensor for measuring

the air gap width during generator operation. A coil etched on a printed circuit board, i.e., a search coil, was the chosen basis for the sensor. The sensor was tested on the laboratory generator and the results were compared to calculations based on finite element simulations. The results showed that the sensor was suitable for measuring the air gap width. Experimentally measured and theoretically calculated sensor signals showed good agreement, and the set-up had a sensitivity of ± 0.4 mm in the range of $4 - 9.5$ mm air gap. The experiments were somewhat compromised by an ill-designed cement pillar guiding the translator of the laboratory generator, and the potential for future improvements of the sensors sensitivity is deemed considerable.

The paper is published in *Journal of Applied Physics*.

The author performed most of the work in this paper.

PAPER X

Wave Climate off the Swedish West Coast

This paper presents and discusses the wave climate off the Swedish west coast. It is based on eight years (1997-2004) of wave data from 13 sites, near shore and offshore, in the Skagerrak and Kattegatt. The data is a product of the WAM and SWAN wave models verified at one site by a wave measurement buoy. It is found that the average energy flux is approximately 5.2 kW/m in the offshore Skagerrak, 2.8 kW/m in the near shore Skagerrak, and 2.4 kW/m in the Kattegatt. Statistical hundred-year waves were estimated to range from approximately $10 - 13$ m in offshore Skagerrak, $6 - 8$ m in near shore Skagerrak, and $6.5 - 9.5$ m in the Kattegat. Discussions on WECs conclude that the design sea state should be chosen with awareness of the fraction of available energy in the sea states that is made obtainable to the WEC, which is a consequence of the chosen WEC system design.

The paper is under review in *Renewable Energy*.

The author performed most of the work in this paper.

PAPER XI

Wave energy from the North Sea: experiences from the Lysekil research site

This paper provides a status update on the development of the Lysekil wave energy research site. It provides a more detailed and thorough overview than what has been published in any of the other papers. The installation of the WEC in the spring of 2006 is illustrated, and the paper includes a discussion on environmental studies at the site and some results on the artificial reefing effects of the installed WEC. Furthermore, almost a full year of sea states, as measured by the wave measurement buoy, is presented with the conclusion that the average energy flux during 2007, excluding August, was 3.4 kW/m.

The invited paper is published in *Surveys of Geophysics* and is available online.

The author is responsible for part of the results, i.e. the sections dealing with the wave climate and WEC output. He also participated to a small degree in the overall writing of the paper.

PAPER XII

Conversion of wave motions to electricity – from theory to full scale experiments

The paper is the first to describe the fundamental ideas behind the concept for wave energy conversion researched at the Centre for Renewable Electric Energy Conversion at Uppsala University. The concept is presented as a grid-oriented approach to electricity production from ocean waves, and the importance of a holistic perspective throughout the WEC system design is pointed out. The paper concludes that mechanical parts should be kept as simple as possible and that overloads, originating in the intermittent nature of the waves, should be handled electrically rather than mechanically when possible.

The paper will appear in the January 2009 issue of *IEEE Power & Energy Magazine*.

The author played a large role in the writing of the paper.

PAPER XIII

Experimental results from an offshore wave energy converter

The object of this paper was to present a detailed description of the electrical system at the Lysekil wave energy research site after it had been expanded with a rectifier and filter. Special attention is given to the power absorption by the generator when it is connected to a non-linear load. The values of the capacitance and resistive load were set high in the experiments to achieve a constant DC level. The results show that the DC load of the generator will play a significant role when the power production of the generator is going to be optimized in the future. A low loading of the generator at high sea states will decrease the power absorption substantially. In the future, with a grid connection, the load of the generators will be regulated by the inverter. It will then be easier to achieve a constant DC voltage in comparison to using only one generator connected to a resistive load.

The peer-reviewed paper was presented by Cecilia Boström at the 27th international conference on *Offshore Mechanics and Arctic Engineering*.

The author wrote the basic programs used for the simulations leading to the data given i Figures 6 and 7, and is responsible for part of Figure 2. He played a small part in the writing of the paper.

PAPER XIV

The Lysekil Wave Power Project: Status Update

The paper provides a status update of the Lysekil project. It was presented for the wave energy community at the 10th World Renewable Energy Conference, WREC, in 2008. The paper briefly covers the wave energy concept, the Lysekil research site, project history, the laboratory set-up, wave climate studies, force measurements, the first offshore wave energy converter, the measuring station, the observation tower, environmental impact, and some previously published results.

The paper was presented by Simon Tyrberg at the *10th World Renewable Energy Conference*.

The author is part of this paper as a function of having been involved in many parts of the Lysekil project as well as having contributed with four figures to the paper, i.e. Figures 1, 4, 5 and 7.

PAPER XV

On the Physics and Economics of Renewable Electric Energy Sources – part I utilization

A method for evaluating renewable energy technologies (RETs), in terms of economy and engineering solutions, is presented and argued for in this paper, part I utilization, and the accompanying paper, part II engineering. RETs can be evaluated through studying the fundamental physics of renewable energy sources and how it matches with the RETs. This match is described by the "Degree of Utilization". The papers argues that if competitive RETs are to be developed, then engineers need to match the technology to the physics of the renewable energy source, resulting in a high degree of utilization. The findings indicate that new innovations should focus on possible full loading hours. This would lead to more economically viable RETs which, in turn, would enable a faster, cheaper and more long-term sustainable integration of environmentally friendly solutions. The first part, Part I utilization, of the two papers focuses on the difference between power and energy, the physics of different energy sources, and their utilization.

The invited peer-reviewed paper was presented by Mats Leijon at the *World Scientific and Engineering Academy and Society – Energy Planning, Energy Saving, Environmental Education*.

The author participated in the writing of the paper and has contributed with Figures 1, 2, and 3.

PAPER XVI

On the Physics and Economics of Renewable Electric Energy Sources – part II engineering

Same as above, only this part of the two papers focuses on the engineering side with a large number of real examples that serve to support the case made in both papers.

The invited peer-reviewed paper was presented by Annika Skoglund at the *World Scientific and Engineering Academy and Society – Energy Planning, Energy Saving, Environmental Education*.

The author participated in the writing of the paper.

11. Svensk sammanfattning

Den här avhandlingens huvudsakliga fokus är en teknik för utvinning av energi ur havsvågor som studeras vid Sveriges Centrum för Förnybar Elenergiomvandling (CFE) vid avdelningen för Elektricitetslära på Uppsala Universitet.

Forskningen riktar sig mot att studera vågenergikonceptet ur ett fysikaliskt, teknologiskt, ekologiskt och ekonomiskt perspektiv. Tekniken har testats under lång tid i verkliga förhållanden och dess övergripande funktion som energiteknik för förnybar elproduktion från havsvågor har verifierats.

I mars 2006 installerades ett första vågkraftverk ett par kilometer ut till havs på den svenska västkusten, i närheten av Lysekil. Sedan dess har vågkraftverket stått på havsbotten i över två och ett halvt år och tagits i drift under tre perioder om sammanlagt ca 12 månader, senast under fem månader av 2008. Under driftperioderna har mätningar kontinuerligt utförts och det elektriska systemet har stegvis uppdaterats med målet att så småningom ansluta vågkraftverket till elnätet.

Vågkraftverk arbetar i en krävande miljö. Stora krafter tillsammans med korrosion och begränsad tillgänglighet för reparationer och underhåll har historiskt lett till att många vågkraftverk gått sönder. Med lärdom taget från detta, och för att minska behovet av underhåll, har vågkraftkonceptet vid Uppsala Universitet inriktats på att vara så mekaniskt enkelt som möjligt. Lösningar som ersatt mekaniska laster med elektriska har favoriserats eftersom dessa är billigare och lättare att hantera. Dessutom har utgångspunkten alltid varit helheten, från uppfångandet av energi ur havsvågor till nätanslutning, vilket tros leda till en robust och hållbar teknik.

Vågkrafttekniken består av ett antal huvudkomponenter. En s.k. direktdriven permanentmagnetiserad synkron linjärgenerator är placerad i en vattentät behållare på havsbotten, och en lina förbinder generatorn med en boj på ytan. Vågorna sätter bojen i rörelse, och bojen driver därigenom generatorn. Den genererade elektriciteten överförs till en mätstuga på land via sjökabel. Under den första testperioden, som varade i cirka två och en halv månad, omvandlades den genererade elektriciteten direkt till värme i dumplaster. I de senare perioderna, som varade i cirka fem månader vardera, likriktades och filtrerades elektriciteten först innan den förbrändes i dumplasterna. Den här avhandlingen är framförallt inriktad på konstruktionen av vågkraftverket samt den första och delvis den andra av de tre mätperioderna.

Rörelsen hos en linjärgenerator varierar i både hastighet och riktning vilket gör att den genererade spänningen och strömmen varierar i både amplitud,

frekvens och fasföljd. Eftersom translatorn, dvs den rörliga delen i en linjärgenerator, måste stanna upp för att byta riktning så kommer generatorn med några sekunders mellanrum inte att producera någon elektricitet. Den genererade effekten är beroende av hastigheten i generatorn, vilket får konsekvensen att effekten varierar kraftigt på sekundskala och kommer att generera effekttoppar som är flera gånger större än medeleffekten. För att uppnå en mer konstant uteffekt, och en spänning med konstant frekvens och ampliud, likriktas och filtreras först den genererade spänningen, sedan växelriktas den till nätfrekvensen och transformeras till önskad amplitud.

En rad studier har gjorts på vågkraftverket vilket har gett många lärdomar och kunskap om det studerade vågkraftkonceptets funktion. Erfarenheter har erhållits i allt från design, konstruktion och installation, till energiabsorption och inverkan av det elektriska systemet, AC som DC, på den genererade elektriciteten. Ett urval av resultat ges i det följande:

- En relativt jämn elproduktion, som är nära konstant över ett tiotal sekunder, har åstadkommits genom likriktning och filtrering. Den genererade effekten följer förändringarna i vågklimatets medeleffekt.
- Långa experiment visar att den optimala dämpningen är oberoende av vågklimat.
- Generatorerna behöver vara dimensionerade för att klara stora variationer i elproduktion p.g.a. att vågklimatet inte kan kontrolleras och att generatorerna är direktdrivna. Detta gör att genererad maxeffekt kommer att vara flera gånger högre än medeleffekten.
- Den andel av vågornas energi som fångats upp, i genomsnitt under en halvtimme och vid konstant elektrisk last, visade ett flackt maximum kring en våghöjd på 1.2 m och en vågperiod på 4.5 s under den första mätperioden. Absorptionen var högst i våghöjder mellan 0.5 och 1.5 m och vågperioder mellan 3.5 och 5 s. Maximalt uppgick den till strax över 24%. Dessa resultat är helt beroende av, och varierar starkt med, den valda kombinationen av boj, generator och elektrisk last.
- Momentana maxeffekter visade sig vara proportionella mot medeleffekten.
- Maximal translatorhastighet och standardavvikelse för genererad effekt minskar med ökad dämpfaktor.
- Belastningsstrategier har studerats och kan appliceras på vågkraftverket för att till viss del styra storleken på de fysiska lasterna.
- Vågkrafttekniken är känslig för stora variationer i vattenstånd. Storleken av förändringarna på den svenska västkusten är dock mestadels så små att dess påverkan är liten.
- DC-nivån i det elektriska systemet kommer att vara av stor betydelse vid optimering av energiproduktionen i framtiden.
- När generatorn är kopplad mot DC-spänning förändras funktionen på så sätt att likriktaren bara leder ström när den genererade spänningen är större än DC-spänningen.

Vågkraftparken på västkusten startades 2004 och nuvarande tillstånd tillåter att den körs till år 2014. Under tiden kommer upp till 10 nätanslutna

vågkraftverk och upp till 30 bojar för biologiska studier att installeras. Idag innehåller vågkraftparken ett vågkraftverk kopplat till en mätstuga på land, en vågmätningsboj, 15 bojar för biologiska studier och en observationmast.

Allt som allt har stor erfarenhet erhållits om vågkraftteknikens funktion och forskningen har kommit en bit på väg mot en energiteknik för förnybar elproduktion som har potential att bli en integrerad del av energisystemet i en nära framtid. Erfarenheterna fungerar som en plattform för den forskning som bedrivs idag och som fortsättningsvis kommer att bedrivas. Det finns många parametar som spelar in i vågkraftsystemet och det är mycket som kommer att förändras och förbättras i den framtida forskningen.

Utöver konstruerandet av vågkraftverket har några kortare studier utförts. En sensor har utvecklats som mäter luftgapets storlek i vågkraftverkets generator. Sensorn består av en spole etsad på ett kretskort. Den mäter luftgapet genom den spänning som induceras när spolen placeras i det varierande magnetfältet i luftgapet. Sensorn har testats på en labbgenerator, som är väldigt lik den i vågkraftverket, och resultaten har jämförts med simuleringar som baserades på finita elementberäkningar. Resultaten visade att sensorn med 95% säkerhet kunde mäta luftgapets storlek till en noggrannhet av 0.4 mm. Potentialen för förbättring av sensorns noggrannhet är stor.

Vågklimatet på den svenska västkusten har studerats utifrån åtta år av vågdata från tretton platser i Skagerrak och Kattegatt, samt genom en vågmätningsboj som varit utplacerad i forskningsparken i närheten av Lysekil sedan 2004. Det genomsnittliga energiflödet för Skagerrak beräknades till 5.2 kW/m på djupt vatten och 2.8 kW/m nära land. I Kattegatt beräknades energiflödet till ca 2.4 kW/m. Den mesta energin, på årsbasis, finns i våghöjder mellan 1 – 3 m och vågperioder mellan 4 – 7 s på djupt vatten, och 1 – 2.5 m respektive 4.5 – 7 s nära land i Skagerrak. Statistiskt framräknade enskilda största våg på hundra år estimeras i Skagerrak till en våghöjd mellan 10 – 13 m på djupt vatten, och mellan 6 – 8 m nära land. För Kattegatt estimeras våghöjden till mellan 6.5 – 9.5 m. En diskussion kring designkriterier för vågkraftverk rekommenderar att det designande vågklimatet bör väljas utifrån hur stor del av vågklimatets energi, på årsbasis, som görs tillgänglig för vågkraftverket.

Slutligen presenterades en metod för jämförande av olika energitekniker, utifrån ekonomiska och ingenjörsmässiga synvinklar, genom att studera de grundläggande egenskaperna hos energikällan och hur tekniken matchar dessa. Jämförelsen sker genom framräknad så kallad utnyttjandegrad. I artiklarna argumenteras för att ingenjörer behöver matcha teknologin med energikällan för att konkurrenskraftig energiteknik för förnybar elproduktion ska kunna utvecklas. Detta bör resultera i en hög utnyttjandegrad vilket ger fler fullasttimmar, mer tillförlitlighet för elnätet och bra ekonomiska förutsättningar. Detta skulle, i sin tur, kunna leda till en snabbare, billigare och mer långsiktigt hållbar integration av miljövänliga energitekniker i samhället.

12. Acknowledgements

Jag har haft det stora privilegiet och nöjet att doktorera i ett fantastiskt spännande ämne. För detta, för allt jag lärt mig under resans gång, för alla givande samtal, och för att jag har fått känna att mitt bidrag och engagemang har varit viktigt, vill jag tacka min handledare *Mats Leijon*.

Although our *contributors* have been acknowledged in the papers, I would like to thank them again for their support. Without these contributions none of the performed work could have been achieved.

Jag vill också ge ett stort tack till de seniorer som jag har haft nöjet att få arbeta med och lära känna. *Janne S.* som varit min biträdande handledare, *Janne I.* som jag alltid sprungit till när teorin har gått mig över huvudet, *Olov* som är en intressant kombination av teoretisk fysiker, galen professor, och nagel i ögat, *Micke* som kom in sent och livade upp stämningen på avdelningen, och *Hans* som varit en stor källa till inspiration och kunskap inom vågkraft och som alltid har halvgalna historier till hands.

Gunnel och *Christina* – tack för att ni gjort livet enklare för mig här på avdelningen.

Magnus – vi har gjort det här tillsammans, från Energisystem och framförallt sen vi började med vågkraften. Du har varit den bästa kollega jag kan tänka mig, men det är ändå ingenting jämfört med hur fina vänner vi har blivit och kommer att förbli.

Simon – tack för att du inspirerade mig till att damma av den gamla felan (och köpa en ny som var jättedyr, och sen en femsträngad). Tack för musiken, sången och seglingen. Jag ser fram emot alla framtida äventyr!

Oskar – som kollega var du en förebild i mitt doktorandarbete. Tack för handledning, skarpa analyser, inspiration och alla givande samtal. Nu är du en god vän som jag delar massa glada minnen med och som jag träffar på Svenssons lite då och då, men det är ju inte så tokigt det heller. Say when!

Ulf – du har fått några droppar whiskey i en påse av mig. Själv har jag fått hjälp med allt jag bett om, från vågkraftverk till fiolstråke, men jag tänker att det nästan går jämt upp med tanke på alla skämt som jag har fått uthärda...

Våggänget, gamla som nya – tack för ett sammarbete som har flutit på bra genom åren. Ibland har det gått lite upp och ner, men vi har alltid lyckats hålla huvudet över ytan. Se till att hålla ihop när det blåser på och försök hålla er på styva linan, annars är det lätt att någon blir sur och sprintar iväg. Jag har fått uppleva mycket spänning tillsammans med er. Oh boj vad jag kommer att sakna er. Det har aldrig saknats hummer i vårt gäng, och aldrig varit långt till tratt.

Kollegor på Ellära – tack för att jag vaknat varje dag och sett fram emot att komma till jobbet (speciellt på fredagar).

Basic Cooking – for a number of great classes (and good times), great food (and fat bellies), great wine (and round feet), but most of all friendship.

Skidgänget – Tack för svettiga dagar i Orsa, stenhård valla, smaklös kexchoklad och hundbajs i spåret. Men framförallt tack för den efterföljande bastun och brädspelen långt in på kvällarna. Vem vinner nästa omgång av Kill Doctor Lucky?

Amy – thank you soo much for proofreading my thesis! I'm surrounded by Swedish people!!

Ett stort tack till alla er som hjälpt mig med korrekturläsning av avhandlingen! *Magnus, Mårten, Simon, Urban, Kalle, Martin, Janne S. och Janne I.*

Fredrik, *Johan*, och *Tor* – mina äldsta vänner. Tack för att ni står ut med min tankspriddhet och för att ni fortfarande tycker om att träffas. Vi ses på Galtande Grisen!

Gustav – tack för min tid som gästforskare på Chalmers (rädda världen-snack, morgonyoga, the French pain), och tack för allt det andra.

Fredrik – för oförståeliga diskussioner om Wavelettransformer, för kvickrötter och stenar.

Maria – (som blir sur om jag inte tackar henne) Tack för allt! Allt!!

Magnus L. – tack för att du förgyllt min tid i Uppsala. Från Fälbiologerna till Gälbotorpet till serenader till svettiga krocketmatcher och till sång så stark att självaste Carl Gustaf stannar upp i sin färd och utropar *Guds frid!*

Ultunae Drängar – tack för några av de bästa stunderna i mitt liv.

Mina nyfunna vänner i *Orphei Drängar* – tack för en fantastisk början på en lång resa.

Framförallt vill jag tacka:

Min kära *svenska familj* för allt stöd genom åren. Snart blir det julotta i Oxberg!

My *American family* for all the kindness, support and good times through the years. You are a crazy bunch!

Malena och *Saga* för att ni är det bästa sällskap jag kan tänka mig när elden sprakar i öppna spisen långt inne i dalaskogarna, och det enda som finns till hands är en kopp kaffe med mazariner och kitbits.

Bibliography

[1] International Energy Agency (IEA). *World Energy Outlook 2006*. Head of Publications Service, IEA, Paris, France, 2006.

[2] D. Mollison, O.P. Buneman, and S.H. Salter. Wave power availability in the NE Atlantic. *Nature*, 263:223 – 226, 1976.

[3] L. J. Duckers. Wave energy; crests and troughs. *Renewable Energy*, 5(2):1444 – 1452, 1994.

[4] J. Falnes and J. Løvstedt. Ocean wave energy. *Energy policy*, 19(8):768 – 775, 1991.

[5] H. Polinder, M.E.C. Damen, and F. Gardner. Linear PM generator system for wave energy conversion in the AWS. *IEEE Trans. on Energy Conversion*, 20(3):583 – 589, 2004.

[6] J.P. Kofoed, P. Frigaard, E. Friis-Madsen, and H.C. Sørensen. Prototype testing of the wave energy converter Wave Dragon. *Renewable energy*, 31(2):181 – 189, 2006.

[7] M.C. Carcas. The OPD Pelamis WEC: Current status and onward programme. *Int. Journal of Ambient Energy*, 24(1):21 – 28, 2003.

[8] C.B. Boake, T.J.T. Whittaker, and M. Folley. Overview and initial operational experience of the LIMPET wave energy plant. pages 586 – 594, Kitakyushu, Japan, 2002. Proc. of the 12th International Offshore and Polar engineering Conference.

[9] R. Waters, M. Stålberg, O. Danielsson, O. Svensson, S. Gustafsson, E. Strömstedt, M. Eriksson, J. Sundberg, and M. Leijon. Experimental results from sea trials of an offshore wave energy system. *Applied Physics Letters*, 90:034105, 2007.

[10] A. Weinstein, G. Fredrikson, M.J. Parks, and K. Nielsen. Aquabuoy – the offshore wave energy converter, numerical modeling and optimization. *Oceans '04. MTTS/IEEE Techno-Ocean '04*, 4:1854 – 1859, 2004.

[11] M. Ruellan, H. Ben Ahmed, B. Multon, C. Josset, A. Babarit, and A.H. Clement. Design methodology for a SEAREV wave energy converter. *Electric Machines & Drives Conference, 2007. IEMDC '07. IEEE International*, 2:1384 – 1389, 2007.

[12] A. Muetze and J.G. Vining. Ocean wave energy conversion – a survey. *Industry Applications Conference, 2006. 41st IAS Annual Meeting. Conference Record of the 2006 IEEE*, 3:1410 – 1417, 2006.

[13] A. Clément, P. McCullen, A. Falcão, A. Fiorentino, F. Gardner, K. Hammar-lund, G. Lemonis, T. Lewis, K. Nielsen, S. Petroncini, T. Pontes, P. Schild, B.-O. Sjöström, H. C. Sørensen, and T. Thorpe. Wave energy in europe: current status and perspectives. *Renewable & Sustainable Energy Review*, 6(5):405 – 431, 2002.

[14] L. Claeson. *Energi från havets vågor (Efn-rapport nr 21)*. Energiforskn-ingsnämnden, Stockholm, Sweden, 1987.

[15] Encyclopædia Britannica. *Ocean*. (2008). Retrieved September 21, 2008, from Encyclopædia Britannica Online: http://www.britannica.com/EBchecked/topic/424285/ocean.

[16] E.ON. *E.ON Netz Wind Report 2004*. E.ON Netz GmbH, Bayreuth, Germany, 2004.

[17] N. Sharmila, P. Jalihal, A.K. Swamy, and M. Ravindran. Wave powered desali-nation system. *Energy*, 29(11):1659 – 1672, 2004.

[18] D. C. Hicks, G.R. Mitcheson, C.M. Pleass, and J.F. Salevan. Delbuoy: ocean wave-powered seawater reverse osmosis desalination system. *Desalination*, 73(1):81 – 94.

[19] Centrum för vindkraftsinformation CVI. *Vindkraft i Elnätet (Faktablad 7)*. Centrum för vindkraftsinformation - CVI, Gotland University, Visby, Sweden, 2005.

[20] M. Leijon, H. Bernhoff, M. Berg, and O. Ågren. Economical considerations of renewable electric energy production – especially development of wave energy. *Renewable Energy*, 28(8):1201 – 1209, 2003.

[21] M. Leijon. Foreseeable cost reductions in energy from renewables. Stockholm, Sweden, 2004. Proc. of Euroscience Open Forum, invited lecture.

[22] C. Falkemo. *Vågenergiboken*. Ingenjörsförlaget, Stockholm, Sweden, 1980.

[23] J. Falnes. *Ocean waves and oscillating systems*. The press syndicate of the Universtiy of Cambridge, Cambridge, United Kingdom, 1st edition, 2002.

[24] João Cruz. *Ocean Wave Energy, Current Status and Future Perspectives*. Springer-Verlag, Berlin Heidelberg, Germany, 2008.

[25] D. Sigurd, L. Stolt, and L. Claesson. *Solceller och vågkraft (Efn/UTR 1983:7, Efn/LET 1983:27)*. Energiforskningsnämnden, Stockholm, Sweden, 1983.

[26] H. Bergström. *Wind resource mapping of Sweden using the MIUU-model*. Wind Energy Report WE2007:1. Air, Water and Landscape Sciences, Depart-ment of Earth Sciences, Uppsala University, Uppsala Sweden, 2007.

[27] J. Brooke. *Wave energy conversion*, volume 6, Elsevier ocean engineering book series. Elsevier, Oxford,UK, 2003.

[28] J. Falnes. A review of wave-energy extraction. *Marine Structures*, 20:185 – 201, 2007.

[29] H. Bernhoff, E. Sjöstedt, and M. Leijon. Wave energy resources in sheltered sea areas: A case study of the Baltic Sea. *Renewable Energy*, 31(13):2164 – 2170, 2006.

[30] U. Henfridsson, V. Neimane, K. Strand, R. Kapper, H. Bernhoff, O. Danielsson, M. Leijon, J. Sundberg, K. Thorburn, E. Ericsson, and K. Bergman. Wave energy potential in the Baltic Sea and the Danish part of the North Sea, with reflections on the Skagerrak. *Renewable Energy*, 32(12):2069 – 2084, 2007.

[31] Girard père et fils. *Pour divers moyens d'employer les vagues de la mer, comme moteurs*. Brevet D'invention De Quinze Ans, Paris, France, 1799.

[32] G. Boyle. *Renewable Energy*. Oxford University Press and The Open University, Oxford and Milton Keynes, UK, 4th edition, 2002.

[33] G. Svensson and R. Hardell. *En svensk vågkraftidé (Efn-rapport nr 12)*. Energiforskningsnämnden, Stockholm, Sweden, 1985.

[34] K. Thorburn. *Electric Energy Conversion Systems: Wave Energy and Hydropower*. Doctoral thesis, Uppsala University, Sweden, 2006.

[35] M. Eriksson. *Modelling and Experimental Verification of Direct Drive Wave Energy Conversion. Buoy-Generator Dynamics*. Doctoral thesis, Uppsala University, Sweden, 2007.

[36] Coordinated Action on Ocean Energy. European Commission. Retrieved September 22, 2008: http://www.ca-oe.net/.

[37] Centre for Renewable Energy Sources. *Ocean Energy Conversion in Europe*. Published by the European Commission in the framework of the Co-ordinated Action on Ocean Energy, 2006.

[38] International Energy Agency (IEA). *IEA-OES, International Energy Agency Implementing Agreement on Ocean Energy Systems, Annual report 2007*. IEA-OES Executive Committee, Paris, France, 2007.

[39] Pelamis Wave Power. Retrieved September 22, 2008: http://www.pelamiswave.com/.

[40] Wave Dragon. Retrieved September 22, 2008: http://www.wavedragon.net/.

[41] Wavegen A Voith and Siemens company. Retrieved September 22, 2008: http://www.wavegen.co.uk/.

[42] R.K. Wangsness. *Electromagnetic fields*. John Wiley & Sons, New York, New York State, USA, 2 edition, 1986.

[43] D. Jiles. *Magnetism and magnetic materials*. Chapman & Hall/CRC, Boca Raton, Florida, USA, 2 edition, 1998.

[44] M. Mathiesen, P.J. Hawkes Y. Goda, E. Mansard, M.J. Martin, E. Peltier, E.F. Thompson, and G. Van Vledder. Recommended practice for extreme wave analysis. *Journal of Hydraulic Research*, 32(6), 1994.

[45] L.R. Muir and A.H. El-Shaarawi. On the calculation of extreme wave heights: a review. *Ocean Engineering*, 13(1):93 – 118, 1986.

[46] J.H.G.M. Alves and I.R. Young. On estimating extreme wave heights using combined Geosat, Topex/Poseidon and ERS-1 altimeter data. *Applied Ocean Research*, 25(4):167 – 186, 2004.

[47] W. Wimmer, P. Challenor, and C. Retzler. Extreme wave heights in the North Atlantic from altimeter data. *Renewable Energy*, 31(2):241 – 248, 2006.

[48] O. Danielsson and M. Leijon. Flux distribution in linear permanent-magnet synchronous machines including longitudinal end effects. *IEEE Trans. on Magnetics*, 43(7):3197 – 3201, 2007.

[49] K. Thorburn and M. Leijon. Farm size comparison with analytical model of linear generator wave energy converters. *Ocean Engineering*, 34(5):908 – 916.

[50] O. Langhamer and D Wilhelmsson. Wave power devices as artificial reefs. Porto, Portugal, 2007. Proc. of the 7th European Wave and Tidal Energy Conference.

[51] O. Danielsson, M. Eriksson, and M. Leijon. Study of a longitudinal flux permanent magnet linear generator for wave energy converters. *International Journal of Energy Research*, 30(14):1130 – 1145, 2006.

[52] M. Eriksson, J. Isberg, and M. Leijon. Theory and experiment on an elastically moored cylindrical buoy. *IEEE Journal of Oceanic Engineering*, 31(4):959 – 963, 2006.

[53] M. Leijon, O. Danielsson, M. Eriksson, K. Thorburn, H. Bernhoff, J. Isberg, J. Sundberg, I. Ivanova, E. Sjöstedt, and O. Ågren. An electrical approach to wave energy conversion. *Renewable Energy*, 31(9):1309 – 1319, 2006.

[54] K. Nilsson, O. Danielsson, and M. Leijon. Electromagnetic forces in the air gap of a permanent magnet linear generator at no load. *Journal of Applied Physics*, 99:034505, 2006.

[55] K. Thorburn, K-E. Karlsson, A. Wolfbrandt, M. Eriksson, and M. Leijon. Time stepping finite element analysis of a variable speed synchronous generator with rectifier. *Applied Energy*, 83(4):371 – 386, 2006.

[56] K. Thorburn and M. Leijon. Analytical and circuit simulations of linear generators in farm. Dallas, USA, 2006. Proc. of IEEE PES T&D conference and exposition.

[57] K. Thorburn, K. Nilsson, O. Danielsson, and M. Leijon. Generators and electrical systems for direct drive energy conversion. London, UK, 2006. Proc. of MAREC 2006 at WMTC 2006.

[58] O. Danielsson, M. Leijon, and E. Sjöstedt. Detailed study of the magnetic circuit in a longitudinal flux permanent-magnet synchronous linear generator. *IEEE Trans. on Magnetics*, 41(9):2490 – 2495, 2005.

[59] M. Eriksson, J. Isberg, and M. Leijon. Hydrodynamic modelling of a direct drive wave energy converter. *International Journal of Engineering Science*, 43(17):1377 – 1387.

[60] I.A. Ivanova, H. Bernhoff, O. Ågren, and M. Leijon. Simulated generator for wave energy extraction on deep water. *Ocean Engineering*, 32(14):1664 – 1678.

[61] I.A. Ivanova, O. Ågren, H. Bernhoff, and M. Leijon. Simulation of wave-energy converter with octagonal linear generator. *IEEE Journal of Oceanic Engineering*, 30(3):619 – 629, 2005.

[62] M. Leijon, H. Bernhoff, O. Ågren, J. Isberg, J. Sundberg, M. Berg, K.E. Karlsson, and A. Wolfbrandt. Multiphysics simulation of wave energy to electric energy conversion by permanent magnet linear generator. *IEEE Transactions on Energy Conversion*, 20(1):219 – 224, 2005.

[63] O. Danielsson, M. Leijon, K. Thorburn, M. Eriksson, and H. Bernhoff. A direct drive wave energy converter – simulations and experiments. Halkidiki, Greece, 2005. Proc. of OMAE 2005: the 24th international conference on mechanics and arctic engineering.

[64] S. Gustafsson, O. Svensson, J. Sundberg, H. Bernhoff, M. Leijon, O. Danielsson, M. Eriksson, K. Thorburn, K. Strand, U. Henfridsson, E. Ericsson, and K. Bergman. Experiments at Islandsberg on the west coast of Sweden in preparation of the construction of a pilot wave power plant. Glasgow, UK, 2005. Proc. of the 6th European Wave and Tidal Energy Conference, EWTEC.

[65] H. Bernhoff and M. Leijon. Conversion of wave energy to electricity. *The Scandinavian Shipping Gazette, The Scandinavian Yearbook of Maritime Technology*, 2004.

[66] K. Thorburn, H. Bernhoff, and M. Leijon. Wave energy transmission system concepts for linear generator arrays. *Ocean Engineering*, 31(11-12):1339 – 1349, 2004.

[67] B. Bolund, E. Segergren, A. Solum, R. Perers, L. Lundström, A. Lindblom, K. Thorburn, M. Eriksson, K. Nilsson, I. Ivanova, O. Danielsson, S. Eriksson, H. Bengtsson, E. Sjöstedt, J. Isberg, J. Sundberg, H. Bernhoff, K-E. Karlsson, A. Wolfbrandt, O. Ågren, and M. Leijon. Rotating and linear synchronous generators for renewable electric energy conversion – an update of the ongoing research projects at Uppsala University. Trondheim, Norway, 2004. Proc. of the Nordic Workshop on Power and Industrial Electronics, NORPIE.

[68] O. Danielsson, K. Thorburn, E. Sjöstedt, and M. Leijon. Simulated response of a linear generator wave energy converter. Toulon, France, 2004. Proc. of ISOPE-2004.

[69] M. Eriksson, K. Thorburn, H. Bernhoff, and M. Leijon. Dynamics of a linear generator for wave energy conversion. Vancouver, Canada, 2004. Proc. of OMAE, the 23rd International Conference on Offshore Mechanics and Arctic Engineering.

[70] I.A. Ivanova, O. Ågren, H. Bernhoff, and M. Leijon. Simulation of a 100 kw permanent magnet octagonal linear generator for ocean wave energy conversion and utilization. *Scientific Technical Review Journal*, 1:239 – 244, 2004.

[71] I.A. Ivanova, O. Ågren, H. Bernhoff, and M. Leijon. Simulation of cogging in a 100 kw permanent magnet octagonal linear generator for ocean wave conversion. Taipei, Taiwan, 2004. Proc. of the International Symposium on underwater technology.

[72] O. Danielsson, K. Thorburn, E. Eriksson, and M. Leijon. Permanent magnet fixation concepts for linear generator. Cork, Ireland, 2003. Proc. of EWEC 2003, the 5th European Wave Energy Conference.

[73] I.A. Ivanova, O. Ågren, H. Bernhoff, and M. Leijon. Simulation of a 100 kw permanent magnet octagonal linear generator for ocean wave conversion. Cork, Ireland, 2003. Proc. of EWEC 2003, the 5th European Wave Energy Conference.

[74] S. Tyrberg. *Offshore surveillance of wave buoys*. Masters thesis, Uppsala University, Sweden, 2007.

[75] O. Danielsson. *Wave Energy Conversion, Linear Synchronous Permanent Magnet Generator*. Doctoral thesis, Uppsala University, Sweden, 2006.

[76] M. Stålberg. *Experimental Test Set-up for Wave Energy Converter Linear Generator*, volume UPTEC ES05 005. Maters thesis, Uppsala University, Sweden, 2005.

[77] S. Gustafsson. *Measuring of waves at Islandsberg and literature survey of wave measurement technology*, volume UPTE F04048. Masters thesis, Uppsala University, Sweden, 2004.

[78] O. Danielsson. *Design of a Linear Generator for Wave Energy Plant*, volume UPTEC F03 003. Masters thesis, Uppsala University, Sweden, 2003.

[79] E. Spooner and M.A. Mueller. *Comparative study of linear generators and hydraulic systems for wave energy conversion*. ETSU/DTI report V/06/00189/REP, University of Durham, School of Engineering, Durham, UK, 2001.

[80] P.R.M. Brooking and M.A. Mueller. Power conditioning of the output from a linear vernier hybrid permanent magnet generator for use in direct drive wave energy converters. *IEE Proc. C Gener. Transm. Distrib.*, 152(5):673 – 681, 2005.

[81] K. Rhinefrank, E.B. Agamloh, A. von Jouanne, A.K. Wallace, J. Prudell, K. Kimble, J. Aills, E. Schmidt, P. Chan, B. Sweeny, and A. Schacher. Novel ocean energy permanent magnet linear generator buoy. *Renewable Energy*, 31(9):1279 – 1298, 2006.

[82] L. Szabo, C. Oprea, C. Festila, and E. Dulf. Study on a wave energy based power system. Vilamoura, Portugal, 2008. Proc. of the 2008 International Conference on Electrical Machines.

[83] V. DelliColli, P. Cancelliere, F. Marignetti, R. DiStefano, and M. Scarano. A tubular-generator drive for wave energy conversion. *IEEE Transactions on Industrial Electronics*, 53(4):1152 – 1159, 2006.

[84] N.M. Kimoulakis, A.G. Kladas, and J.A. Tegopoulos. Power generation optimization from sea waves by using a permanent magnet linear generator drive. *IEEE Transactions on Magnetics*, 44(6):1530 – 1533, 2008.

[85] Significant wave heights on a hourly basis at the Lysekil research site. Retrieved September 22, 2008: http://islandsberg.angstrom.uu.se/.

[86] Norman E. Dowling. *Mechanical Behaviour of Materials*. Prentice-Hall, Inc., New Jersey, USA, 2nd edition, 1999.

[87] SMS Sveriges Mekanstandardisering. *Fasteners M – Terminology, generalities, tolerances and mechanical properties for bolts, screws, studs and nuts*. SIS – Standardiseringskommissionen i Sverige and SMS – Sveriges Mekanstandardisering, Gothenburg, Sweden, 1990.

[88] Maskinaktiebolaget Karlebo. Editors: B. Lindström, B. Rundqvist, R. Crafoord, and L. Hågeryd. *Karlebo handbok*. Liber AB, Fälth & Hässler, Värnamo, Sweden, 15th edition, 2005.

[89] Tibnor. *Handelsstål 2006, Sortiment – Toleranser – Produktion*. Tibnor, Solna, Sweden, 2006.

[90] J. Sundberg and O. Langhamer. Environmental questions related to point-absorbing linear wave-generators: impacts, effects and fouling. Glasgow, Scotland, 2005. Proc. of the 6th European Wave and Tidal Energy Conference.

[91] T.W. Thorpe and M.J. Picken. Wave energy devices and the marine environment. *IEE Proceedings A (Science, Measurement and Technology)*, 140(1):63 – 70, 1993.

[92] N. Mårtensson and L. Claeson. *On the Wave Climate of the Southern Baltic. (Report A:15)*. Department of Hydraulics, Chalmers University of Technology, Gothenburg, Sweden, 1987.

[93] L. Claeson. *Vågkraftverk i svenska farvatten, Tillgängliga vattenområden – inledande studie (Rapport GR:19)*. Gruppen för Vågenergiforskning, Gothenburg, Sweden, 1980.

[94] M.T. Pontes. Assessing the european wave energy resource. *Journal of Offshore Mechanics and Arctic Engineering, Transactions of the ASME*, 120(4):226 – 231, 1998.

[95] M.T. Pontes and R. Aguiar. A nearshore wave energy atlas for portugal. *Journal of Offshore Mechanics and Arctic Engineering*, 127(3):249 – 255, 2005.

[96] A. Beyene and J.H. Wilson. Comparison of wave energy flux for northern, central, and southern coast of California based on long-term statistical wave data. *Energy*, 31:1856 – 1869, 2006.

[97] B. Broman, T. Hammarklint, K. Rannat, T. Soomere, and A. Valdmann. Trends and extremes of wave fields in the north-eastern part of the Baltic proper. *Oceanologia*, 48:165 – 184, 2006.

[98] A. Jönsson, B. Broman, and L. Rahm. Variations in the Baltic Sea wave fields. *Ocean Engineering*, 30:107 – 126, 2002.

[99] The WAMDI Group. The WAM model – A third generation wave prediction model. *Journal of Physical Oceanography*, 19:1775 – 1810, 1988.

[100] S.F. Wornom, D.J.S. Welsh, and K.W. Bedford. On coupling the SWAN and WAM wave models for accurate nearshore wave predictions. *Coastal Engineering Journal*, 43(3):161 – 201, 2001.

[101] Johan Ribrant. *Reliability performance and maintenance,* A *survey of failures in wind power systems*, volume XR-EE-EEK 2006:009. Masters thesis, Royal Institute of Technology, Stockholm, Sweden, 2006.

Acta Universitatis Upsaliensis

Digital Comprehensive Summaries of Uppsala Dissertations from the Faculty of Science and Technology 580

Editor: The Dean of the Faculty of Science and Technology

A doctoral dissertation from the Faculty of Science and Technology, Uppsala University, is usually a summary of a number of papers. A few copies of the complete dissertation are kept at major Swedish research libraries, while the summary alone is distributed internationally through the series Digital Comprehensive Summaries of Uppsala Dissertations from the Faculty of Science and Technology. (Prior to January, 2005, the series was published under the title "Comprehensive Summaries of Uppsala Dissertations from the Faculty of Science and Technology".)